MECHANISMS OF CELL VOLUME REGULATION IN MOUSE OOCYTES: THE ROLE OF ZONA PELLUCIDA DETACHMENT IN THE INITIATION OF GLYCINE-DEPENDENT OSMOREGULATION

CHYNA ORTMAN

This thesis is submitted to the Faculty of Medicine as a partial fulfillment of the M.Sc. program in Cellular and Molecular Medicine

Cellular and Molecular Medicine

Faculty of Medicine

University of Ottawa

Abstract

Mouse oocytes and early preimplantation (PI) embryos possess a novel mechanism for regulating their cell volume which involves the accumulation of the organic osmolyte glycine via the glycine transporter, GLYT1. When the oocyte is still housed within the follicle, oocyte volume is completely determined by its strong adhesion to its rigid extracellular matrix, the zona pellucida (ZP). Shortly following ovulation, the ZP will detach from the oocyte and GLYT1 will become active, allowing the oocyte to independently regulate its own cell volume. These two mechanisms unfold at a very similar time course, with speculation that detachment precedes GLYT1 activation. However, their relative timing has yet to be confirmed. Moreover, much about these mechanisms, such as if they are coupled, remains unknown. Here I explore the relationship between GLYT1 activation and oocyte-ZP detachment, with the data demonstrating that detachment precedes GLYT1 activation.

I have found that the inhibition of oocyte-ZP detachment prevents the activation of GLYT1, which implies that GLYT1 activation requires detachment of the ZP from the oocyte. Previous data from our laboratory found that the oocyte-ZP adhesion is released via the action of a metalloproteinase (MP). MP's are protease enzymes whose catalytic mechanism involves a metal. Therefore, in an attempt to uncover the relationship between detachment and GLYT1 activation, metalloprotease inhibitors were used. Based on these results, I hypothesized that removal of the ZP would accelerate the activation of GLYT1. However, no acceleration was found. Lastly, as TIMPs are an important regulator of MP activity, I tested whether they were able to prevent the MP responsible for ZP detachment. However, detachment still preceded as normal in the presence of TIMPs. Overall, I have built on the previous data from our laboratory to provide further understanding into the two

independent cell volume regulation mechanisms of oocyte-ZP detachment and GLYT1 activation.

Abstract ii

Table of Contents iv

List of Figures viii

List of Tables x

List of Abbreviations xi

Acknowledgments xv

Table of Contents

1.0 Introduction 1

1.1 Folliculogenesis and oogenesis 1

1.2 Cell communication within the ovarian follicle 4

1.3 Meiotic Arrest 5

1.4 Meiotic Resumption 6

1.5 Ovulation 12

1.7 Culture media inflicted "2-cell block" and the changes required to overcome it 14

1.8 Osmolarity, osmolality, tonicity and molarity 16

1.9 Cell volume responses to changes in tonicity 17

1.10 Cell volume regulation with acute recovery: inorganic ions 18

1.11 Cell volume regulation with long-term homeostasis: organic osmolytes 19

1.12 Glycine as an organic osmolyte 22

1.13 The glycine transporter GLYT1 23

1.14 Cell volume regulation prior to ovulation: oocyte-zona pellucida adhesion 27

1.15 ZP composition and role 28

1.16 Synthesis, secretion and assembly **29**

1.17 Metalloproteases **32**

1.18 ZP detachment inhibition through chemical inhibitors **35**

1.19 ZP detachment inhibition through endogenous inhibitors: TIMPs **36**

1.20 Summary **37**

2. Significance and overall objective **38**

3. Specific aims and hypotheses **41**

4. Materials and Methods **43**

4.1 Chemicals and pharmaceutical agents **43**

4.2 Oocyte culture media **43**

4.3 Animals **44**

4.4 Superovulation **44**

4.5 Oocyte isolation and collection **45**

4.6 Oocyte culture **45**

4.7 Maintaining meiotic arrest **49**

4.8 Oocyte-ZP adhesion assay **49**

4.9 [^{3}H]-Glycine transport measurements **50**

4.10 Removal of the zona pellucida **52**

4.11 Time-lapse imaging with environmental control chamber **52**

4.12 Zona pellucida detachment inhibition with small molecule chemical inhibitors **53**

4.13 ZP detachment inhibition with TIMPs **53**

4.14 Data analysis **56**

5. Results **57**

5.1 The oocyte-ZP adhesion release precedes GLYT1 activation **57**

5.1a. GLYT1 activation over time for groups of oocytes 57

5.1b. Oocyte-ZP adhesion over time 59

5.1c. Timing of activation of GLYT1 vs oocyte-ZP detachment 61

5.1d. Meiotic competence of oocytes 63

5.1e. GLYT1 activation over time for individual of oocytes 65

5.1f. GLYT1 transporter recovery following 1000mOsM shock 70

5.1g. Oocyte adhesion assay at different concentrations 72

5.1h. GLYT1 transporter recovery following 450 mOsM shock 74

5.1i. GLYT1 activity and oocyte-adhesion assay both performed on individual oocytes 76

5.2. Detachment of ZP is required for the activation of GLYT1 ..... **79**

5.2a. Effects of metallopeptidase inhibitors 79

5.2b. GLYT1 activity and protease inhibitors 83

5.2c. Inhibitor reversibility on oocyte-ZP adhesion 85

5.2d. Inhibitor reversibility on GLYT1 activity 87

5.3 Removal of ZP does not accelerate GLYT1 activation in oocytes **89**

5.3a. Oocyte volume in ZP intact and ZP free oocytes 89

5.3b. GLYT1 activity in ZP-free and ZP-intact oocytes 93

5.3c. GLYT1 activity and osmolarity induced cell volume change 95

5.3d. Inhibition of GLYT1 activity in ZP-intact and ZP-free oocytes 97

5.4 TIMPs did not inhibit the release of the ZP from the oocyte **99**

6. Discussion **101**

6.1 The oocyte-ZP release precedes the activation of GLYT1 101

6.2 Oocyte-ZP detachment is required for GLYT1 activation..... 103

6.3 Removal of the ZP did not accelerate GLYT1 activation in oocytes..... 105

6.4 TIMPs did not inhibit the release of the ZP from the oocyte..... 107

7. Conclusion..... 109

8. Significance 110

9. Literature cited..... 111

List of Figures

Figure 1: Folliculogenesis

Figure 2: Meiotic arrest and resumption

Figure 3: Cell volume regulatory mechanisms

Figure 4: The structure of a zona pellucida glycoprotein (ZPG)

Figure 5: Glycine transport for groups of oocytes during oocyte maturation

Figure 6: Oocyte-ZP detachment during oocyte maturation

Figure 7: GLYT1 activity assay vs oocyte-ZP adhesion assay time course in GV oocytes

Figure 8: Meiotic competence of oocytes after osmotic shock

Figure 9: Average glycine transport for individual oocytes during oocyte maturation

Figure 10: GLYT1 activity assay of groups vs individual

Figure 11: GLYT1 transporter recovery following 1000 mOsM hypertonic shock

Figure 12: The oocyte-ZP adhesion assay with 1000 mOsM and 450 mOsM medium

Figure 13: GLYT1 transporter recovery following 450 mOsM hypertonic shock

Figure 14: The GLYT1 activity and oocyte-adhesion assays performed on an individual oocyte

Figure 15: Inhibitor dose response after 1.5 hr incubation

Figure 16: Inhibitor dose response after 4 hr incubation

Figure 17: Glycine transport in oocytes in the presence of protease inhibitors

Figure 18: Inhibitor reversibility for oocyte detachment

Figure 19: Inhibitor reversibility for GLYT1 transport

Figure 20: Zona pellucida removal and volume decrease

Figure 21: Average oocyte diameter over time

Figure 22: GLYT1 activity in ZP-intact and ZP-free oocytes

Figure 23: GLYT1 activity in ZP-free oocytes

Figure 24: GLYT1 activity in ZP-intact and ZP-free oocytes in the presence or absence of MMP inhibitors

Figure 25: TIMPs and oocyte detachment

List of Tables

Table 1: Summary of chemicals and compounds used

Table 2: Summary of pharmaceutical agents used

Table 3: Summary of recombinant proteins used

List of abbreviations

AC = adenylyl cyclase

ADAM = a disintegrin and metalloproteases

ADAMTS = metalloproteinase with thrombospondin motifs

ADAMTSL = ADAMTS-like

ATP = adenosine triphosphate

ART = assisted reproductive technologies

ACVS = animal care and veterinary services

BSA = bovine serum albumin

BMP = bone morphogenic protein

cAMP = cyclic adenosine monophosphate

CDC = cell division cycle

CDK = cyclin dependent kinase

CEEF = cumulus expansion-enabling factors

CGC = cumulus granulosa cells

cGMP = cyclic guanosine monophosphate

COC = cumulus oocyte complex

CNS = central nervous system

CTP = C-terminal propeptide

CTS = C-terminal subdomain

CX = connexin

CZB = Chatot Ziomek Bavister embryo culture medium

ECM = extracellular matrix

EDTA = tetrasodium ethylenediaminetetraacetic acid

EGF = epidermal growth factor

EGFR = epidermal growth factor receptor

ER = endoplasmic reticulum

FSH = follicle stimulating hormone

GC = granulosa cell

GDF = growth differentiation factor

GPR = G-protein-coupled receptors

GLYT = glycine transporter

GTP = guanosine triphosphate

GV = germinal vesicle

GVBD = germinal vesicle break down

HA = hyaluronic acid

Hepes = 4-(2-hydroxyethyl)-1-piperazineethanesulfonic acid

i.p. = intra-peritoneal

IVF = *in vitro* fertilization

IVM = *in vitro* maturation

KSOM = potassium supplemented Simplex Optimized Medium for embryo culture

LH = luteinizing hormone

MAPK = mitogen-activated protein kinase

MGC = mural granulosa cell

MI = meiosis I

MII = second meiotic division

MP = metalloproteinase

MMP = matrix metalloproteinase

MPF = M phase-promoting factor

MYT = myelin transcription factor

NIH = national institutes of health

NPPC = natriuretic peptide precursor

NPR = natriuretic peptide receptor

NTS = N-terminal subdomain

NTT = neurotransmitter transporters

OsM = osmoles per liter

PDE = phosphodiesterase

PGC = primordial germ cell

P = post-natal day

PI = preimplantation

PKA = protein kinase A

PKMYT = membrane-associated Tyrosine- And Threonine-Specific Cdc2- Inhibitory kinase

PMSG = pregnant mare serum gonadotropin PVA = polyvinyl alcohol

PVS = perivitelline space

RVD = regulatory volume decrease

RVI = regulatory volume increase

SEM = standard error of the mean

Ser = serine

SLC = solute carrier

TIMP = tissue inhibitors of metalloproteinase

Thr = threonine

TMD = transmembrane domain

Tyr = tyrosine

TZP = transzonal projections

VRAC = volume-regulated anion channels

ZP = zona pellucida

ZPD = zona pellucida domain

ZPG = zona pellucida glycoproteins

Acknowledgements

The work compiled in this thesis was performed under the supervision of Dr. Jay Baltz (Department of Cellular and Molecular Medicine, University of Ottawa, Ottawa Hospital Research Institute, Chronic Disease Program, Obstetrics and Gynecology). I would like to thank Dr. Baltz for being such an exceptional mentor to me throughout my Master's degree. His immense knowledge and passion for research is truly inspiring. This degree could not have been possible without his continuous guidance and support, while always encouraging me to do my best and to continue pushing through when times got tough.

I would also like to thank the members of my Thesis Advisory Committee: Dr. Barbara Vanderhyden (Department of Cellular and Molecular Medicine, University of Ottawa, Ottawa Hospital Research Institute, Cancer Therapeutics Program) and Dr. Christopher Kennedy (Department of Cellular and Molecular Medicine, University of Ottawa, Ottawa Hospital Research Institute, Chronic Disease Program). These remarkable scientists helped me become a better researcher through their insightful comments and challenging questions, greatly improving the quality of my work.

I would like to further extend my thanks to my colleagues in the Baltz lab that I had the pleasure of working with. First, I would like to thank Mrs. Megan Meredith and Ms. Taylor McClatchie who taught me all the technical laboratory skills and the basics of oocyte and embryo culture. Additionally, I would like to thank Dr. Allison Tscherner and Dr. Angus Macaulay for extending their knowledge, advice and technical skills. I would especially like to thank Ms. Emily McIntosh, my colleague, roommate and best friend for her unending support and for showing me the true value of friendship, which has only continued to strengthen over the course of our graduate studies.

Finally, I would like to thank all of my family and friends for their endless love and encouragement throughout this graduate program, I would not be who or where I am today without you guys. I would also like to give a special mention to Richad Hirani who I'm so appreciative to have in my life for his endless patience and support. And lastly, to the love of my life and furry companion, Nala, for always radiating happy and loving energy and for bringing so much joy into my life.

This graduate work was supported by Canadian Institutes of Health Research (CIHR) (Contract grant number: PJT152991) obtained by Dr. Baltz. I would also like to thank the financial support of the University of Ottawa Graduate and Postdoctoral Studies Admission Scholarship programs.

1.0 Introduction

1.1 Folliculogenesis and oogenesis

In female mammals, oogenesis begins during fetal development resulting in the formation of the ovum. Primordial germ cells (PGCs) undergo proliferation as they migrate to the developing gonads from the extraembryonic region (Coticchio et al., 2013). Once they reach the gonadal ridge, PGCs have differentiated into oogonia within the ovary. The female germ cells are stored within the ovary as primordial follicles, where a non-growing oocyte is arrested in meiotic prophase I surrounded by a single layer of flattened early granulosa cells (GCs), serving as the source for developing follicles and oocytes throughout a female's reproductive life. As primordial follicles are recruited into the growth phase, the GCs become cuboidal in shape and enclose the oocyte, forming the primary follicle (Eppig, 2001). Throughout fetal development, as the growth of the oocyte is occurring concomitantly with follicle growth, the oocyte will remain arrested in meiotic prophase I. Simultaneously, the oocyte begins to synthesize and secrete glycoproteins, forming a rigid extracellular coat surrounding the oocyte that is known as the zona pellucida (ZP). As the oocyte grows, the ZP also continues to increase in thickness. Following ZP formation, the oocyte maintains communication with the GCs via cytoplasmic processes called transzonal projections originating from the GCs that penetrate the ZP to form gap junctions that support the health of the growing oocyte during folliculogenesis (Alam & Miyano, 2019; Da Silva-Buttkus et al., 2008; Simon et al., 1997;Wassarman & Litscher, 2013;).

A primary follicle will transition into a preantral or secondary follicle as the oocyte grows, characterized by a great increase in oocyte size along with increased proliferation of the GCs that form multiple layers (Coticchio et al., 2013). The follicle will develop a distinct

layer of theca cells that form the outer layers of the follicle and are separated from the GCs by a basement membrane. Fluid begins to accumulate between the GCs, causing the follicle to swell by increased volume and fluid filled spaces form which coalesce into a single, large, fluid-filled cavity known as the follicular antrum (Hirshfield, 1991). These events mark the transition from pre-antral to early antral follicle. The follicles that are destined to become fully mature gain sensitivity to follicle stimulating hormone (FSH) that is released from the pituitary gland and binds to its receptors expressed in GCs, which induces continual proliferation and differentiation of GCs and supports oocyte growth. The formation of the antrum causes a division into two distinct cell types: cumulus cells directly surrounding the oocyte and mural granulosa cells (MGCs) lining the follicular wall (Salustri et al., 2004). At this stage the follicle is fully mature, also known as a Graafian follicle.

As the oocytes complete their growth phase, reaching a maximal size of ~75 - 85 μm (in mice), they acquire meiotic competence, wherein they gain the ability to progress beyond prophase I of meiosis (Demeestere et al., 2012; Wassarman et al., 1979). In response to luteinizing hormone (LH) from the pituitary gland that binds to its receptors in GCs, fully mature oocytes in the antral follicle will undergo meiotic maturation prior to ovulation, progressing through the first meiotic cycle. They then re-arrest at metaphase II until the point of fertilization (Eppig, 2001; Jamnongjit et al., 2005). In humans, typically a single dominant follicle will become activated to mature, undergoing ovulation into the oviduct, while the rest of the developing follicles will undergo atresia (Coticchio et al., 2013). In mice, during a natural cycle, 6 - 16 oocytes are stimulated to undergo ovulation, with variation dependent on strain (Silver, 1995).

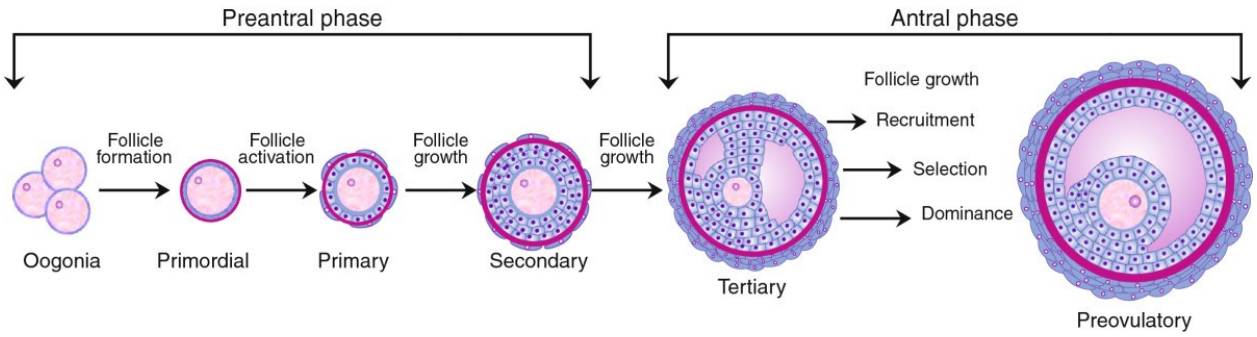

Figure 1: Folliculogenesis. Schematic sequence of follicular development, proceeding from the primordial follicle through to the antral follicle. The preantral phase begins with the formation and growth of primordial follicles which are surrounded by a single layer of flattened granulosa cells. It then leads to the formation of a primary follicle with cell layer becoming cuboidal in shape, and a secondary follicle cuboidal cells proliferate to form multiple layers. The antral phase consists of the formation of the tertiary follicle, where fluid begins to accumulate to form the cavity known as the follicular antrum. Follicle growth continues through the phases of recruitment, selection, dominance reaching the preovulatory stage, also known as the Graafian follicle. Light pink = oocyte, dark pink = basal membrane, light purple = granulosa cells, dark purple = theca cells. This image was used with permission from Araújo, V.R., Gastal, M. O., Figueiredo, J.R., & Gastal, E. L. (2014). In vitro culture of bovine preantral follicles: A review. *Reproductive Biology and Endocrinology: RB&E, 12, 78.*

1.2 Cell communication within the ovarian follicle

Throughout folliculogenesis, direct cell-cell communication by intercellular channels known as gap junctions allows for bi-directional signaling between the oocyte and the GCs. Gap junctions allow for the exchange of small metabolites (< 1 kDa), inorganic ions and second messengers (Bruzzone et al., 1996). Two adjacent cells are connected across their plasma membranes, with each cell contributing one half of a channel, known as a connexon, and thus the connection of the connexons forms a complete gap junction. Each connexon is made up of an oligomerization of protein subunits called connexins (CX), with six assembled together into a hexameric pore structure on each cell (Goodenough et al., 1996; Makowski et al., 1977). The two gap junction isoforms CX43 and CX37 are known to play a vital role in oogenesis. CX43 is responsible for forming a connection between GCs, with permeability decreasing in response to LH, while gap junctions that link the surrounding GCs to the oocyte are composed of CX37 (Norris et al., 2008; Simon et al., 1997). This functional syncytium provides the appropriate molecular signals and nutrients for oocyte growth and acquisition of developmental competence, and in turn supports follicular organization, proliferation and differentiation (Coticchio et al., 2013).

The other major form of communication between the oocyte and GCs is through paracrine signaling, wherein paracrine factors bind to and activate receptors on the opposite cell type. Oocyte derived paracrine factors, such as growth differentiation factor-9 (GDF-9) and bone morphogenic proteins (BMPs) BMP-15 and BMP-6 are some of the leading determinants of follicular development (Emori & Sugiura, 2014). Conversely, GC derived paracrine signaling via KIT/KITL leads to the activation of numerous intracellular signaling cascades that stimulate oocyte growth and development (Kidder & Vanderhyden, 2010).

1.3 Meiotic Arrest

Meiosis that begins during embryonic development arrests immature oocytes in late prophase until the time ovulation is triggered by a surge in LH. Meiosis resumes as LH acts on the GCs surrounding the oocyte (Dekel, 2005). For the resumption of meiosis, the activation of maturation- or M phase-promoting factor (MPF) is critical. The G_2/M regulator, MPF, is comprised of a complex with an enzymatic subunit, cyclin dependent kinase (CDK) 1 and a regulatory subunit, cyclin B (Eppig et al, 2004). In meiotically arrested oocytes, MPF is inactive due to reversible inhibitory phosphorylation of CDK1 resulting from the synthesis and maintenance of high levels of cyclic adenosine monophosphate (cAMP). High cAMP levels activate protein kinase A (PKA) which phosphorylates and activates the substrates WEE1 G2 Checkpoint Kinase (WEE1) and Membrane-Associated Tyrosine- And Threonine-Specific Cdc2-Inhibitory Kinase (PKMYT1, commonly called MYT1), responsible for the negative regulation of CDK1 through phosphorylation (Liu et al., 2013). In contrast, PKA phosphorylates and inhibits the cell division cycle 25 (CDC25) phosphatase on threonine (Thr)- 14 and tyrosine (Tyr)- 15 (Pan & Li, 2019). To maintain prophase I arrest, CDC25 must remain inactive to prevent the dephosphorylation and activation of CDK1 (Liu et al., 2013; Wigglesworth et al., 2013).

The synthesis of cAMP from its adenosine triphosphate (ATP) precursor is attributed to the constitutively active G-protein-coupled receptors (GPR) 3 and GPR12 (in mice) which activate the enzyme adenylyl cyclase (AC) at the oocyte plasma membrane (Liu et al., 2013). High levels of cAMP are maintained by inhibition of phosphodiesterase (PDE) 3A, which is responsible for the degradation of cAMP via hydrolysis (Norris et al., 2009) . The maintenance of PDE3A in an inactive state is dependent on high levels of cyclic guanosine monophosphate (cGMP) and also on its diffusion through gap junctions into the oocyte since

it is synthesized in the surrounding MGCs (Norris et al., 2009; Richard & Baltz, 2014). cGMP is produced from guanosine triphosphate (GTP) by the transmembrane guanylyl cyclase natriuretic peptide receptor 2 (NPR2) found on the membrane of cumulus granulosa cells (CGCs) (Robinson et al., 2012). The ligand natriuretic peptide precursor C (NPPC) produced in the MGCs exerts biological action by binding and activating NPR2 in the CGCs (Zhang et al., 2010). Thus, this series of steps results in high levels of cAMP and therefore maintains meiotic arrest.

1.4 Meiotic Resumption

The prophase-arrested oocyte is characterized by its clearly visible, large nucleus with a single nucleolus at its center, also referred to as the germinal vesicle (GV). At the time of ovulation, stimulated by an LH surge, the oocyte resumes meiosis I (MI) and within 1 - 3 hr the oocyte undergoes a disappearance of its nucleus and nucleolus as the nuclear envelope breaks down, which is known as germinal vesicle break down (GVBD). During growth, the oocyte acquires the ability to resume meiosis, also known as the acquisition of meiotic competence (Wassarman et al., 1979). Meiotic maturation involves the condensation of chromosomes, GVBD, meiotic spindle formation and extrusion of the first polar body. The oocyte then re-arrests at metaphase of the second meiotic division (MII) (Sorensen & Wassarman, 1976). However, mice oocytes that are <60μm in diameter are meiotically incompetent, remaining indefinitely arrested at prophase I, failing to undergo GVBD. This is likely due to the relative amounts of cell cycle components within the meiotically incompetent oocyte, wherein CDK1 is low, resulting in insufficient CDK1 to dimerize with

cyclin B1 and re-localize from the cytoplasm to the nucleus (Kanatsu-Shinohara et al., 2000; Solc et al., 2010).

Meiotic resumption is stimulated *in vivo* when LH binds to its receptors that are restricted exclusively to the MGCs. This induces the MGCs to produce and release the epidermal growth factor (EGF)-like growth factors epiregulin and amphiregulin, which bind to the EGF receptor (EGFR) located on the CGCs (Franciosi et al., 2014; Park et al., 2004). Consequently, EGFR undergoes autophosphorylation and activation of several signalling pathways, one of which includes mitogen-activated protein kinase (MAPK) signaling in the cumulus cells (Prochazka & Nemcova, 2019). The initiation of MAPK activity through EGFR kinase causes gap junction closure, through MAPK phosphorylation of connexin 43 (Norris et al., 2010). Simultaneously, LH acts to stimulate a decrease in cAMP concentrations in the oocyte, which in turn leads to the inactivation of the PKA pathway (van den Hurk & Zhao, 2005). Additionally, MAPK activation evokes upregulation of MPF activity through inhibition of MYT1, responsible for inhibitory phosphorylation of CDC25. The activation of CDC25 phosphatase catalyzes the dephosphorylation of CDK-1 at serine (Ser) -287 (van den Hurk & Zhao, 2005). Thus, this series of steps taken together are all essential requirements for meiotic resumption.

Prior to the LH surge, the concentration of cGMP is at a uniformly high level of ~2 - 4 μM. However, within 1 min of the LH surge, the decreased production of cGMP in the granulosa cells along with the activation of a cGMP-specific phosphodiesterase causes a decrease in cGMP concentration in the peripheral granulosa cells. As a result, cGMP diffuses out of the oocyte down its concentration gradient, such that by 20 min the cGMP concentration throughout the follicle is uniformly low at ~100nM. This rapid diffusion

occurs prior to the decrease in gap junction permeability, which occurs by 30 - 60 min post LH exposure (Shuhaibar et al., 2015).

Through steps that remain to be completely understood, the maintenance of low cGMP concentrations within the follicle occurs via decreased levels of follicular NPPC by a slower response of ~2 hr after LH receptor stimulation. It is known that the decrease in NPPC peptide is associated with a reduction of *Nppc* expression, which may occur in response to EGFR activation, and therefore, it is suggested that there is a possibility this may be responsible (Liu et al., 2013). The fall in NPPC is most likely too slow to account for the initial rapid decrease in cGMP, however it could play an important role in the maintenance of low levels of cGMP later. Following the loss of NPPC-stimulated production of cGMP, PDE3A is activated causing the hydrolysis and thus decreased levels of cAMP, leading to the re-initiation in meiosis.

LH acting on receptors on GCs rapidly decreases cGMP through two complementary pathways: the dephosphorylation and inactivation of NPR2 leading to decreased production of cGMP, along with cGMP hydrolysis through increased activation of PDE5. Independent of NPPC concentration decrease, NPR2 undergoes a rapid decrease in activity. This decrease is also not due to a decrease in NPR2 protein concentration, but rather is caused independently by the dephosphorylation of seven juxtamembrane Ser and Thr of NPR2 (Egbert et al., 2014; Shuhaibar et al., 2016). This dephosphorylation in turn leads to the inactivation of NPR2, reducing the production of cGMP. In mice, there are several phosphodiesterases responsible for hydrolyzing cGMP, however PDE5 is of particular interest as its activity is increased by phosphorylation by PKA but is independent of EGFR kinase activity (Egbert et al., 2014; Egbert et al., 2016; Robinson et al., 2012). Therefore, the

activation through phosphorylation of PDE5, along with the dephosphorylation and inactivation of NPR2, together lower the levels of cGMP in the follicle in response to LH.

Meiotic resumption in the oocyte in response to LH is comprised of various complex processes, with some steps of the mechanisms that remain unknown. Further research is required to elucidate these many components of signaling pathways to completely understand what is needed for the oocyte to achieve developmental competence.

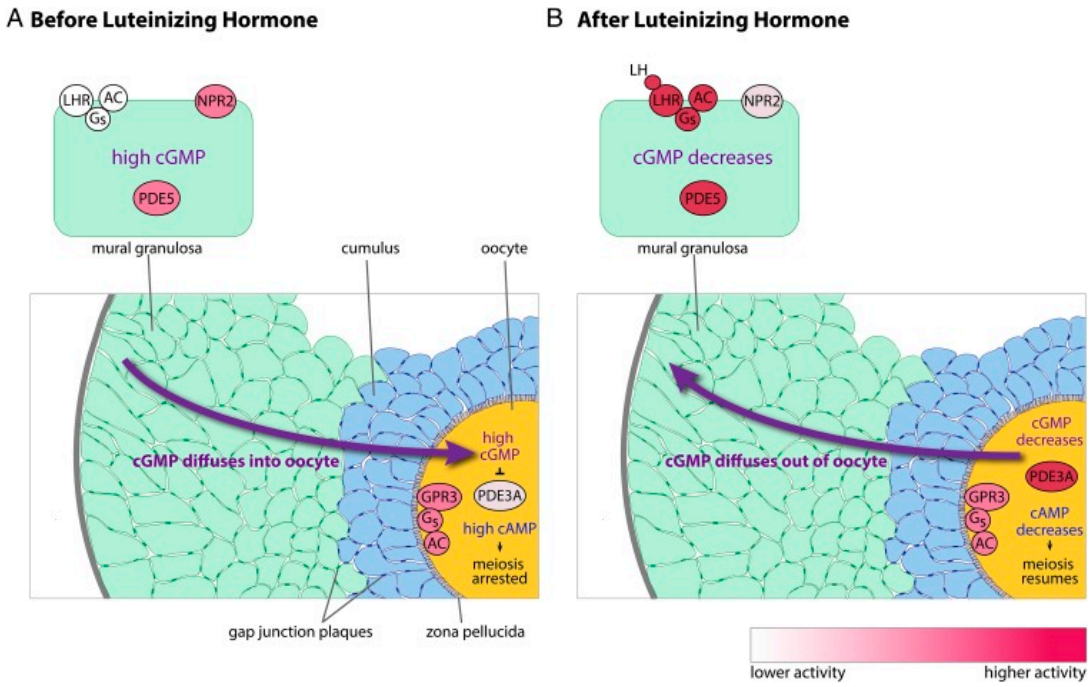

Figure 2: Meiotic arrest and resumption. (A) Prior to surge, meiotic arrest is maintained by high levels cAMP in the oocyte produced by GPR3 in the oocyte that is constitutively active. An elevated concentration of cAMP within the oocyte is maintained due to the inhibition of the phosphodiesterase PDE3A responsible for the hydrolysis of cAMP. The activity of PDE3A is inhibited via cGMP which is produced at high rates through the binding NPPC from the mural granulosa cells to its NPR2 receptor. cGMP diffuses through gap junctions to the oocyte to thus maintain meiotic arrest in the oocyte. **(B)** Upon the surge in LH, as it binds to its receptors on the mural granulosa cells, cGMP levels decrease due to NPR2 activity and an increase in PDE5 activity. Since levels of cGMP are low within the follicle cells, levels within the oocyte follow an outward diffusion, reaching a uniformly low level throughout the entire follicle. This leads to the activation of PDE3A which hydrolyzes cAMP. The low level of cAMP in the oocyte thus causes meiosis to resume. This image was obtained with permission from: Shuhaibar L.C., Egbert J.R., Norris, R.P., Lampe P.D.,

Nikolaev V.O., Thunemann M., Wen L., Feil R., and Jaffe L.A. (2015). Intercellular signaling via cyclic GMP diffusion through gap junctions restarts meiosis in mouse ovarian follicles. PNAS; 112:5527-5532.

1.5 Ovulation

Ovulation is the rupture of the antral follicle, with release of the cumulus oocyte complex (COC) into the oviduct, where it has the potential to become fertilized. Toward mid-cycle, ovulation is induced by a surge in LH (and FSH) that is synthesized and secreted by the anterior pituitary gland. This results in the activation of numerous signaling cascades, while affecting all cell types of the ovarian follicle. LH induces meiotic maturation (as discussed above), with the release of the oocyte from prophase of the first meiosis with the progression through to metaphase of second metaphase, where it re-arrests as a mature egg (Eppig, 1996; Eppig et al., 2004; Wassarman et al., 1979).

LH signaling action is restricted to the receptors on the surrounding MGCs, as neither the CGCs nor the oocyte express the required LH receptors. Consequently, they rely on transfer of signals and intracellular mediators from the MGCs via gap junctions to relay the ovulatory response (Park et al., 2004). The activation of one of the major signaling pathways involves the release of EGF which stimulates intracellular signaling and changes in gene expression in the CGCs, leading to hyaluronic acid secretion and expansion of the cumulus cells or mucification.

Mucification of the COC is essential for oocyte extrusion from the follicle, to undergo successful ovulation and hence fertility for subsequent development of the zygote. The process of mucification commences when FSH stimulates the CGCs of the COC to synthesize hyaluronic acid (HA), an important macromolecule contributing to the make-up of the extracellular matrix (Nagyová et al., 2000). Among the CGCs, HA is secreted to embed them in an expansive gelatinous matrix (Chen et al., 1993; Fülöp et al., 2003; Salustri et al., 1992; Vanderhyden et al., 1990). Another major player in cumulus expansion is the oocyte, which releases soluble factors known as cumulus expansion-enabling factors

(CEEFs) necessary to induce HA synthesis through the transcription of the main enzyme Hyaluronan synthase (Has) 2 (Richards, 2005). Oocytes acquire the ability to secrete these factors during their growth period. They are secreted as they undergo GVBD to become mature eggs, with the capability lost following fertilization. Although the identities of these CEEFs remain unknown, previous evidence suggests that a likely candidate is GDF-9 (Nagyová et al., 2000).

1.6 Development of culture media for growing and maturing oocytes and embryos *in vitro*

Considerable progress has been made over the years, with significant work done in the past to develop and optimize culture media suitable for the complete development of preimplantation embryos through to the blastocyst stage in *in vitro* environments, playing a major role in the treatment of infertility. For over a century, numerous modifications were made to improve culture media such as varying the energy sources, osmolarity, pH and amino acid composition to correct for the numerous conditions that resulted in incomplete embryo development. Eventually, these various experimental contributions led to the first successful human embryo *in vitro* fertilization (IVF). Embryo culture and transfer resulting in a live birth was accomplished, as reported by Steptoe and Edwards in 1978 (Steptoe & Edwards, 1978).

Early attempts to culture embryos *in vitro* were performed in a variety of different solutions. The first attempts that were largely unsuccessful began with embryo culture done in undefined complex biological fluids, such as blood plasma and serum (Alexandre, 2001). It was later discovered that preimplantation embryonic development could be achieved *in vitro* when specific stages of embryos were culture in simple balanced salt solutions such as

Krebs-Ringer, Tyrode's and Gey's (Adams, 1956; Brinster, 1963). Upon modification to Krebs-Ringer solution, the first major breakthrough was accomplished by the addition of serum albumin and glucose to the balanced salt solution, permitting successful *in vitro* culture for 8-cell mouse embryos to develop to viable blastocysts (Whitten, 1956). However, this medium was unfortunately still inadequate for culture as it did not support development at earlier stages (McLaren & Biggers, 1958). The range of preimplantation (PI) embryo stages supported in *in vitro* culture was extended from the 2-cell stage embryos to blastocyst through the addition of lactate as a metabolic substrate (Whitten, 1957), though it still did not permit fertilized oocyte cleavage. Lastly, pyruvate was the crucial addition that allowed for support of the earliest stage oocyte development through to the 2-cell stage (Biggers et al., 1967). These findings eventually led to the development of the classic mouse embryo culture medium known as M16 (Whittingham, 1971) that was commonly used for numerous years, with this medium being comparable to contemporary human embryo culture medium.

1.7 Culture media inflicted "2-cell block" and the changes required to overcome it

Through to the 1980s, the development of an optimized culture medium remained a major research focus for the purpose of overcoming the reoccurring fundamental problem of developmental blocks in PI embryos. In mice, the cessation of development occurred as an arrest in late G_2 stage of the second embryonic cell cycle that was not due to cell death. (Goddard & Pratt, 1983). Advances in the improvement of embryo culture media transpired through contributions from the National Cooperative Program on Non-Human In Vitro Fertilization and Preimplantation Development, funded by the US National Institute of Child Health and Human Development of the National Institutes of Health (NIH) which led to the

production of two widely used successful media, CZB (Chatot Ziomek Bavister embryo culture medium) (Chatot et al., 1989) and KSOM (potassium supplemented Simplex Optimized Medium for embryo culture) (Lawitts & Biggers, 1991). The key features of these media that eliminated the developmental block in mouse embryos at the 2-cell stage (and similar developmental blocks in other species) were the decrease in osmolarity, as well as the inclusion of amino acids, such as glutamine, which more completely supported volume regulatory requirements of the oocyte and early embryo (Van Winkle et al., 1990; Lawitts & Biggers, 1992).

Decreasing the osmolarity of media was found to be one of the major changes that prevented arrest in embryo development. The fluid of the mouse oviduct ranges between 300 - 310 mOsM (Collins & Baltz, 1999), while CZB and KSOM have substantially lower osmolarities of 275 mOsM and 250 mOsM respectively (Baltz, 2013; Lawitts & Biggers, 1993). In contrast, the medium known as Whittingham's M16 which was previously the standard medium to culture mouse embryos (Whittingham, 1971), had an osmolarity closer to physiological range with an osmolarity of 290 mOsM. Accordingly, this medium did not allow for the development of fertilized eggs through to the blastocyst stage, but instead suffered from the 2-cell block (Hogan et al., 1994). As a result, experiments were conducted to test the hypothesis that early stages of PI embryos were sensitive to increased osmolarity. This was accomplished by raising the osmolarity of KSOM culture media either through raising the concentration of NaCl or adding the inert trisaccharide raffinose, with results demonstrating a block at the 2-cell stage once again (Lawitts & Biggers, 1992; Hadi et al., 2005).

Early PI embryos are very sensitive to increased osmolarities such that high osmolarity media led to a decrease in cell volume — cell shrinkage. However, when organic

compounds such as glutamine, betaine and glycine were present in media with high osmolarity, oocytes and early PI survival and development was enhanced (Biggers et al., 1993; Lawitts & Biggers, 1992; Van Winkle et al., 1990). These compounds were found to act as organic osmolytes – organic molecules that are uncharged and small in size, with the ability to osmotically support cells without disturbing physiology (Hoffmann et al., 2009; Lang et al., 1998;). Early embryos are extremely sensitive to small increases in osmolarity in an *in vitro* environment and this exemplifies how critical volume regulation is for development as discussed below.

1.8 Osmolarity, osmolality, tonicity and molarity

Osmosis is the net movement of water across a semipermeable membrane, controlled by a concentration gradient where the water flows from a lower towards a higher solute concentration in order to equalize the concentration of both sides (Strange, 2004). Osmolarity is the measure of solute concentration, expressed as osmoles per liter (OsM). Osmolality is also a measure of osmotic strength of a solution but measured in osmoles per kilogram. However, for dilute solutions such as most that are physiologically relevant, the difference between the two measures is insignificant and thus they can be used interchangeably (Baltz, 2001). Molarity is the number of moles of solute concentration per litre of solution. It is important to note that molarity and osmolarity are often not equal. Osmolarity takes into account solute dissociation in solutions while molarity does not. In solutions with non-ionic solutes that do not dissociate or interact, molarity and osmolarity will be equivalent. Whereas ionic compounds, such as NaCl (1 mole) would dissociate into two individual ions in water (2 osmoles). Tonicity, in contrast, is context specific. It

measures the osmotic pressure exerted on a semi-permeable membrane, accounting for the pressure exerted by solutes that are unable to cross the membrane. The semi-permeable membrane of the cell allows water to pass freely through aquaporin channels, while inhibiting the transport of most solutes. However, some solutes that are small, hydrophobic, non-polar or polar but uncharged, are able to freely diffuse across the membrane (Cooper, 2000), and thus do not have an effect on tonicity.

1.9 Cell volume responses to changes in tonicity

The water flux across a cell membrane is driven by the osmotic gradient between the intracellular and extracellular environment. When there is no difference between environments (i.e., they are isotonic) and thus no net flow of water in or out of the cell, the volume remains stable and the cell is in homeostasis. Any deviations in the external (or internal) solution concentration will cause the cell to change volume through water loss or gain (Lang et al., 1998). When a cell is exposed to a low tonicity solution, the water will influx into the cell, resulting in cell swelling. In contrast, when placed in a high tonicity solution, cells will undergo shrinkage as the water effluxes from the cell.

The function and survival of cells are extremely dependent on the ability to regulate their own volume, with changes influencing physiological processes such as cell migration, proliferation and cell death. These cell functions are influenced by changes in cell volume macromolecular crowding, alterations in intracellular ionic strength, and changes in the mechanical and chemical properties of the lipid bilayer (Hoffmann et al., 2009). In somatic cells, two main pathways are initiated in response to hypertonicity that both fall under activation through MAP kinase cascades, which include activation of the p38 family and

SAPK/JNK pathway (Hoffmann et al., 2009; Sheikh-Hamad & Gustin, 2004). Both of these pathways are also present in preimplantation embryos as the ability to sense and respond to osmotic stress induced by the osmolarity of their environment is of great importance (Fong et al., 2007; Natale et al., 2004). This is especially critical in the case of hypertonicity induced cell volume decrease that leads to developmental arrest in embryos. Thus, if left unchecked, these alterations in cell volume would eventually lead to disruption in metabolic and enzymatic activities required for cell function and ultimately lead to cell stress, eventually becoming lethal (Mongin & Orlov, 2001). Correspondingly, to regain equilibrium, cells have developed mechanisms to sense and counter the perturbations to their cell volume. The cellular response to a loss in volume from a hypertonic environment is to increase inorganic ion transport into the cell, inducing water influx to increase cell volume. The mechanism for restoration of cell volume under these conditions is referred to as regulatory volume increase (RVI). In turn, when cells swell in a hypotonic environment, they will activate a volume regulatory mechanism that includes the release of nonessential organic osmolytes and ions to induce water efflux known as regulatory volume decrease (RVD).

1.10 Cell volume regulation with acute recovery: inorganic ions

Cells are consistently working to balance their intracellular osmolarity with their external environment as imbalances occur. Fluctuations in solute concentrations expose cells to hypo- or hypertonic conditions causing cells to respond by rapid swelling or shrinking, respectively. Over the long term, this state of stress can lead to cell damage such as disruption of the cell cycle and eventually become fatal. Consequently, cells have developed membrane transport mechanisms to respond to perturbations in cell volume so as to return to

homeostasis. One way in which cells correct acute decreases in cell volume is through a coupled exchange of inorganic ions along with osmotically driven influx of water to increase cell volume (Hoffmann et al., 2009). This is primarily mediated via the membrane proteins NHE1 and AE2. The SLC9 family member, NHE1, regulates the influx of one Na^+ ion per H^+ ion effluxed, causing an increase in intracellular pH due to the H^+ efflux (Orlowski & Grinstein, 2004). AE2, the SLC4 family anion exchanger, activated via the pH increase, mediates the passage of one Cl^- ion into the cell coinciding with the discharge of HCO_3^-, resulting in no net change in pH when coupled with NHE1 activity, since H^+ and HCO_3^- neutralize each other (Orlowski & Grinstein, 1997). The activation of this coupled exchange rapidly restores cell volume through the accumulation of Na^+ and Cl^-, without a net effect on pH. However, over the long term, substantial increases of intracellular ionic strength can be detrimental (Yancey et al., 1982).

1.11 Cell volume regulation with long-term homeostasis: organic osmolytes

The influx of inorganic ions is an effective mechanism for quick recovery from acute decreases in cell volume. However, ion accumulation and thus increased ionic strength within the cell disrupts and alters protein structure in turn affecting protein function, membrane potential and metabolism (Lang et al., 1998). Cells thus respond by accumulating small, uncharged, organic compounds, replacing a portion of the intracellular inorganic ions. These organic osmolytes are able to provide osmotic support over a large range of concentrations without compromising cellular biochemistry (Yancey et al., 1982). Many different types of organic osmolytes are transported from the external environment by their corresponding organic osmolyte transporter. Organic osmolytes utilized by cells for osmotic

support include the polyalcohols sorbitol and inositol, glycerophosphorylcholine, and amino acids such as glutamine, glycine, proline, taurine and betaine, as well as some of their derivatives (Baltz, 2001; Lang et al., 1998). Of these organic osmolytes, glycine has been found to play a critical role in osmoregulation in early embryos, with an excellent ability at protecting successful development of an unfertilized eggs through to the 2-cell stage embryos in the presence of increased salt concentration or osmolarity (Hadi et al., 2005 ;Van Winkle et al., 1990).

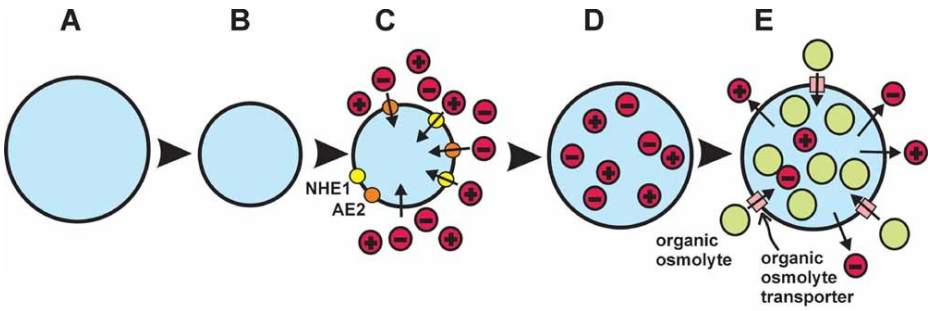

Figure 3: Cell volume regulatory mechanisms. When a cell **(a)** decreases in cell volume **(b)**, it will respond by accumulating inorganic ions as a form of acute recovery. A common mechanism for this is the activation of Na^+/H^+ exchanger NHE1coupled with HCO_3^-/Cl^- exchanger AE2 **(c)**. The accumulation of Na^+ and Cl^- into the cell increases the intracellular osmolarity, allowing for the cell to return to normal size **(d)**. In some cells, such as the mammalian oocyte, the increased ionic strength of the cell is, however, detrimental over the long term. This led to some cells evolving the ability to accumulate organic osmolytes, via specific transporters to replace a portion of the inorganic ions in the cell while still maintaining intracellular osmolarity **(e)**. This image was adapted with permission from (Baltz & Zhou, 2012).

1.12 Glycine as an organic osmolyte

Glycine is the simplest stable amino acid obtainable through hydrolysis of proteins. Glycine was one of the first amino acids to be discovered (in 1820) and was isolated from gelatin. Glycine does not need to be acquired through food and is therefore one of several non-essential amino acids as it can be biosynthesized in the body from serine and threonine (Razak et al., 2017). At physiological pH, glycine exists as a zwitterion possessing both an acidic and basic functional group and thus contains a net charge of zero.

Glycine has shown to be an extremely effective osmoprotectant for embryos against increases in osmolarity (Hadi et al., 2005; Van Winkle et al., 1990). In the presence of glycine, one cell embryos are able to develop through the 2-cell stage, avoiding the 2-cell block, in media increased by as much as 70 mOsM more hypertonic (Hadi et al., 2005). Consistent with this, osmolarity increased to levels similar to those found in the oviduct (~300 mOsM) were able to sustain *in vitro* embryo culture through to the blastocyst stage when 1mM glycine was added to culture media but not without (Dawson & Baltz, 1997; Hadi et al., 2005; Van Winkle et al., 1990). Additionally, the amount of intracellular glycine oocytes and embryos accumulate varies proportionally with the external osmolarity (Dawson et al., 1998; Steeves et al., 2003).

Glycine is accumulated to high levels in early embryos *in vivo* as it is very abundant in their environment. The levels of glycine in oviductal fluid range from 0.5 - 3.0 mM (Guérin et al., 1995; Harris et al., 2005) and glycine is thus available in an amount sufficient for osmoprotection as the half-maximally effective external concentration of glycine is about 50 μM (Hammer & Baltz, 2002). Levels of endogenous glycine are very low within GV

oocytes and MI eggs, however as they gain the ability to regulate their cell volume and glycine transport is activated, the levels of freely soluble glycine start to accumulate reaching high levels in eggs and early PI embryos, with concentrations ranging from ~4 - 10 pmoles in MII eggs, 1 cell and 2 cell embryos. However, the amount of glycine starts to decrease over subsequent preimplantation development. As the morulae and blastocyst stages are reached, levels decrease to 0.1 - 0.3 pmoles (Schultz et al., 1981; Tartia et al., 2009; Van Winkle & Dickinson, 1995). The transport of glycine into oocytes and PI embryos has been shown to occur predominantly via the GLYT1 transporter.

1.13 The glycine transporter GLYT1

The transport of glycine occurs via two glycine transporters (GLYT): GLYT1 and GLYT2, encoded by the *Slc6a9* gene and *Slc6a5* gene respectively. GLYT1 and GLYT2 belong to the family of high affinity Na^+/Cl^--dependent neurotransmitter transporters (NTT) or solute carrier 6 (SLC6) family (Kristensen et al., 2011). This family includes additional transporters for GABA, monoamines neurotransmitters: serotonin, dopamine, and norepinephrine, and the amino acids betaine, proline and taurine (Kristensen et al., 2011) . GLYT1 and GLYT2 are both transmembrane proteins, sharing ~50 % homology in their amino acid sequence, with variation found mainly in the N-terminus (Aragón & López-Corcuera, 2003; Eulenburg et al., 2005). Despite the conservation in sequence between these two transporters and their involvement in the regulation of synaptic glycine concentrations for neurotransmission, there remains clear differences in their function, transport mechanism, and cellular distribution (Supplisson & Bergman, 1997). GLYT2 is unable to transport sarcosine (López-Corcuera et al., 1991) and its expression is restricted to glycinergic neurons

in the brainstem, spinal cord and cerebellum (Zafra & Giménez, 2008). GLYT1 is expressed in glia where it mediates the reuptake of glycine, but is also expressed outside of the central nervous system (CNS), and can transport sarcosine with high affinity (Borowsky et al., 1993).

Due to GLYT1's function as a neurotransmitter reuptake transporter at synapses in the brain, extensive pharmaceutical studies have been conducted to develop specific GLYT1 inhibitors to treat schizophrenia (Aroeira et al., 2014). These inhibitors have allowed for a better understanding of the function GLYT1 in glycine transport in the brain but also in cell volume regulation. Previously in our lab, a highly selective inhibitor for GLYT1 known as ORG23798 was used to demonstrate that glycine transport in PI mouse embryos occurs via GLYT1. The inhibition of GLYT1 blocked glycine transport in cleavage stage embryos, eliminating the developmental support provided by glycine through its osmoprotective effects when osmolarity is increased (Steeves et al., 2003; Tartia et al., 2009). GLYT1 thus plays an important role in intracellular osmotic support, maintaining cell volume homeostasis and thus healthy, normal sized oocytes and early embryos (Dawson & Baltz, 1997; Steeves et al., 2003; Van Winkle et al., 1990). However, the mechanism by which GLYT1 is activated remains unknown. As this method of volume regulation is of particular importance to oocyte and preimplantation embryos, further understanding is required.

The activity of the glycine transporter GLYT1 is low in mature preovulatory oocytes in meiotic prophase I, and GV oocytes. Once ovulation is triggered *in vivo* or oocytes are mechanically removed from the ovarian follicle, the oocyte resumes meiotic maturation, undergoing GVBD, and at such time GLYT1 activity will initiate, with the upregulation of the transport of glycine occurring at a similar time course to GVBD. Although GLYT1 activation and meiotic progression are taking place at the same time, these processes

nonetheless are not coupled, as GLYT1 activation still occurred when meiotic progression was inhibited, maintaining oocytes in GV arrest (Tartia et al., 2009). Within several hours following the initiation of meiotic maturation, the activity of GLYT1 continues to rise, with large amounts of free glycine correspondingly accumulated, reaching maximal transport by 4 - 5 hours. The activation of GLYT1 seems to occur *in vivo* as well since GV oocytes present undetectable levels however MII eggs matured in vivo have similar levels of glycine found in a 1-cell embryo, indicating that glycine utilized for cell volume regulation is accumulated after ovulation is triggered (Tartia et al., 2009). In early PI mouse embryogenesis, the activity of GLYT1 and glycine accumulation are maximal at the 1- and 2- cell stages and persist through to the 4-cell stage. However, GLYT1 activity is restricted to cleavage stage embryos before compaction, with levels gradually declining to extremely low levels in 8-cell embryos and becoming completely inactive by the blastocyst stage (Tartia et al., 2009; Van Winkle et al., 1988).

The osmoprotection of embryos through GLYT1 activity is essential against increased osmolarity. It was found that when early cleavage stage embryos were transferred from 250 to 350 mOsM culture medium, GLYT1-mediated glycine uptake occurred immediately, without any delay (Steeves et al., 2003). This differs in contrast to previously described mammalian organic osmolyte transporters which respond to increased osmolarity with a lag time of hours or days (Garcia-Perez & Burg, 1991; Kwon & Handler, 1995; Pastor-Anglada et al., 1996). This indicates that the activity of GLYT1 occurs independently of protein synthesis, which requires a longer period of time. This was further confirmed when culturing 1-cell embryos with cycloheximide, an inhibitor of protein synthesis, which resulted in no effects on glycine accumulation (Steeves et al., 2003). As protein synthesis was not necessary, it was of interest to determine the time during oogenesis that GLYT1 is

first expressed and when activation can first occur. Upon investigation by previous lab members, it was found that *Slc6a9a* mRNA expression was detectable in growing mouse oocytes as early as post-natal day (P) 5 and continued to increase throughout oogenesis (Richard et al., 2017). Although two isoforms for *Slc6a9* exist in rodents, the *Slc6a9b* isoform was not identified throughout any stage of oogenesis while *Slc6a9a* was present (Guastella et al., 1992; Richard et al., 2017). Furthermore, SLC6A9 protein synthesis increased during oogenesis with expression detected as early as P11 and a maximum level reached by P21. As SLC6A9 is being synthesized, it simultaneously localizes to the periphery of the oocyte and embeds into the plasma membrane as a transmembrane protein. This localization to the plasma membrane concurs with the oocyte's development of the capacity for GLYT1 activation (Richard et al., 2017). For mature oocytes from adult ovaries, the activity of GLYT1 occurs once the oocyte has acquired meiotic competence and similarly for neonatal oocytes which occurs as the oocyte reaches ~65 - 70 μm in diameter. Therefore, in each case, the ability for oocytes to independently control their own cell volume occurs once oocytes have grown to nearly full size and have acquired meiotic competence (Richard et al., 2017).

In addition to glycine accumulation, oocytes require the ability to release intracellular glycine as a response to severe increases in cell volume. To counteract volume increase and prevent swelling-induced bursting, mammalian cells have developed a key regulatory volume decrease mechanism through volume-regulated anion channels (VRAC) which activate and open within seconds upon osmotic swelling, reaching maximal activity within several minutes. VRACs are made up of LRRC8 proteins, with LRRC8A also known as SWELL1 being one of the essential subunits to combine with any of its paralogs (LRRC8B-E) to form a heteromeric complex (König & Stauber, 2019). These channels are permeable to

several organic osmolytes and allow for a controlled efflux of ions, organic osmolytes and osmotically driven water from the cell (Deneka et al., 2018). Upon the efflux of an anion such as Cl^- via VRAC, there is cation coupling with the release of K^+ via K^+ channels (Hoffmann et al., 2009). Therefore, cell swelling recovery is mediated through KCl efflux via coupled channels together with the release of organic osmolytes through VRAC. This efflux balanced with the influx of glycine via the GLYT1 transporter and NaCl influx via NHE1 and AE2 allows for cells to control their size, maintaining homeostasis.

1.14 Cell volume regulation prior to ovulation: oocyte-zona pellucida adhesion

Prior to the LH surge that triggers ovulation, before cell volume control occurs through the transport of glycine, oocytes are unable to independently control their own volume. Instead, oocyte volume is determined by its strong adhesion to the extracellular coat, the ZP (Tartia et al., 2009). Shortly following ovulation, the oocyte progressively loses its adhesion to the ZP and as this occurs the oocyte decreases in cell volume, concurrently forming a space between the inner surface of the ZP and the oocyte surface, forming the perivitelline space (PVS) (Dandekar & Talbot, 1992; Inoue et al., 2007). It had previously been thought that the development of the PVS occurred as a result of a decrease in oocyte cell volume as the first polar body is released through transition to the MII phase, however it was shown in our laboratory that this was not truly the case. In reality, the large majority of the cell volume decrease occurred as the oocyte entered into the MI phase, prior to emission of the first polar body (Tartia et al., 2009). By this time, GLYT1 is completely active, with activation occurring with a similar time course to oocyte-ZP detachment (Tartia et al., 2009). Thus, the initiation of independent cell volume regulation involves two distinct processes

that are completed within several hours following the triggering of ovulation: detachment of the ZP from the oocyte and the activation of GLYT1 (Tartia et al., 2009).

1.15 ZP composition and role

The ZP is a thick and rigid extracellular matrix surrounding the mammalian oocyte and early PI embryos, with the protein content (~1 - 30 ng) and thickness (~1 - 25 μm) varying significantly between species (Wassarman, 1988). The ZP is made up of three glycoproteins known as ZP1, ZP2 and ZP3, with a fourth ZP protein (ZP4) found in humans and many other mammalian species. All ZP glycoproteins (ZPGs) share common features in the makeup of their polypeptide chain which include: an N-terminal signal sequence, large bipartite ZP domains (ZPD) which consists of ~270aa with 8 conserved cysteine residues, two subdomains known as a N-terminal subdomain (NTS) and a C-terminal subdomain (CTS), and a C-terminal propeptide (CTP), with transmembrane domain (TMD). These glycoproteins are held together through noncovalent bonds and although the ZP is tough and rigid, it is also quite porous, allowing for the passage of various macromolecules including enzymes, antibodies and small viruses (Wassarman, 1988; Wassarman & Litscher, 2021). Furthermore, the oocyte remains tightly adhered to the ZP transmembrane proteins by oocyte microvilli extending into the zona matrix, along with a connection to the oocyte through transzonal projections (TZPs) that extend through the ZP from the surrounding cumulus cells (Baena & Terasaki, 2019; Gilula et al., 1978; Tartia et al., 2009).

The ZP has many different roles, with one of great importance being the regulation of interactions between the spermatozoa and egg during fertilization. The ZP is responsible for modulating oocyte-sperm binding through the ZP3 glycoprotein, while inducing bound

sperm to undergo an exocytotic event, known as the acrosomal reaction. Once the sperm is bound, the ZP acts as a barrier for the fertilized egg to prevent polyspermy from taking place (Bleil & Wassarman, 1980; Wassarman, 2005; Wassarman, 2008). Additionally, the ZP plays an essential role as a barrier prior to implantation and influences oogenesis through control of communication between the oocyte and its surrounding follicle cells (Wassarman et al., 1999). Additionally, each individual ZPG plays a critical role in the make-up of the ZP, and thus, any gene mutations leading to protein inactivation causes detrimental effects on both the ZP formation and female fertility (Liu et al., 1996; Rankin et al., 1996; Rankin et al., 1999; Rankin et al., 2001).

1.16 Synthesis, secretion and assembly

As the oocyte grows, the ZP is concurrently increasing in size and thickness, with formation complete as the oocyte reaches full growth at ~80 μm in diameter. For example, during oocyte growth as the rate of ZPG synthesis largely increases, the glycoprotein ZP3 increases in mRNA transcripts copies from previously undetectable levels, up to levels reaching as high as ~300,000 copies as the oocyte reaches mid-growth. This is followed by a drastic drop in copies to almost undetectable levels as the stage of the unfertilized egg is reached. Simultaneously, ZPGs are being synthesized and packaged in secretory vesicles to transport the nascent protein to the plasma membrane of the oocyte for formation of the ZP from the innermost surface outward, with the earliest synthesized layers at the periphery (Wassarman, 1988). These proteins initially exist in a transmembrane form, which will eventually be cleaved for incorporation into the matrix. The cleavage is likely accomplished by a peptidase that acts a secretase or sheddase located at the oocyte surface, with the

location of cleavage being at or near a well-conserved furin site just distal to the TMD, leading to the release of the CTP ectodomain. It has been proposed previously in the literature that a furin or another related convertase could be the possible candidate peptidase responsible for this cleavage, however this remains controversial and further studies are required to elucidate the unknown mechanism of ZPG secretion and assembly that follows ZPG biosynthesis (Litscher et al., 1999; Williams & Wassarman, 2001; Zhao et al., 2002).

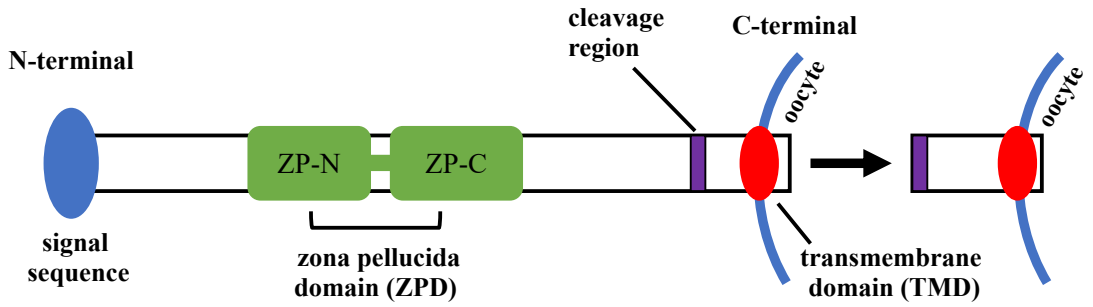

Figure 4: The structure of a zona pellucida glycoprotein (ZPG). The structure of glycoproteins that make up the rigid extracellular ZP have been highly conserved in mammals over many years. In mice and humans, the glycoproteins are synthesized as precursor polypeptides and their structure includes an N-terminal signal sequence, a bipartite ZP domain (ZPD) which contains an N-terminal subdomain (also known as ZP-N) and a C-terminal subdomain (also known as ZP-C), and a transmembrane domain of the C-terminal propeptide (CTP). The cleavage region is the area responsible for releasing the transmembrane domain by an unknown protease, allowing for the secretion of ZPGs and assembling to form the ZP. This was adapted based on a figure in (Zhao et al., 2003).

1.17 Metalloproteases

Of the four main types of proteases, the metalloproteases (MP) are the most diverse, with the general family of MPs including matrix metalloproteinases (MMPs), a disintegrin and metalloproteases (ADAMs), and a disintegrin and metalloproteinase with thrombospondin motifs (ADAMTSs) (Przemyslaw et al., 2013). These subfamilies of MPs are all endopeptidases classified based on their main shared structural feature of having three highly conserved histidines that ligate a zinc atom (Zn^{2+}) in the active site of their catalytic domain (Cui et al., 2017). Their function primarily involves the degradation and thus regulation of the various components making up the extracellular matrix (ECM).

The MMP subfamily comprises a multitude of enzymes, and although their catalytic domains are structurally very similar, they are functionally very different due to characteristics such as cellular localization, substrate preference, whether they are secreted or membrane bound, and structural domain organization (Raeeszadeh-Sarmazdeh et al., 2020;Yong et al., 2001). Currently, 23 distinct MMPs are known in humans and 24 in mice (Klein & Bischoff, 2011). The first discovered MMP, known as MMP-1 or collagenase-1, was identified in 1962 through the observation of collagen degradation in tadpole embryogenesis (Gross & Lapiere, 1962). MMPs play a role in numerous biological functions, some of which include cell proliferation, differentiation, apoptosis, angiogenesis and immune function (Galliera et al., 2015). As these enzymes play a role in cell function, with capabilities of extensive destruction, their activity is highly regulated. MMP regulation begins at the level of transcription, as MMPs are not continually expressed and their ability to be transcribed depends on cell activation. The second level of regulation occurs post-

translation, wherein MMPs are produced as biologically inactive zymogens due to the zinc ion in their active site bound by a cysteine residue of the pro-domain. Thus, disruption of the cysteine and zinc interaction requires proteolytic removal of their pro-domain by activating factors. The last means of control for MMP activity is through inhibition via direct interaction with their natural inhibitor known as tissue inhibitors of metalloproteinases (TIMPs) (Galliera et al., 2015; Yong et al., 2001).

ADAMs are integral membrane glycoprotein, with a few exceptions, that are typically bound through a C-terminal transmembrane segment (Andreini et al., 2005; Porter et al., 2005). They are responsible for cleaving other proteins anchored in the membrane leading to their release from the cell surface, while also affecting their function. To date there have been 30 ADAMs identified, half of which contain a catalytic site consensus sequence and are thus considered to be catalytically active, while the other half mainly function as modulators in cell-matrix or cell-cell interactions (Blobel & Apte, 2006). ADAMTSs are secreted proteases, thereafter either bind extracellular matrix components, or attach to the cell surface. Both ADAM and ADAMTS proteins are composed of a multidomain structure, with initial synthesis as a zymogen, with most but not all, cleaved by furin to become activated either within the secretory pathway or at the cell surface. All ADAMs that are catalytically active contain a pro-domain in their structure. This helps with folding of the metalloprotease domain in the endoplasmic reticulum (ER), keeping it inactive until the point at which the pro-domain is cleaved. Following cleaving of the pro-domain, the catalytic activity of ADAMs is regulated by additional mechanisms such as phosphatase inhibitors, calcium and activation of G-protein coupled receptors (Blobel & Apte, 2006). ADAMTSs are structurally and evolutionarily related to ADAM enzymes, as well as more distantly related to MMP enzymes. Upon discovering ADAMTS1, it was initially thought to be a

variant of ADAM. Soon afterward, as all 19 ADAMTS were discovered, it was found that they all share a common structural characteristic of a central thrombospondin type 1 sequence repeat (TSR) motif found within the distinct C-terminal ancillary domain. Moreover, the number of TSRs present within the domain varies from 0 (ADAMTS4) to 14 (ADAMTS9 and 20) (Blobel & Apte, 2006). Despite the ADAM's and ADAMTS's many similarities in structure, they individually possess a lot of variability in their motifs and structure which influence their substrate specificity, localization and interaction partners. Furthermore, unlike ADAMs, all ADAMTS are catalytically active (Kelwick et al., 2015; Blobel & Apte, 2006). Indeed, a family of ADAMTS-like (ADAMTSL) proteins exist, which are structurally very similar to ADAMTS, however they lack a catalytic site and are thus not true proteases but are just proteins secreted in the ECM (Blobel & Apte, 2006).

Typically, under normal conditions MMP, ADAM and ADAMTS gene expression and activity levels remain low within tissues, helping to maintain homeostasis. Therefore, dysregulation inducing an aberrant expression or upregulation in activity has become a biomarker for various kinds of diseases, some of which include different types of cancer, chronic inflammation, along with neurological and cardiovascular disorders (Galliera et al., 2015; Jackson et al., 2010). Additionally, various members of the ADAMTS protease family play a key role in the development of reproductive organs, along with multifaceted roles in male and female fertility (Russell et al., 2015). Due to their importance as a therapeutic target, there has been a growing interest for a better understanding of their structure and function for the development of selective synthetic inhibitors.

1.18 ZP detachment inhibition through chemical inhibitors

As the onset of independent cell volume regulation occurs once ovulation is triggered, the oocyte transitions from a passive mechanism dependent on their direct contact with the ZP to a unique mechanism of glycine-dependent volume control via GLYT1. The first step towards independent cell volume regulation is the detachment of the ZP from the oocyte, which is followed by a decrease in cell volume, formation of the perivitelline space and the activation of GLYT1. However, the mechanism for ZP detachment from the oocyte was unknown.

In attempts to uncover this mechanism, our lab previously investigated oocyte-ZP detachment and hypothesized that the detachment requires activation of a cell-surface protease, as this is analogous to the mechanism of how transmembrane ZP proteins are secreted during ZP biosynthesis (Qi et al., 2002; Zhao et al., 2002). It is possible that the peptidase responsible for oocyte-ZP detachment is the same as that which releases ZPGs during synthesis through its reactivation or with oocyte-ZP detachment occurring via an independent peptidase. Therefore, the process began by performing a bioinformatics screen using the MEROPS database of proteases to generate a transcript list of peptidases expressed in oocytes that may be possible candidates responsible for the detachment (Macaulay et al., 2023). Additionally, a list of corresponding peptidase inhibitors was also compiled from MEROPS. To identify the likely candidates responsible, various peptidase inhibitors were tested for prevention of ZP-oocyte detachment, with results demonstrating that the inhibitors marimastat and batimastat responsible for inhibition of M10 and M12 family of MPs, along with an ADAM10-selective inhibitor known as GI254023X were effective. Consequently, the data in our laboratory suggests that the oocyte-ZP adhesion is released via the action of a metalloproteinase, with the likely candidates from the ADAM subfamily of the M12 family

of MPs, however future work is still required to further elucidate the mechanism and identification of the MP involved.

1.19 ZP detachment inhibition through endogenous inhibitors: TIMPs

TIMPs are important endogenous inhibitors of MPs, with their initial discovery characterized as inhibitors of MMPs. However, over time the known scope of their inhibition broadened to include ADAMs and ADAMTSs. Four TIMP paralogous genes have been identified in the animal and human genome, which encode TIMPs 1 to 4 (Brew & Nagase, 2010). TIMPs consist of 184-194 amino acids, which are subdivided into N- and C-terminal domains that are stabilized by three conserved disulfide bonds (Jackson et al., 2017) . TIMP-1 and -3 are glycoproteins, while TIMP-2 and -4 are not glycosylated. Each TIMP is categorized in respect to their structure, activity and biological function and inhibit multiple MPs with diverse efficacies that thus trigger various cellular responses (Brew & Nagase, 2010). The inhibition through TIMPs occurs via tight binding to MPs in a 1:1 stoichiometry, wherein the TIMP N-terminus domain also known as the inhibitory domain, will bind with its cysteine residue to the MP catalytic Zn^{2+} to block the MP active site (Brew & Nagase, 2010; Raeeszadeh-Sarmazdeh et al., 2020).

Thus, to further investigate the role of MPs and the mechanism of oocyte-ZP release, pharmacological MP inhibitors will be tested along with the natural inhibitors, TIMPs, to see whether TIMPs are similarly able to regulate the MP responsible for oocyte-ZP detachment.

1.20 Summary

Prior to ovulation, the GV oocyte tightly adheres to the rigid extracellular matrix shell, the ZP, and in turn does not control its own volume. However, as the fully grown oocyte is ovulated or removed from the follicle, it will resume meiosis and the key developmental event of the oocyte acquiring the ability to independently control its own volume will commence. The initial step in this process is the detachment of the ZP from the oocyte, possibly via cleavage of the transmembrane ZPGs that likely occurs by an unknown MP. At the same time, GLYT1 becomes activated to accumulate glycine as an organic osmolyte. But how these two processes of oocyte-ZP detachment and GLYT1 activation are connected remains to be elucidated, with further investigations needed to better understand the mechanism behind it.

2. Significance and overall objective

Over time, IVF alongside several other forms of assisted reproductive technologies (ART) have become commonly used treatments for the increasing rates of human infertility. ART includes any fertility-related treatments that involve manipulating eggs or embryos (Jain & Singh, 2022). Additionally, these procedures are also used for the manipulation of animal models for the purposes of research, domestic and commercial use. Successful outcomes from ART depend on the ability to obtain healthy oocytes and effectively maintain embryo development *in vitro* prior to implantation. Therefore, a better understanding of oocyte and PI embryo physiology is required, including in regard to the mechanisms of cell volume as they play a major role in *in vitro* development. As previously discussed, early embryos are very sensitive to perturbations in their cell volume (Baltz, 2001; Tscherner et al., 2021) and proper development in culture strongly depends on the appropriate osmotic conditions alongside the oocyte's ability to adapt to changes in their external environment.

Currently, at the frontier of clinical ART is the use of the technique *in vitro* maturation (IVM), which involves maturation of oocytes in culture, resulting in prolonged periods of time spent outside of their normal *in vivo* environment. Oocyte maturation is a delicate process as it involves multiple steps such as nuclear and cytoplasmic maturation which must occur to produce a healthy and fertilizable oocyte. Thus, as oocytes are maturing and undergoing these vital processes *in vitro*, this can impact the overall health and development of PI embryos. Although IVM has advantages such as the elimination of side-effects from drug stimulation, there tends to be poorer development of PI embryos from oocytes matured through IVM than compared to embryos matured from oocytes *in vivo* (Fadini et al., 2009; Mikkelsen & Lindenberg, 2001). Thus, appropriate *in vitro* conditions are

necessary to eliminate osmotic stressors caused by culture techniques used in ART as oocytes undergo development.

Functional cell volume regulation is of particular importance to oocytes and early embryos, especially when culturing oocytes *in vitro*, in most likely sub-optimal conditions. Oocytes and early embryos have adapted by developing a unique mechanism of independent cell volume regulation, involving the intracellular transport of glycine via the GLYT1 transporter. Prior to ovulation and the activation of GLYT1, cell volume is controlled via the strong adhesion between the ZP and the oocyte. Since these osmoregulatory mechanisms found in mouse models are also present in human oocytes and embryos, this indicates the importance of GLYT1 as a general cell volume control mechanism employed in oocytes, allowing for research advancements determined in mice to be applied to human oocytes and embryos as well (Hammer et al., 2000). However, much about the mechanisms of these two processes remains unknown. The mechanisms by which the oocyte detaches from the ZP and the activation of GLYT1 could be related, as they occur with very similar time courses during the same period in oocyte maturation. But whether these two processes are coordinated in some way is undetermined. Further investigations are needed to better understand the development of independent cell volume regulation in oocytes and PI embryos.

An increase in our knowledge of oocyte physiology to maintain healthy, fertilizable oocytes would further advance oocyte culture technologies and consequently the current treatment protocols used for women undergoing infertility issues. In addition, further understanding of the essential cell volume regulation mechanisms of ZP detachment and GLYT1 activity would be beneficial to enhance oocyte survival and development *in vitro.*

Therefore, **the overall objective of my thesis was to determine the relationship between the mechanism of GLYT1 activation and oocyte-ZP detachment**. Using mice as the animal model along with a combination of functional studies, pharmacological manipulations, and molecular biology techniques, I have investigated the precise temporal relationship between ZP-adhesion release and GLYT1 activation, their possible relationship to one another and the mechanisms controlling ZP detachment to determine potential effects on GLYT1 activation. The findings from my research have provided further insight into the important aspects of independent cell volume regulation after ovulation and provide a better understanding of oocyte physiology. Consequently, a more complete understanding of the independent cell volume regulation mechanisms could help to improve human IVM culture conditions to maintain healthy and competent oocytes for women undergoing infertility treatments. In conclusive, the overall hypothesis for my thesis is that oocyte-ZP detachment activates GLYT1, which would predict that detachment must precede GLYT1 activation, and that prevention of detachment would in turn prevent GLYT1 activation.

3. Specific aims and hypotheses

Specific aim 1: Compare the timing of GLYT1 activation to oocyte-ZP release

The detachment of the oocyte from the ZP was previously shown to occur at a very similar time course to glycine transport via GLYT1 though with oocyte-ZP release appearing to slightly precede GLYT1 activation (Richard et al., 2017; Tartia et al., 2009). However, their relative timing has only been inferred from separate experiments and thus the precise temporal relationship remains unknown.

Therefore, I hypothesized that oocyte-ZP adhesion release precedes GLYT1 activation.

Specific aim 2: Determine whether release of oocyte-ZP adhesion is required for GLYT1 activation

If, as hypothesized above, oocyte-ZP adhesion release precedes GLYT1 activation, it is possible that release of the physical interaction between the oocyte surface and the ZP provides the initial signal for GLYT1 activation or is required before GLYT1 can become active. Data from our laboratory has shown that oocyte-ZP detachment can be prevented by MP inhibitors selective for extracellular peptidases expressed in mouse oocytes (Macaulay et al., 2023). Therefore, utilizing MP inhibitors, I will investigate whether GLYT1 activity still develops with its normal time course in oocytes when oocyte-ZP release has been prevented.

Therefore, I hypothesized that detachment of the ZP is required for the activation of GLYT1.

Specific aim 3: Determine if GLYT1 activation is sped up when the ZP is removed

In correlation with specific aim 2, if the data supports the above hypothesis that preventing the oocyte-ZP release suppresses the activation of GLYT1, I will follow by

chemically removing the ZP from the oocyte to determine if GLYT1 activation is accelerated.

Therefore, I hypothesized that the removal of the ZP would accelerate GLYT1 activation in oocytes.

Specific aim 4: Identify if TIMPs regulate the ZP release from the oocyte

In accordance with previous work from our laboratory that demonstrated oocyte-ZP detachment can be prevented by chemical MP inhibitors, I sought to determine whether natural TIMPs, the key endogenous regulators of MP activity, would similarly prevent ZP-oocyte detachment.

Therefore, I hypothesized that TIMPs would inhibit the release of the ZP from the oocyte.

4. Materials and Methods

4.1 Chemicals and pharmaceutical agents

The chemicals and solutions used for experiments were all embryo tested or cell culture grade where available. All chemicals, compounds and pharmaceutical agents were obtained from sources listed below in Table 1 and Table 2.

4.2 Oocyte culture media

Oocytes were cultured in a modified version of potassium simplex optimized medium (mKSOM), which was modified from classical (unmodified) KSOM by replacing polyvinyl alcohol (PVA, 1 mg/ml, cold-water soluble) with bovine serum albumin (BSA), along with glutamine being omitted as it can be transported by GLYT1 (Lawitts & Biggers, 1993). mKSOM contained: NaCl (95 mM), KCl (2.5 mM), KH_2PO_4 (0.35 mM), $MgSO_4.7H_2O$ (0.2 mM), Na lactate (10 mM), Glucose (0.2 mM), Na pyruvate (0.2 mM), NaHCO3 (25 mM), $CaCl_2.2H_2$) (1.7 mM), Tetrasodium ethylenediaminetetraacetic acid (EDTA)(0.01 mM), K penicillin G (0.16 mM), Streptomycin SO_4 (0.03 mM) and 1mg/ml PVA. The medium used for oocyte collection and handling was identical to mKSOM except for the addition of 21 mM of 4-(2-hydroxyethyl)-1-piperazineethanesulfonic acid (Hepes) with the reduction of NaOH to 4 mM (pH adjusted with NaOH to 7.4), and this is referred to as Hepes-mKSOM (also known as KFHM). The osmolarities of mKSOM and Hepes-mKSOM were 250 mOsM and 240 mOsM respectively, with osmolarity measured with a Vapro 5520 osmometer (Wescor, Logan, UT) to confirm it was within ± 5 mOsM of the nominal value. For desired experiments, KSOM osmolarity was adjusted using D(+) raffinose and confirmed by

osmometer (Vapro 5520, Wescor, Logan, UT) as previously described (Dawson & Baltz, 1997).

4.3 Animals

All animal protocols were approved by the Animal Care Committee of the University of Ottawa Faculty of Medicine and conform to the Canadian Council on Animal Care guidelines. Female CD1 strain mice were obtained from Charles River (St-Constant, QC, Canada) and used to obtain fully-grown oocytes from mice with an age range of 4 - 7 weeks. This strain (along with CF1) has been used as a model system in our laboratory to investigate culture effects as it is known to be produce oocytes and embryos that are sensitive to *in vitro* conditions and osmolarity (Biggers, 1998; Hadi et al., 2005).

The University of Ottawa Animal Care and Veterinary Services (ACVS) facility provided animal care. All animals were maintained on a 12 hr light-dark cycle and were provided unrestricted access to Teklad Global 18% protein rodent diet 2018 (Envigo, Indianapolis, IN) and water. All animals were sacrificed by cervical dislocation.

4.4 Superovulation

To obtain sufficient numbers of oocytes for experimental use, a standard superovulation protocol was utilized (Hogan et al., 1994; Dawson & Baltz, 1997). Female mice received an intra-peritoneal (i.p.) injection of 5 IU pregnant mare serum gonadotropin (PMSG), an FSH-like hormone, to stimulate ovarian folliculogenesis.

4.5 Oocyte isolation and collection

Isolation of fully GV stage oocytes was completed by surgically excising ovaries approximately 44 hr post-PMSG injection. COCs were released from ovarian tissue by mincing with a razor blade, followed by their collection. The cumulus cells were removed from GV oocytes by denuding with repeated gentle pipetting by a narrow-bore flame pulled Pasteur pipette. All steps for collection and handlings were performed using Hepes-mKSOM.

To obtain *in vitro* matured MI and MII oocytes, GV oocytes were isolated from cumulus cells and cultured in microdrops of mKSOM for 1.5 hr to 4 hr or overnight (22 hr), as specified (Wassarman et al., 1979).

4.6 Oocyte culture

Culture of oocytes was carried out by following the standard protocols routinely used in our laboratory (Dawson & Baltz, 1997; Lawitts & Biggers, 1993). For experiment replicates, pools of oocytes were collected from several female mice, unless otherwise stated. Three drops of 50 µL mKSOM were placed in a 35 mm culture dish (Falcon, Corning NY, USA) and submerged with filter-sterilized embryo culture-grade mineral oil (Sigma Aldrich, St. Louis, MO, USA). When using hydrophobic inhibitors, mineral oil was omitted and oocytes were cultured in 750 µL of mKSOM in 4-well plates (Falcon, Corning NY). Culture media was pre-equilibrated in an incubator at 37ºC with 5% CO_2 in air and 100% humidity (Lawitts & Biggers, 1993) for a minimum of 2 hr prior to use. Oocytes were washed through three drops of pre-equilibrated culture media to minimize the carryover of media from collections or previous treatments and left to culture in the final drop. Plates with oocytes were returned to the incubator to culture for an experiment-specific time frame.

Table 1: Summary of chemicals and compounds used

Name of Chemical or Compound	Source
4-(2-hydroxyethyl)-1-piperazineethane-sulfonic acid (HEPES)	Sigma Aldrich (St. Louis, MO, USA)
[^{3}H]-glycine ([2-^{3}H]-glycine; ~42-60 Ci/mmol)	Perkin Elmer (Boston, MA, USA), American Radiolabeled Chemicals (ARC)(St. Louis, MO, USA)
Calcium chloride ($CaCl_2$)	Sigma Aldrich (St. Louis, MO, USA)
Dimethyl Sulfoxide (DMSO)	Calbiochem (La Jolla, CA, USA)
Ethanol	Sigma Aldrich (St. Louis, MO, USA)
Glucose, D-(+)	Sigma Aldrich (St. Louis, MO, USA)
Glycine	Sigma Aldrich (St. Louis, MO, USA)
K penicillin G	Sigma Aldrich (St. Louis, MO, USA)
Magnesium sulfate heptahydrate ($MgSO_4$)	Sigma Aldrich (St. Louis, MO, USA)
Mineral Oil	Sigma Aldrich (St. Louis, MO, USA)
Sodium bicarbonate ($NaHCO_3$)	Sigma Aldrich (St. Louis, MO, USA)
Sodium chloride (NaCl)	Sigma Aldrich (St. Louis, MO, USA)
Sodium lactate	Sigma Aldrich (St. Louis, MO, USA)
Sodium pyruvate	Sigma Aldrich (St. Louis, MO, USA)
Potassium chloride (KCl)	Sigma Aldrich (St. Louis, MO, USA)
Potassium phosphate monobasic (KH_2PO_4)	Sigma Aldrich (St. Louis, MO, USA)
Polyvinyl alcohol (PVA)	Sigma Aldrich (St. Louis, MO, USA)

Raffinose pentahydrate, D-(+)	Sigma Aldrich (St. Louis, MO, USA)
Sarcosine	Sigma Aldrich (St. Louis, MO, USA)
Scintillation fluid	Scintiverse BD, Fisher Scientific (Pittsburg, PA, USA)
Sodium Chloride (NaCl)	Sigma Aldrich (St. Louis, MO, USA)
Streptomycin SO_4	Sigma Aldrich (St. Louis, MO, USA)
Tetrasodium ethylenediaminetetra-acetic acid (EDTA)	Sigma Aldrich (St. Louis, MO, USA)

Table 2: Summary of pharmaceutical agents used

Pharmaceutical Agent	Source	Action
Acidic Tyrode's Solution (pH 2.5)	Sigma Aldrich (St. Louis, MO, USA)	Zona pellucida (ZP) removal
Batimastat	Sigma Aldrich (St. Louis, MO, USA)	Broad spectrum matrix metalloproteinase (MMP) inhibitor
GI254023x	Sigma Aldrich (St. Louis, MO, USA)	Selective metalloproteinase inhibitor for ADAM10
Milrinone	Sigma Aldrich (St. Louis, MO, USA)	Maintains meiotic arrest in oocytes by inhibiting PDE3
Marimastat	Sigma Aldrich (St. Louis, MO, USA)	Broad spectrum matrix metalloproteinase (MMP) inhibitor
Pregnant mare serum gonadotropin (PMSG)	Merck, supplied by Inervet (Canada Corp, Kirkland, QC, Canada)	Stimulation of ovarian follicle growth *in vivo* (hormone)

4.7 Maintaining meiotic arrest

Maintenance of prophase I arrest (GV-arrest) depends on high levels of intracellular cAMP. GVBD was inhibited *in vitro* by using Milrinone (Table 2), which selectively inhibits PDE3 and thus prevents the degradation of cAMP. When meiotic arrest was required for specific experiments, 10 μM Milirone was added to culture medium.

4.8 Oocyte-ZP adhesion assay

An assay was developed in our laboratory to distinguished between the various stages of oocyte-ZP adhesion: completely attached, partially attached and completely detached (Tartia et al., 2009). Oocytes were collected and denuded, followed by exposure to a hypertonic solution of either mKSOM (1000 mOsM or 450 mOsM) or Hepes-mKSOM (1000 mOsM) by addition of NaCl, with osmolarity measured to confirm it was within ± 5 mOsM of the nominal value. Oocytes were classified as completely attached to the ZP if the oocyte and the ZP together formed a concave disc shape. Oocytes were classified as completely detached from the ZP if the oocyte shrunk within the ZP and left a clearly visible space between the surrounding shrunken oocyte and the ZP. Partial attachment to the ZP was classified if the oocyte was in an intermediate stage of attachment and detachment, where some areas of the oocyte adhered to the ZP while other areas left a space between the ZP. Immediately following transfer to the hypertonic solution, oocytes were visually examined by taking a photo using a Nikon E4500 camera mounted on a Zeiss Axiovert microscope within 5 min. A quantitative detachment score was assigned to each oocyte in the image from 0 - 1 = fully attached, 1.5 - 4.5 = partially attached and 5 - 6 = fully detached. To determine detachment score, a virtual radial reticle was used, which was divided into 6 equal

sextants (with each sector at 60°) and centered on the oocyte in the recorded image. Each sector was given a score of 0 if fully attached, 0.5 if partially attached and 1 if fully detached. To maximize the number of sectors at either a score of 0 or 1 (rather than 0.5) in oocytes that were still partially attached, the reticle was rotated to adjust for this before scoring. The scores from each sector were then added up to provide an overall detachment score for each individual oocyte. In experiments where oocyte viability was assessed after the assay was complete, oocytes were returned to mKSOM following hypertonic shock, and left to culture overnight 5% CO_2 in air at 37 °C. Meiotic maturation was assessed the next day, by checking for the presence of a first polar body indicating its progression through meiosis into a mature MII egg. When a detachment score time course was performed, time zero was placement of the oocytes in culture following collection, after an average collection time of 12 min before they were placed into culture.

4.9 [^{3}H]-Glycine transport measurements

The rate of glycine transport in oocytes was measured by following a detailed protocol published by our laboratory (Baltz & Richard, 2013). [^{3}H]-glycine is used as a method for measuring the rate of GLYT1-specific glycine transport in oocytes and embryos, to follow previous work demonstrated by our laboratory (Dawson et al., 1998; Steeves et al., 2003; Steeves & Baltz, 2005; Tartia et al., 2009). Oocytes were isolated and collected as described above and incubated until a desired time point. Time zero was placement of the oocytes in culture following collection, after an average collection time of 12 min before they were placed into culture. Following incubation, oocytes were washed through three 50 µl drops of pre-equilibrated (5%CO2/air; 37ºC) mKSOM under an oil. Oocytes were then

incubated for 10 minutes (Steeves et al., 2003; Tartia et al., 2009) in mKSOM that contained either 1μM of [^{3}H]-glycine for groups of oocytes (~10 oocytes per group) or 3 μM for individual oocytes (Baltz, 2013)(Dawson et al., 1998), to ensure that accumulated glycine could be easily detected above background in single oocytes (this was later accounted for by dividing by 3). Following incubation, oocytes were washed through 7 drops of ice-cold Hepes-mKSOM and transferred with minimal excess media to a scintillation vial. The same amount of medium from the final wash drop, without the presence of oocytes, was expelled into a separate scintillation vial to be used as a measure for background. These counts were subtracted from the counts obtained from the oocyte samples. The vials were filled with 4mL of scintillation fluid (Scintiverse BD, Fisher Scientific, Pittsburgh, PA, USA) and vortexed. The total molar amount of accumulated [^{3}H]-glycine was quantified by a scintillation counter (LS 6500, Beckman Coulter, Brea, CA), with a 5 min counting period per sample (Dawson et al., 1998). To prepare [^{3}H]-glycine incubation drops, a more concentrated mKSOM (70 mKSOM), which had only 70% of the normal amount of sterilized water, was added. This more concentrated mKSOM allowed for the direct addition of the stock concentration of radioactively labelled glycine. Additionally, the amount of filter sterilized water added was adjusted to bring it to the normal concentrations in mKSOM once all components were added to the final drop. New glycine was always tested prior to experimentation by confirming the presence of the expected non-saturable transport by incubating oocytes with 5 mM unlabelled glycine or 5 mM unlabelled sarcosine, in addition to the 1 μM of [^{3}H]-glycine and comparing these to control uptake in the absence of either unlabeled glycine or sarcosine.

To allow for the rate of glycine transport to be converted from counts per minute (CPM) to concentration, standard curves were completed weekly. Known serial dilutions of

the ^{3}H-labeled glycine stock were used in construction of the standard curve. Two 15 mL conical tubes were filled with 5 mL and 7.5 mL of filter-sterilized water, for 1:5000 and 1: 7500 dilutions and 1 µl of the stock solution of [^{3}H]-glycine was added to each tube. Five serial twofold dilutions were performed from each tube and 5 µl from each dilution tube was added to separate scintillation vials. In addition, 5 µl of filter-sterilized water was instead added to the scintillation vial which was used as a background measure. Scintillation fluid was added and measured on the scintillation counter as described above. Standard curves were constructed from the measured CPM vs. amounts of [^{3}H]-glycine. The rate of transport by oocytes was calculated in femtomoles of [^{3}H]-glycine per oocyte per minute of incubation.

4.10 Removal of the zona pellucida

Groups of oocytes were isolated and collected as described above and briefly exposed (30 seconds) to a small drop of acidic Tyrode's solution (Hogan et al., 1994)(stored at -20 ºC) pre-warmed for ~30 minutes at 37ºC. Oocytes were visually monitored until the zona pellucida was successfully dissolved and then immediately transferred through three drops of Hepes-mKSOM to wash away any excess Tyrode's solution, neutralizing its acidity, and additionally washed through five 50µl drops of mKSOM to allow for recovery before utilization in further experimentation.

4.11 Time-lapse imaging with environmental control chamber

Time-lapse images were taken to create a video of live oocyte volume change over time by using a Nikon E4500 camera mounted on a Zeiss Axiovert microscope equipped

with an environmental control chamber. Oocytes were maintained at 37 °C in 5% CO_2 and air, with images taken every 2 min up to 1 hr, followed by every 20 min up to 3 hr with brightfield mode with phase contrast and 20x objective. PVA was omitted in the mKSOM that was used in the environmental control chamber, to facilitate the attachment of oocytes to the bottom of the chamber to maintain them in place for imaging.

4.12 Zona pellucida detachment inhibition with small molecule chemical inhibitors

The pharmacological broad range metalloproteinase inhibitors (Table 2): marimastat, batimastat, responsible for inhibiting M10 and M12 family MMPs and the selective inhibitor for ADAM10 (Table 2), GI254023x were used to prevent ZP-oocyte detachment. All inhibitors were dissolved in DMSO, aliquoted into smaller samples and stored at -20 ºC for up to two months. Experimental concentrations of inhibitors ranged from 1 µM up to 50 µM. Inhibitors were added to 750 µL of mKSOM in 4-well plates without the presence of oil, as batimastat has low aqueous solubility and will partition out of media and into oil.

4.13 ZP detachment inhibition with TIMPs

The physiological inhibitors of metalloproteases, TIMPs-1 to -4 were used for experimentation to determine whether they were able to prevent ZP-oocyte detachment. TIMPs were obtained commercially where mouse genes had been expressed as recombinant proteins (MyBioSource, San Diego, CA, USA) through bacterial expression in E. coli as the host for TIMP-1, 3 and 4 or with mammalian expression in human embryonic kidney (HEK) 293 cells as host for TIMP-2 production (Table 3). All proteins were reconstituted in deionized sterile water to a concentration of 1 mg/mL, aliquoted into smaller samples and

stored at -20 ºC for short periods until use. Once reconstituted, the desired recombinant TIMP protein was added directly to mKSOM, for a final concentration of 1 μM in oocyte culture media (based on concentrations found in literature) and incubated until the desired time point in a microdrop under oil, unless combined with chemical inhibitors where oocytes were incubated without the presence of oil as described above.

Table 3: Summary of recombinant proteins used

Recombinant Mouse Protein	Source	Action	Molecular Weight	Expression Host
Tissue inhibitor of metalloproteinase 1 (TIMP-1)	MyBioSource (San Diego, CA, USA)	Endogenous matrix metalloproteinase (MMP) inhibitors	19.88 kDa	E.coli
Tissue inhibitor of metalloproteinase 2 (TIMP-2)	MyBioSource (San Diego, CA, USA)	Endogenous matrix metalloproteinase (MMP) inhibitors	22 kDa	HEK 293 cells
Tissue inhibitor of metalloproteinase 3 (TIMP-3)	MyBioSource (San Diego, CA, USA)	Endogenous matrix metalloproteinase (MMP) inhibitors	24.182 kDa	E.coli
Tissue inhibitor of metalloproteinase 4 (TIMP-4)	MyBioSource (San Diego, CA, USA)	Endogenous matrix metalloproteinase (MPP) inhibitors	25.774 kDa	E.coli

4.14 Data analysis

Graphs were prepared with Prism 8 (GraphPad Software, San Diego, CA). Data for continuous variables were expressed as mean ± SEM unless otherwise noted. Statistical analysis was also completed through Prism, using a two tailed t-test when comparing the means between two groups, or either one-way or two-way ANOVA with Tukey's multiple comparisons test when comparing three or more groups, with either all means compared or each mean compared to control (t = 0) where specified. For inhibitor dose-response data, nonlinear least squares regression was used to fit a curve of the form (detachment score) = (score with no inhibitor)/(1+[inhibitor]/IC50) where [inhibitor] designates the inhibitor concentration. The score at infinite inhibitor concentration was constrained to 0. The variables determined by the fit were thus the score with no inhibitor (i.e., [inhibitor] = 0) and the IC50. 95% confidence intervals were calculated for IC50 using Prism. To compare the time-dependence between two curves, the dependent variables were both transformed to fraction of maximum. The minimum values (MIN) were taken to be the average at t = 0 and the maximum (MAX) the average at t = 150. MIN was subtracted from each value and then each value transformed to fraction of MAX using the equation:

fraction = [value-MIN)]/[MAX-MIN]

The plots were then fit to a sigmoidal curve which spanned from 0 to 1 of the form:

fraction = $(t^S)*1/(t^S + t_{0.5}{}^S)$ where t = time, S = slope, and $t_{0.5}$ is the time at half-maximum (i.e., fraction = 0.5), which were all determined by the regression. The $t_{0.5}$ (IC50 in Prism equation) was compared by F-test.

5. Results

5.1 The oocyte-ZP adhesion release precedes GLYT1 activation

The initiation of independent cell volume regulation involves two distinct processes that are completed within several hours following the trigger of ovulation or isolation from the follicle: ZP adhesion release from the oocyte and activation of the GLYT1 transporter. Previous data from our laboratory has shown that GLYT1 activation and oocyte-ZP detachment follow a very similar time course (Tartia et al., 2009; Richard et al., 2017), with their relative timing inferred from separate experiments. Therefore, my objective was to investigate the precise temporal relationship between the two distinct cell volume regulation processes to thus determine whether oocyte-ZP adhesion release precedes the activation of GLYT1.

5.1a. GLYT1 activation over time for groups of oocytes

To determine the timing of GLYT1 activation, glycine transport was measured in GV oocytes during meiotic maturation into the MI stage *in vitro* (Figure 5). Groups of ~10 denuded oocytes were subject to the GLYT1 activity assay (1 µM [^{3}H]-glycine) at 15 min intervals from a period of 0 hr to 1.5 hr, followed by assays at 30 min intervals up to 4 hr.

Over the first 0.5 hr, GLYT1 activity in recently isolated GV oocytes remained nearly quiescent. However, GLYT1-mediated glycine transport gradually became increasingly activated, reaching half-maximal activation by 1.5 hr, with maximal capacity reached by 3 hr.

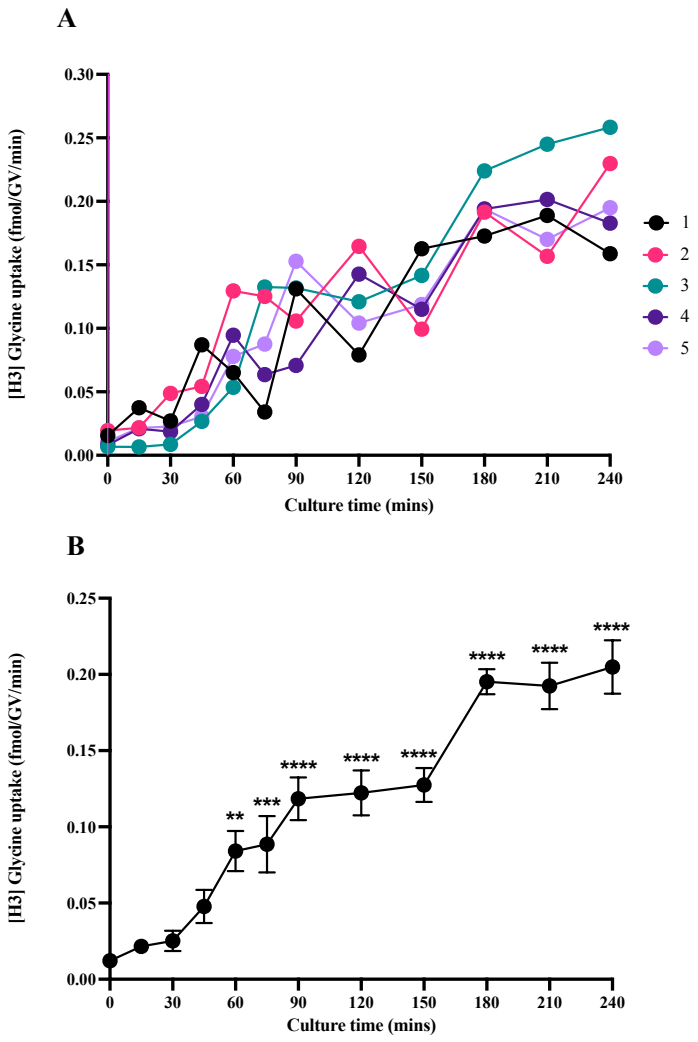

Figure 5: Glycine transport for groups of oocytes during oocyte maturation

(A) The rate of [^{3}H]-glycine transport by GLYT1 was measured in GV oocytes during meiotic progression into the MI stage *in vitro*. Groups of denuded oocytes were incubated with 1 µM [^{3}H]-glycine in KSOM media under oil for 10 min at the various time points post isolation from follicles, with the rate of transport expressed as total glycine (fmoles) per oocyte per minute from 0 hr to 4 hr. Each of the five experiments are shown separately **(B)** The average rate of [^{3}H]-glycine transport by GLYT1 in groups of oocytes shown in (A) for an N = 5. Tested by one-way ANOVA with multiple comparisons, each mean compared to t = 0.

5.1b. Oocyte-ZP adhesion over time

To examine the relationship between oocyte-ZP adhesion and GLYT1 activity, the time course of oocyte-ZP detachment assay was performed (Figure 6). After a specified period in culture, oocytes were placed in hypertonic media (1000 mOsM Hepes-mKSOM) to induce hypertonic shock and oocyte shrinkage. Previously in our laboratory, oocyte-ZP adhesion was qualitatively scored as attached, partially attached or detached. To keep with previous work, oocyte detachment was divided into the same categories with oocyte-ZP attachment as a score of 0 - 1.0, partially attached from 1.5 - 4.5 and detached 5.0 - 6.0. The results showed that oocytes were fully attached immediately after isolation from the follicle, while detachment increased with time post-isolation from the follicle and all oocytes became completely detached by 2.5 hr. These results were also consistent with previous work (Richard et al., 2017).

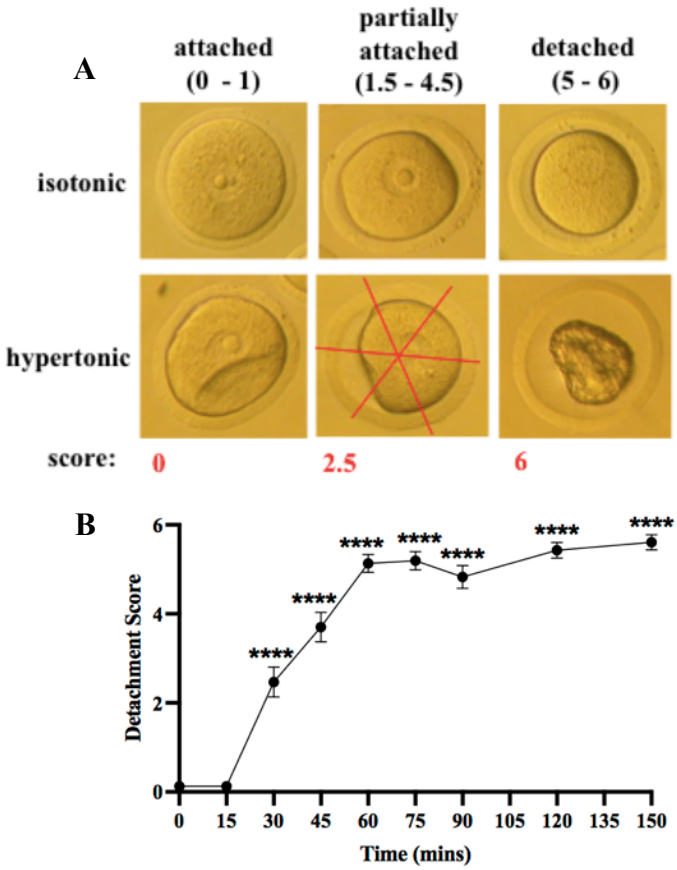

Figure 6: Oocyte-ZP detachment during oocyte maturation

The average oocyte-ZP detachment score was measured in GV oocytes during meiotic progression into the MI stage *in vitro*. Oocytes were hypertonically shocked (1000mOsM Hepes-mKSOM) at various time points over the course of 2.5 hr (a time at which the ZP has completely detached from the oocyte) to determine the detachment status of the ZP from the oocyte. **(A)** Oocyte-ZP attachment was scored as 0 - 1.0, partially attached from 1.5 - 4.5 and detached 5.0 - 6.0 using a virtual radial reticle, which was divided into 6 equal sextants (with each sector at 60°) and centered on the oocyte in the recorded image (in red). **(B)** Oocyte-ZP detachment score graphed as a function of time. Denuded oocytes in groups of ~12 were collected and incubated in KSOM under oil for each repeat. Repeated for an N = 5. Tested by one-way ANOVA with multiple comparisons, each mean compared to t = 0.

5.1c. Timing of activation of GLYT1 vs oocyte-ZP detachment

Since the precise temporal relationship between the two distinct cell volume regulation processes was unknown, the GLYT1 activity assay and oocyte-ZP adhesion assay time courses (as shown above) were compared. Taken together, these results suggest that oocyte-ZP detachment precedes GLYT1 activation by 20 min.

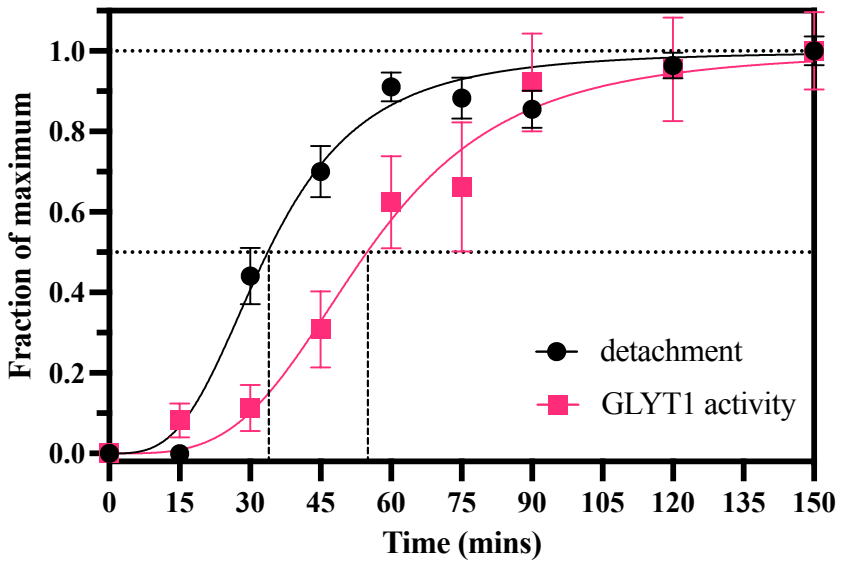

Figure 7: GLYT1 activity assay vs oocyte-ZP adhesion assay time course in GV oocytes

The average rate of [^{3}H]-glycine transport by GLYT1 for groups of oocytes is plotted here in comparison to the average oocyte-ZP detachment score (Figure 5B and Figure 6). Glycine transport and oocyte-ZP detachment, the two processes of independent cell volume regulation, occur at a similar time course, with oocyte-ZP detachment preceding GLYT1 activation by 20 min. The $t_{0.5}$ was compared by F-test and $t_{0.5}$ values of the fits were 34 min for detachment and 55 min for GLYT1, which were significantly different (P = 0.0002).

5.1d. Meiotic competence of oocytes

Although there is a shift between oocyte-ZP detachment and GLYT1 activation by 20 min, the timing of these two mechanisms is extremely similar therefore I used another method to confirm my hypothesis. I performed both the oocyte-ZP adhesion assay and the GLYT1 activity assay on individual oocytes to correlate a specific detachment score with a corresponding glycine uptake for each oocyte at various time points.

Prior to performing both assays on the same oocyte, the health of the oocyte was assessed following a hypertonic shock from high osmolarity exposure (Figure 8). The measurement for oocyte health was based on the meiotic competence of the oocyte, being the ability to progress to MII. The hypertonic shock did not show a detrimental effect on the oocytes when shock was performed 0.5 hr post isolation from the follicle, with progression to MII greater than 80%. However, when oocytes were shocked 4 hr post isolation from the follicle, they had a harder time recovering, with only 74% of oocyte progressing through the MII phase, demonstrating a significant difference from the control.

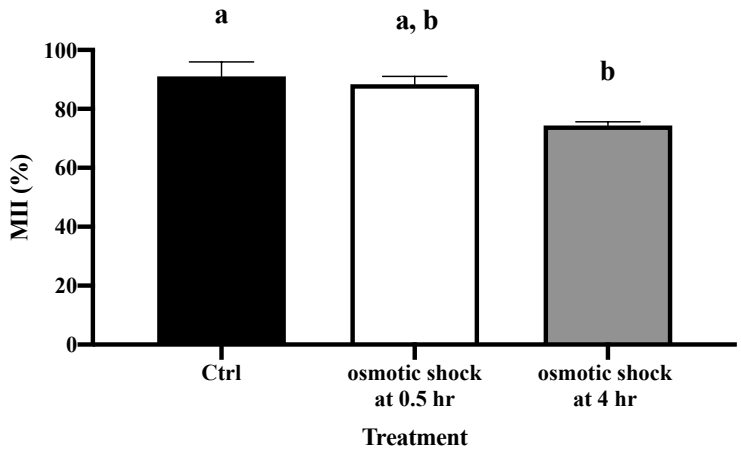

Figure 8: Meiotic competence of oocytes after osmotic shock

The oocyte-ZP adhesion assay was performed on groups of ~12 denuded oocytes with 1000 mOsM Hepes-mKSOM at 0.5 hr and 4 hr post isolation from the follicle. Oocytes were recovered in 250 mOsM mKSOM and left to culture overnight. After 16 hr, meiotic competence was assessed for each oocyte (based on the release of the second polar body). Repeated for an N = 3. The difference between means for meiotic competency were analyzed by ANOVA with Tukey test. The means that do not share the same letter are significantly different (*$P < 0.05$).

5.1e. GLYT1 activation over time for individual of oocytes

The activation of GLYT1 was measured in individual oocytes (Figure 9), following the same time course listed above (for groups of oocytes in 1a). However, small groups of oocytes were incubated with 3 μM [^{3}H]-glycine and each oocyte was individually placed in a separate vial for scintillation counting. Individual oocytes demonstrated the same trend in GLYT1 activity as compared to groups of oocytes.

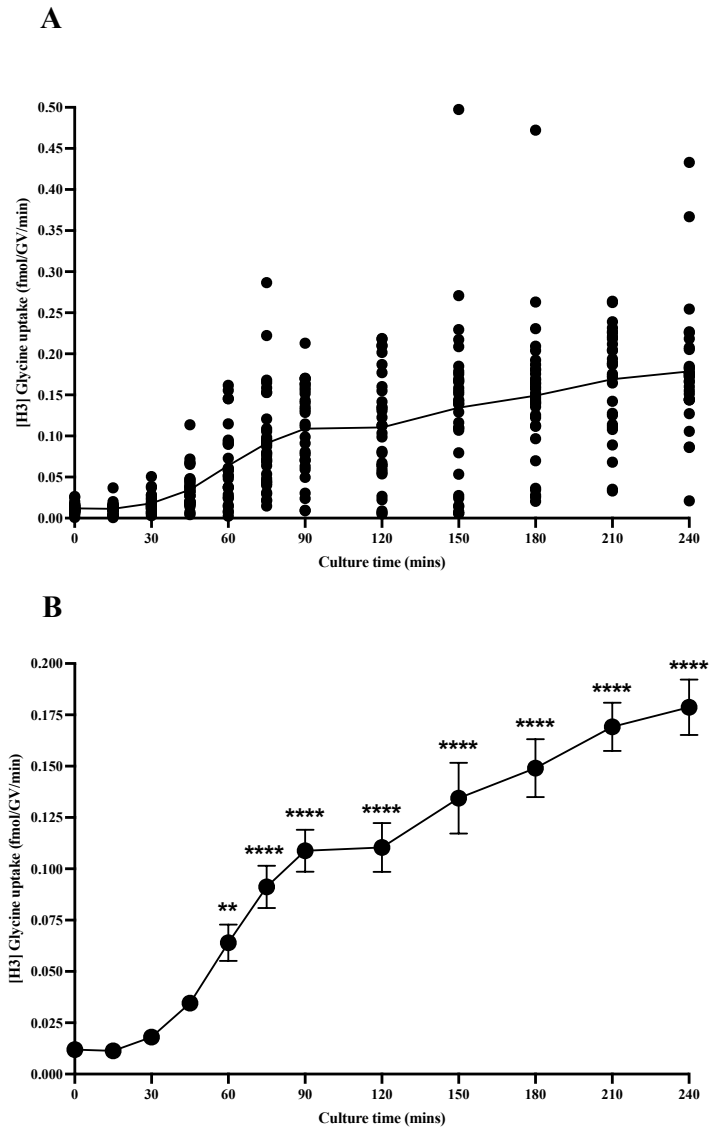

Figure 9: Average glycine transport for individual oocytes during oocyte maturation

(A) The rate of [^{3}H]-glycine transport by GLYT1 was measured in individual GV oocytes during meiotic progression into the MI stage *in vitro*. Small groups of oocytes (~5-7) were incubated with 3 µM [^{3}H]-glycine and then each oocyte was separated for individual readings with the scintillator at the various time points post isolation from the follicle. The rate of transport expressed as total glycine (fmoles) per oocyte per minute from 0 hr to 4 hr.

Experiments were completed for a total of N = 5 which were combined here. On data points where the error bars aren't visible, they are smaller than the data point symbol. **(B)** The average rate of [^{3}H]-glycine transport by GLYT1 for the individual oocytes shown in (A). Tested by one-way ANOVA with multiple comparisons, each mean compared to t = 0.

The average rate of glycine transport by GLYT1 in individual oocytes (Figure 9B) is compared to the average rate of transport for groups of oocytes (Figure 5B). When comparing each time course (Figure 10), individual and groups of oocytes followed the same time course of GLYT1 activation.

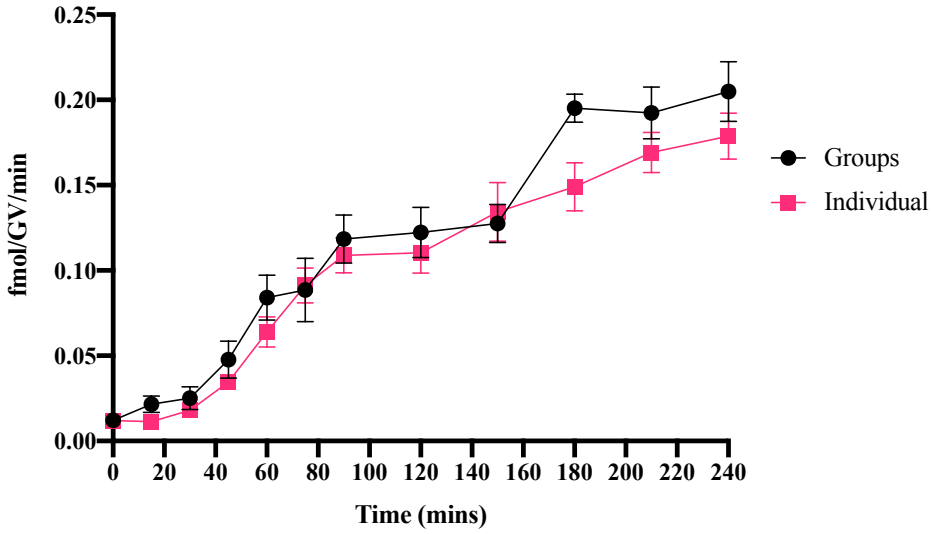

Figure 10: GLYT1 activity assay of groups vs individual

The average rate of [^{3}H]-glycine transport by GLYT1 for groups and individual oocytes compared to see if their rates follow the same trend (Figure 5B and Figure 9B). A 2-way ANOVA was performed for main effects of group vs individual and time. Time is highly significant ($P<0.0001$), while group vs. individual did not have a significant effect ($P = 0.38$), there is no significant difference between GLYT1 when measured as groups or individually.

5.1f. GLYT1 transporter recovery following 1000mOsM shock

To further investigate the relationship between GLYT1 activity and oocyte-ZP adhesion, oocytes were hypertonically shocked and GLYT1 activity was then measured (Figure 11). Groups of ~7 denuded oocytes were osmotically shocked with 1000 mOsM mKSOM following culture for 1.5 hr post isolation from the follicle and returned to 250 mOsM mKSOM to allow for oocyte volume recovery. To determine the shortest recovery time required for GLYT1 to recover from the osmotic shock, oocytes were incubated for 0, 5 and 10 min after the shock, prior to performing the GLYT1 activity assay. No difference was observed in the various recovery times, with GLYT1 activity remaining low. This may indicate that, after a 1000 mOsM hypertonic shock, oocytes either require a recovery time longer than 10 min or are damaged enough that GLYT1 activity is lost. I therefore investigated whether the detachment assay could be performed at lower osmolarity and whether GLYT1 would then recover.

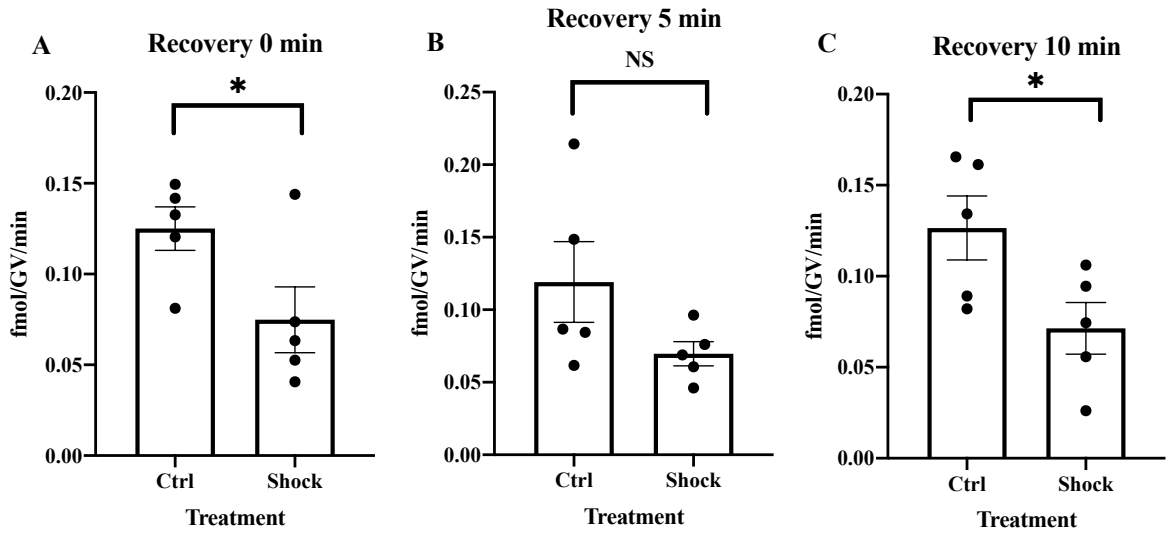

Figure 11: GLYT1 transporter recovery following 1000 mOsM hypertonic shock

The rate of [^{3}H]-glycine transport by GLYT1 was measured following exposure to a hypertonic shock of 1000 mOsM mKSOM on the same cohort of oocytes. The assays were performed on groups of oocytes that were incubated for 1.5 hr following removal from the follicle. Oocytes were left to recover from the hypertonic shock for **(A)** 0 min, **(B)** 5 min or **(C)** 10 min prior to performing the GLYT1 activity assay (n = 5). The difference between means was analyzed by t-test (*P < 0.05), with recovery times marginally significant but with an overall downward trend for all groups.

5.1g. Oocyte adhesion assay at different concentrations

The standard protocol in our laboratory when hypertonically shocking oocytes for the oocyte-ZP adhesion assay is to use a media with an osmolarity of 1000 mOsM as it provides a clear visualization of ZP detachment. In this case, since oocytes must remain viable for further measurements following the hypertonic shock, with minimal time between measurements, the osmolarity of the shock media was decreased to allow for a faster recovery and to cause less damage to the oocytes.

Another oocyte-ZP adhesion assay time course was performed, using mKSOM with an osmolarity decreased down to 450 mOsM mKSOM (Figure 12), following the same time course and protocol as listed above in section 1c, Figure 3. The results from Figure 3, where oocytes were hypertonically shocked with 1000 mOsM Hepes-mKSOM were used here to compare with the oocytes hypertonically shocked at 450 mOsM. The hypertonic shock medium at the two osmolarities: 450 mOsM and 1000 mOsM, showed similar means for detachment score over time. Therefore, 450 mOsM mKSOM was used to determine whether GLYT1 would recover after the detachment assay was performed with 450 mOsM mKSOM.

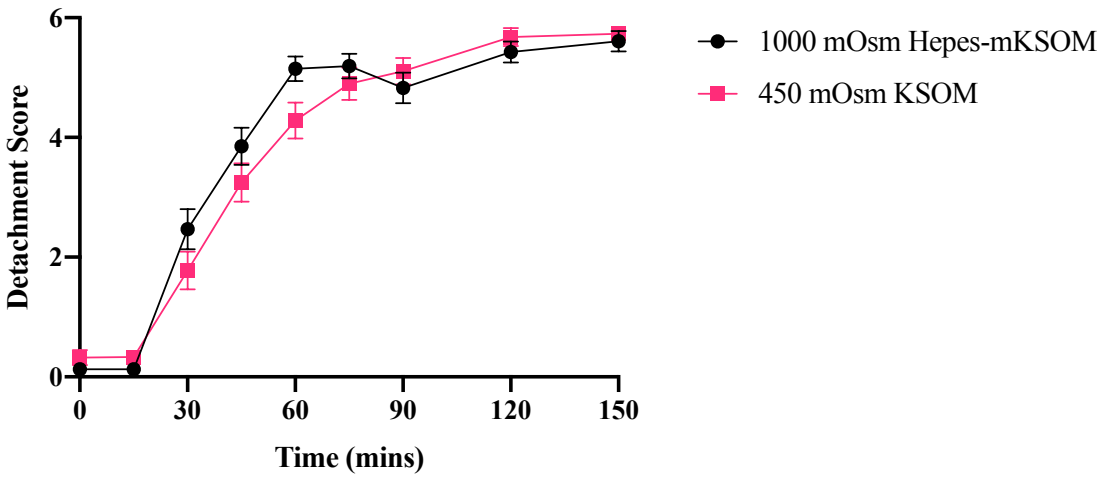

Figure 12: The oocyte-ZP adhesion assay with 1000 mOsM and 450 mOsM medium

The oocyte-ZP adhesion assay time course from 0 to 2.5 hr (a time at which oocytes are completely detached from the ZP) was performed on GV oocytes following removal from the follicle. Denuded oocytes in groups of ~10 were incubated in 250 mOsM mKSOM for the various time points. At which point, an osmotic shock was performed in a drop of 1000 mOsM Hepes-mKSOM or 450mOsM mKSOM. An average was taken for an n = 5 at each time point. A 2-way ANOVA was performed to compare the main effects of osmolarity and time. Time was highly significant ($P < 0.0001$), while osmolarity did not have a significant effect ($P = 0.10$).

5.1h. GLYT1 transporter recovery following 450 mOsM shock

To determine the recovery time of GLYT1 after a hypertonic shock, oocytes were shocked in 450 mOsM mKSOM (Figure 13) following the same protocol as above in 5.1b, Figure 6. In contrast to 1000 mOsM, oocytes were able to fully recover by 5 min and 10 min. Therefore, going forward we chose to use a hypertonic shock of 450 mOsM on the oocytes with a recovery time of 7.5 min to limit the time between assays.

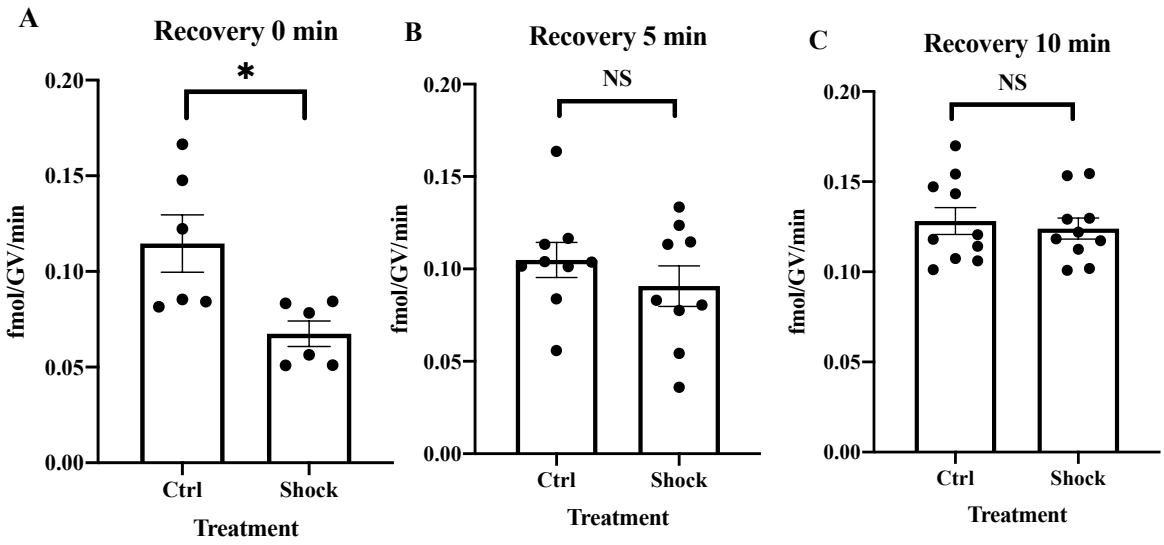

Figure 13: GLYT1 transporter recovery following 450 mOsM hypertonic shock

The rate of [^{3}H]-glycine transport by GLYT1 was measured following exposure to a hypertonic shock of 450mOsM mKSOM on the same cohort of oocytes. The assays were performed on groups of oocytes that were incubated for 1.5 hr following removal from the follicle. Oocytes were left to recover from the hypertonic shock for **(A)** 0 min, **(B)** 5 min or **(C)** 10 min prior to performing the GLYT1 activity assay (recovery 0 min, n = 6, recovery 5 min, n = 9, recovery 10 min, n = 10.) The difference between means was analyzed by t-test (*$P < 0.05$).

5.1i. GLYT1 activity and oocyte-adhesion assay both performed on individual oocytes

To directly correlate ZP-release with GLYT1 activity, both assays were performed on the same individual oocytes (Figure 14). Oocytes were cultured prior to experimentation, with experiments performed in 15 min intervals up to 1 hr, followed by 30 min intervals up to 2.5 hr post isolation from the follicle. Oocytes were osmotically shocked with 450 mOsM mKSOM and imaged immediately using a Nikon E4500 camera mounted on a Zeiss Axiovert microscope to measure their ZP detachment score. Oocytes were left to recover in 250 mOsM mKSOM for 7.5 min prior to performing the GLYT1 activity assay, where an individual oocyte was incubated for 10 min in 3 μM [^{3}H]-glycine. Since all oocytes were going through stages of development at different times, this allowed for the association of a specific oocyte detachment score with a specific rate of glycine transport. GLYT1 activity turns on when the oocytes partially detach from the ZP, between a score of 3 and 4.

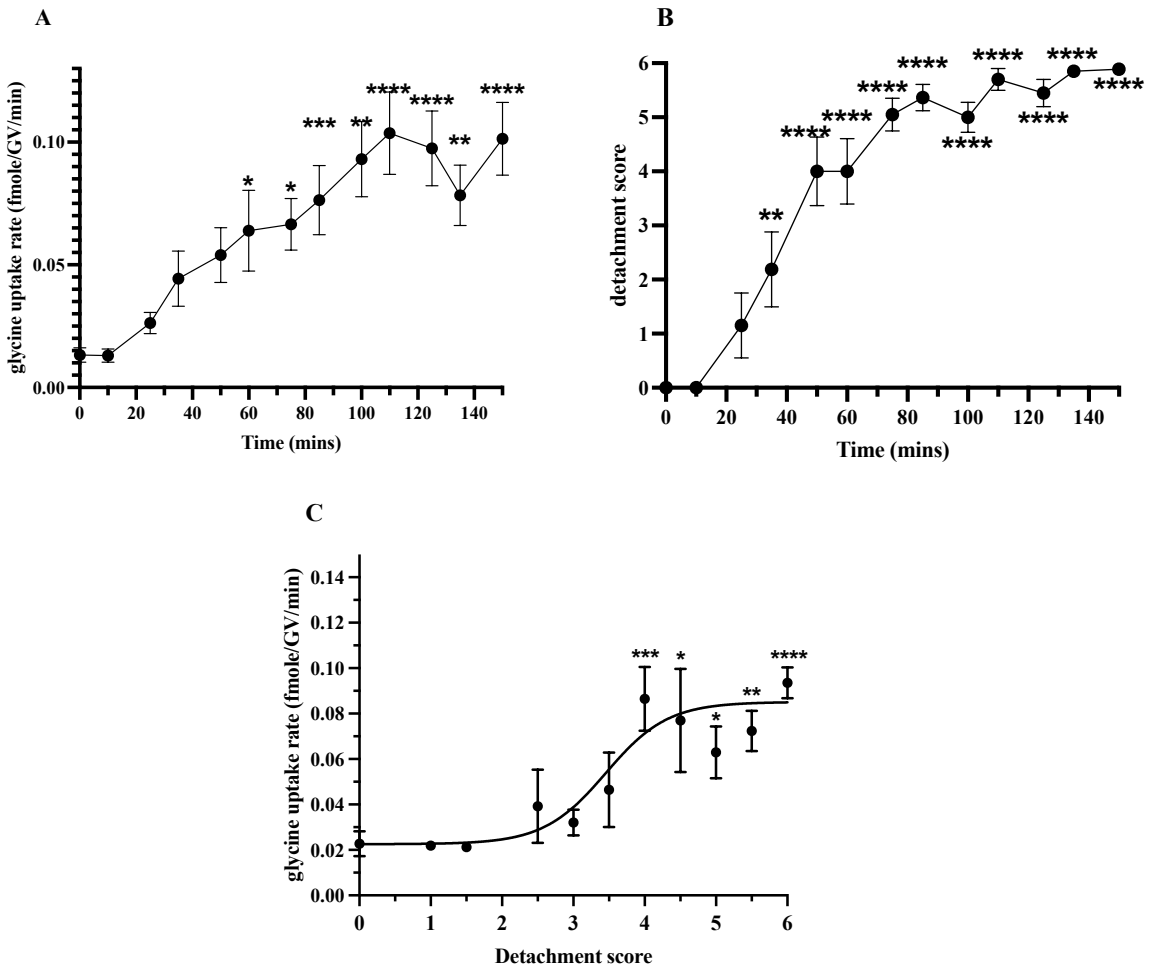

Figure 14: The GLYT1 activity and oocyte-adhesion assays performed on individual oocytes

(A) The GLYT1 activity assay and oocyte-ZP adhesion assay were performed on the same individual oocyte to directly correlate ZP release with GLYT1 activation (n = 10 per time point). GV oocytes were incubated in 250 mOsM mKSOM for various times points from 0hr to 2.5 hr, followed by an osmotic shock in 450 mOsM mKSOM to determine the detachment score. All oocytes were left to recover for 7.5 min prior to performing the GLYT1 activity assay, where individual oocytes were incubated in 3 μM [^{3}H]-glycine for 10 min. **(A)**

GLYT1 activity vs time, with one-way ANOVA performed to compare all means to control (t = 0). **(B)** Detachment score vs time, with one-way ANOVA performed to compare all means to control (t = 0). **(C)** GLYT1 activity vs detachment score. The circles represent an oocytes detachment score and the corresponding amount of glycine taken up at that time (mean ± SEM, n = 10). The data was fit to a sigmoidal dose-response curve.

5.2. Detachment of ZP is required for the activation of GLYT1

5.2a. Effects of metallopeptidase inhibitors

To assess metallopeptidase involvement in oocyte-ZP detachment, inhibitors were used to prevent their activity. Two broadly selective inhibitors for members of the M10 and M12 families of metallopeptidases, known as marimastat and batimastat, were used, as well as one selective small molecule inhibitor for ADAM10, known as GI254023x. These had been identified in a screening performed by another member of the laboratory, A. Macaulay (Macaulay et al., 2023). To investigate their relative potencies, dose-response curves were performed. In Figure 15 below, groups of ~10 denuded oocytes were cultured in 250 mOsM mKSOM for 1.5 hr post isolation from the follicle, in the presence of one of the three metalloprotease inhibitors at multiple concentrations from 0 μM to 40 μM. Following culture, oocytes were osmotically shocked in 1000 mOsM to clearly determine detachment score. At 1.5 hr, the IC50 for least potent inhibitor, marimastat, was 7.6 μM (95% CI 4.2 - 15.3), whereas batimastat was 6.4 μM (95% CI: 3.8 - 11.3), and the most potent was GI254023x with an IC50 of 2.2 μM (95% CI 1.5 - 3.6).

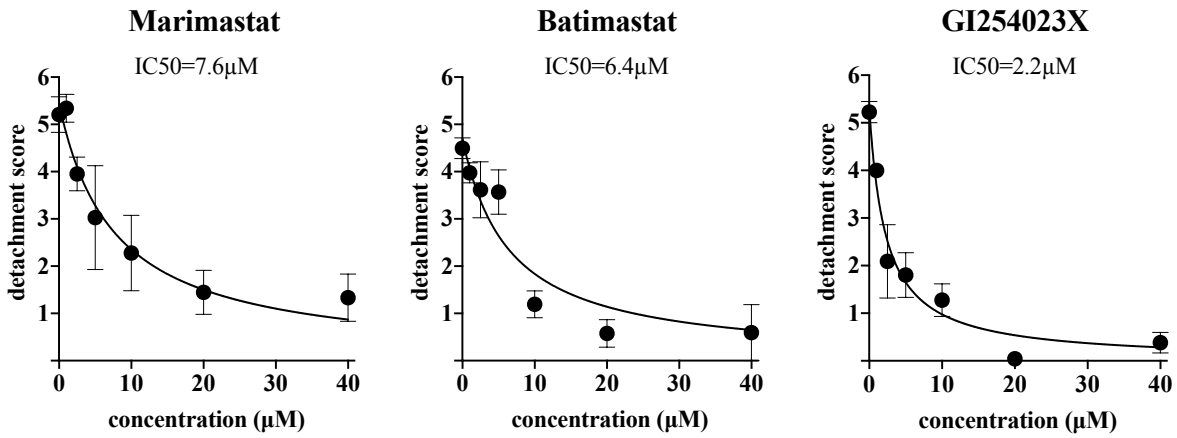

Figure 15: Inhibitor dose response after 1.5 hr incubation

The oocyte-ZP adhesion assay was performed on groups of oocytes incubated for 1.5 hr in mKSOM with the addition of the metalloprotease inhibitors marimastat, batimastat and GI254023X at the various concentrations. At 1.5 hr, oocytes were osmotically shocked in 1000 mOsM Hepes-mKSOM. An average was taken for an n = 5 at each concentration.

To test whether the inhibition of oocyte-ZP detachment would persist for a longer period of time, the same metallopeptidase inhibitors were tested at 4 hr post-isolation from the follicle (Figure 16), as oocytes have completely detached from the ZP by such time (Richard et al., 2017; Tartia et al., 2009). The same protocol from Figure 10 was used (with the highest concentration for marimastat increased to 50 μM as marimastat was found to be the least effective). At 4 hr, each inhibitor still significantly blocked ZP detachment. The IC50 was 18 μM for marimastat (95% CI 13 - 25), 1.4 μM (95% CI 0.6 - 2.5) for batimastat and 1.7 μM (95% CI 0.7 - 3.0) for GI254023x.

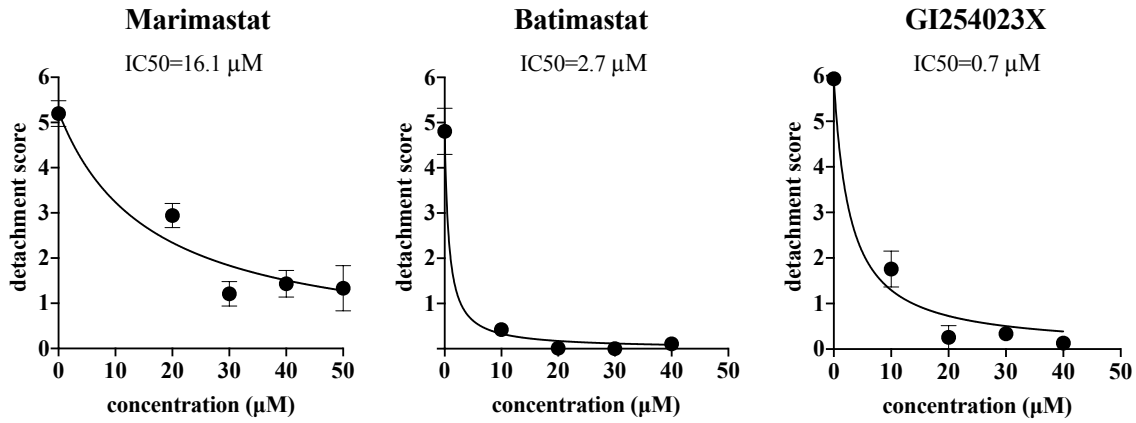

Figure 16: Inhibitor dose response after 4 hr incubation

The oocyte-ZP adhesion assay was performed on groups of oocytes incubated for 4 hr in mKSOM with the addition of the metalloprotease inhibitors marimastat, batimastat and GI254023X at the various concentrations. At 4 hr, oocytes were osmotically shocked in 1000 mOsM Hepes-mKSOM. An average was taken for an n = 5 at each concentration.

5.2b. GLYT1 activity and protease inhibitors

Since GI254023x and batimastat were found to be the most potent inhibitors, only these two were used for most experiments going forward. To test whether ZP release is required for GLYT1 activation, the GLYT1 activity assay was performed on oocytes in the presence of the metalloprotease inhibitors (Figure 17). Groups of ~10 denuded oocytes were cultured for 4 hr in control media (250 mOsM mKSOM with 10 μM Milrinone only) or a high concentration of either GI254023x or batimastat (40 μM of inhibitor, plus 10 μM Milrinone). Milrinone was included to maintain arrest at the GV stage. The protocol for the GLYT1 activity assay on groups used here was the same as described above, with the additional of 40 μM inhibitor in the radioactive drop for the treatment group. Both inhibitors were able to prevent GLYT1 activity when compared to the control. Out of the three, batimastat was the most effective. Overall, these data suggests that ZP release from the oocyte is involved in the activation of GLYT1.

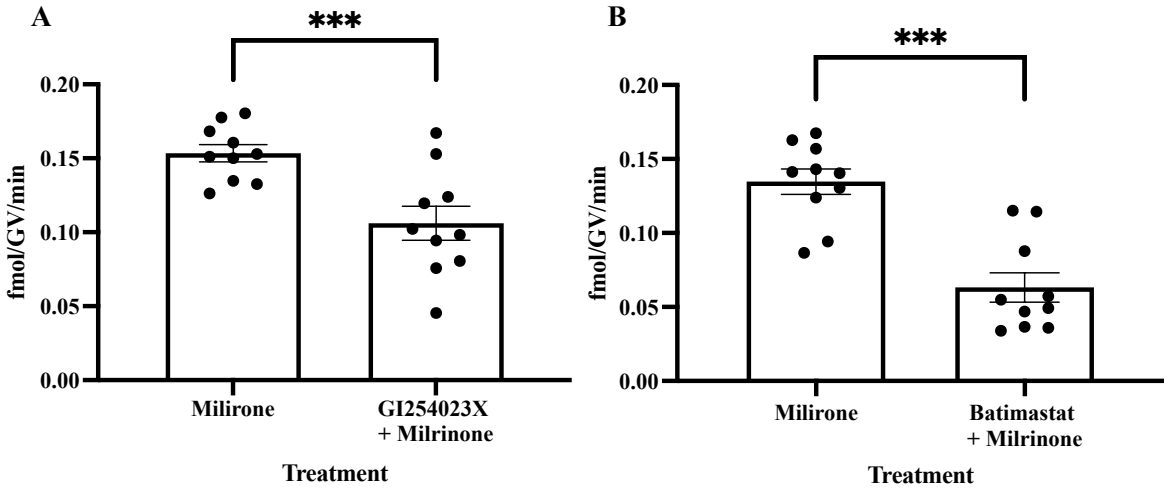

Figure 17: Glycine transport in oocytes in the presence of protease inhibitors

The rate of [^{3}H]-glycine transport by GLYT1 measured in oocytes exposed to 40 μM GI254023X or batimastat (n = 7 and n = 8, respectively) at 4 hr post isolation from the follicle. Groups of oocytes were incubated in mKSOM with Milrinone (control), plus addition of inhibitor (treatment). Milrinone was included to maintain arrest at the GV stage. GI254023x and batimastat were both effective at inhibiting GLYT1 transport. The significant difference between the presence and absence of GI254023X/batimastat was determined by t-test analysis (*$P < 0.05$). An average was taken from an N = 10.

5.2c. Inhibitor reversibility on oocyte-ZP adhesion

Batimastat and GI254023x were tested for a reversible inhibitory effect (Figure 18). Groups of ~10 denuded oocytes were cultured in control media (250 mOsM mKSOM) or with the addition of a high concentration of inhibitor (40 μM) for 4 hr. Both groups maintained oocyte-ZP attachment as expected. However, when oocytes cultured in GI254023x were washed out of inhibitor and left to culture in inhibitor-free media, they became partially detached by 0.5 hr and completely detached by 2.5 hr, with detachment scores at such points very similar to the control. Whereas in contrast, batimastat was ineffectively reversible, with no detachment by 0.5 hr and only partial detachment by 2.5hr.

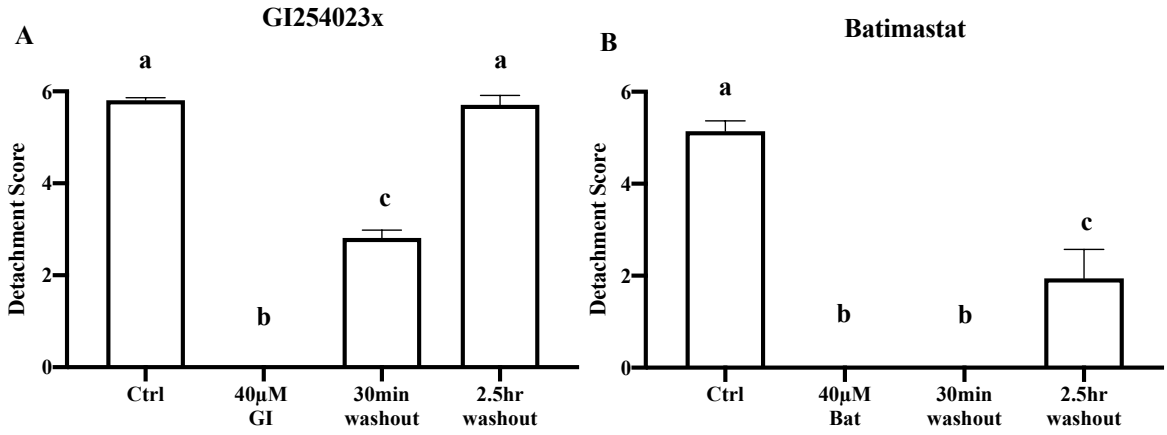

Figure 18: Inhibitor reversibility for oocyte detachment

The oocyte-ZP adhesion assay was performed on oocytes exposed to protease inhibitors, followed by inhibitor washout to test reversibility. Groups of oocytes incubated in mKSOM with a selective inhibitor of either **(A)** GI254023x and **(B)** Batimastat at a concentration of 40 µM for 4 hr. Oocytes were hypertonically shocked with 1000 mOsM Hepes-mKSOM following removal from inhibitor after an incubation of either 0.5 hr or 2.5 hr. GI254023x inhibition was reversible after inhibitor was washed out. Batimastat was very poorly reversible by 2.5 hr. An average was taken from an n = 6 for ctrl and 40 µM GI groups and an n = 3 for each washout group. The means that do not share the same letter are significantly different ($P < 0.05$ by ANOVA with Tukey's test).

5.2d. Inhibitor reversibility on GLYT1 activity

To determine the reversibility of the inhibition of oocyte-ZP detachment with GI254023x on the activity of GLYT1, the GLYT1 activity assay was performed after washout of the inhibitor (Figure 19). Groups of ~10 denuded oocytes were cultured in 40 μM GI254023x with 10 μM of Milrinone for 4 hr. Oocytes were split into two groups, with one group going straight into the GLYT1 activity assay and the other group left to culture in inhibitor-free media for 2.5 hr before performing the assay. There was no significant difference between GLYT1 activity when exposed to inhibitor and after washing it out.

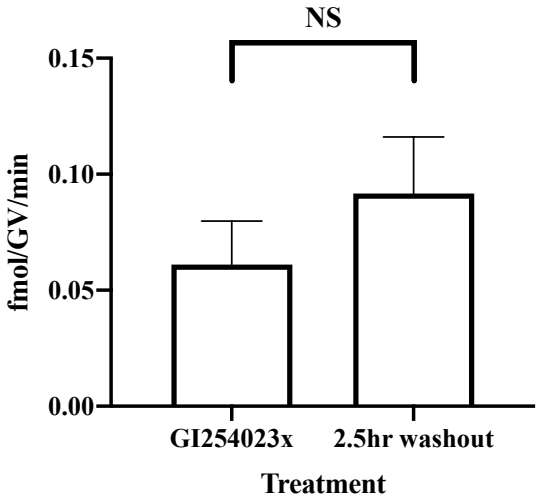

Figure 19: Inhibitor reversibility for GLYT1 transport

The rate of [^{3}H]-glycine transport by GLYT1 was assessed for reversibility after exposure to MMP inhibitor GI254023x. All oocytes were cultured in 40 µM GI254023X and 10 µM of Milrinone for 4 hr, followed by half the oocytes placed in the GLYT1 activity assay and the other half washed out of inhibitor and left to culture for 2.5 hr before performing the assay. An average was taken from an N = 3. Statistical analysis was performed using a two tailed t-test, with no significant difference found between means of groups (P = 0.3740).

5.3 Removal of ZP does not accelerate GLYT1 activation in oocytes

Prior to ovulation, oocyte size and volume are passively determined by its strong adhesion to the ZP. However, upon ovulation or removal from the follicle, oocyte-ZP attachment starts to release and the oocyte volume decreases, forming a distinct perivitelline space between the ZP and the oocyte. Since the oocyte-ZP attachment releases as GLYT1 activates, leading to commencement of independent cell volume regulation, we predicted that removal of the ZP would accelerate GLYT1 activation in oocytes.

5.3a. Oocyte volume in ZP intact and ZP free oocytes

To determine whether volume decrease was accelerated upon ZP removal, a series of images were taken of oocytes using a Nikon E4500 camera mounted on a Zeiss Axiovert microscope equipped with an environmental control chamber (Figure 20). Oocytes were maintained at 37 °C in 5% CO_2 and air, with images taken every 2 min up to 1 hr, followed by every 20 min up to 3 hr with brightfield mode and phase contrast at 20x objective. Acid Tyrode's solution was used to rapidly solubilize the glycoproteins that form the ZP (Gordon & Talansky, 1986; Nicolson et al., 1975). This removes the ZP matrix around the oocyte, while leaving the innermost layer of ZP proteins unaffected and attached as transmembrane proteins in the oocyte plasma membrane, as previously reported (Coonrod et al., 2004; Macaulay et al., 2023). Immediately following collection, half the oocytes were exposed to Acid Tyrode's (details listed materials and methods) to remove the ZP and the other half were left unaffected. The oocytes exposed to Acid Tyrode's were washed with mKSOM to remove any excess, followed by pooling all oocytes together (ZP-free and ZP-intact) to place

into an environmental chamber with PVA-free mKSOM as this allows oocytes to stick and remain attached to the bottom of the chamber for imaging.

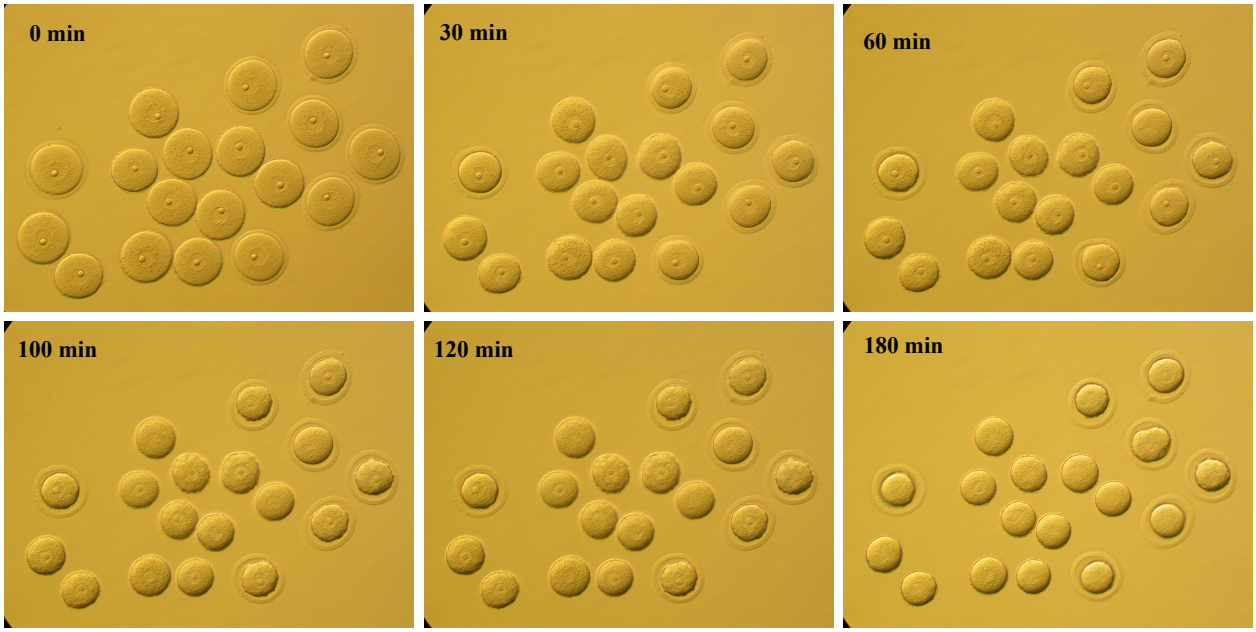

Figure 20: Zona pellucida removal and volume decrease

A series of photos were taken (only a few examples are presented here) to measure volume decrease over time for ZP intact and ZP-free oocytes. The ZP was removed from oocytes with Acid Tyrode's to see whether it would increase the rate of volume decrease. Oocytes were cultured in 250 mOsM PVA free mKSOM in a chamber at 37°C, 5%CO_2 and air, with photos taken every 2 min up to 1 hr, followed by every 20 min up to 3 hr.

To determine if the volume decrease was accelerated in ZP-free oocytes, the compilation of photos used to create the video were used to take an average diameter from each oocyte (Figure 21). Oocyte volume was calculated with assumption that it could be approximated as a sphere, with an average taken from two measured diameters of each oocyte which were converted to microns. Averages were taken from ZP-intact and ZP-free oocytes with each group containing ~10 oocytes each. ZP removal showed no acceleration in oocyte volume decrease in comparison to ZP-intact oocytes. Fully grown oocytes at ~85 μm decreased in volume down to ~60 μm in 3 hr at the same rate for both ZP-intact and ZP-free oocytes.

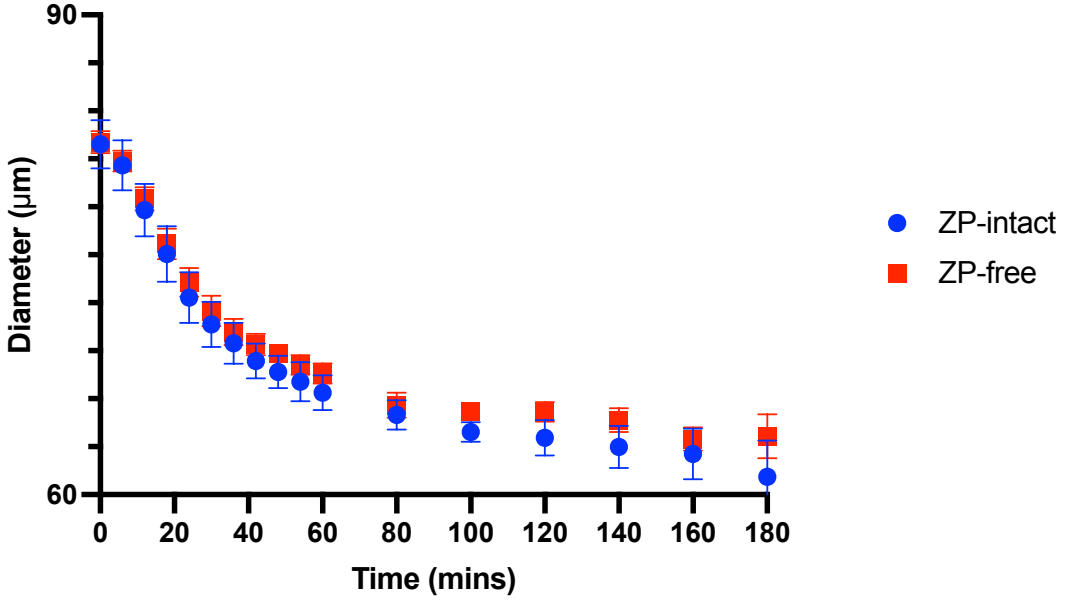

Figure 21: Average oocyte diameter over time

The rate of volume decrease was measured in oocytes with and without their ZP over 3 hr. All oocytes were cultured in 250mOsM PVA free mKSOM in a chamber at 37°C, 5%CO_2 and air, with photos taken every 2 min up to 1 hr, followed by every 20 min up to 3 hr. An average was taken from an N = 3. Performed 2-way ANOVA of main effects (ZP vs no ZP, time). Variation with time was significant ($P < 0.0001$) and ZP vs no ZP was not significant ($P = 0.49$).

5.3b. GLYT1 activity in ZP-free and ZP-intact oocytes

To determine whether removal of the ZP accelerates GLYT1 activity in oocytes, the rate of glycine transport was measured over time for ZP-free and ZP-intact oocytes (Figure 22). Oocytes were collected and divided into two groups with ~10 oocytes per group and one group had their ZP removed with Acid Tyrode's. All oocytes were cultured in mKSOM with 10 μM Milrinone for a desired time point post isolation from the follicle until the GLYT1 activity assay was performed (following the protocol for groups of oocytes listed above). Interestingly, ZP-free oocytes showed no faster increase in GLYT1 activity when compared to ZP-intact oocytes.

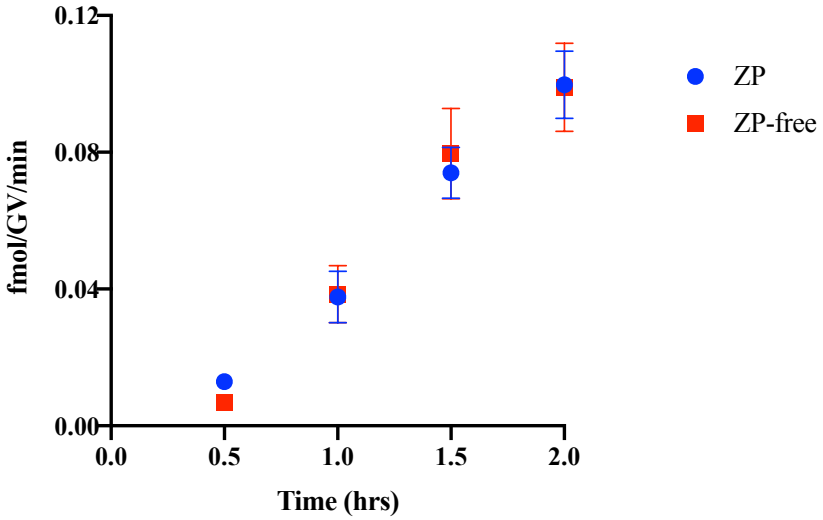

Figure 22: GLYT1 activity in ZP-intact and ZP-free oocytes

The rate of [^{3}H]-glycine transport by GLYT1 was measured in ZP-intact and ZP-free oocytes. Both groups were incubated in mKSOM with 10 µM of Milrinone for the desired time point post isolation from the follicle, followed by incubation within the same radioactive drop with 1 µM [^{3}H]-glycine in mKSOM under oil for 10 min. An average was taken from an N = 5. Performed 2-way ANOVA of main effects (ZP vs no ZP, time). Variation with time was significant ($P < 0.0001$) while ZP vs no ZP showed no difference ($P = 0.99$).

5.3c. GLYT1 activity and osmolarity-induced cell volume change

To determine if GLYT1 activation is stimulated by a decrease in cell volume, the rate of glycine transport was measured in oocytes cultured in isotonic or hypertonic media (Figure 23). Oocytes were collected, their ZP removed with Acid Tyrode's and they were immediately placed in media of 250 mOsm or 310 mOsM. Osmolarity was increased with D(+)-raffinose as previously described (Dawson & Baltz, 1997). Oocytes were incubated for 50 min prior to measuring GLYT1 activity, as this point is right before GLYT1 activity largely starts to increase. The protocol used for the GLYT1 activity assay on groups of oocytes was the same as listed above, however the osmolarity of the radioactive drops for both groups were increased to 310 mOsM. The activity of GLYT1 did not increase when oocyte volume was decreased experimentally, which suggests a volume decrease on its own does not activate GLYT1.

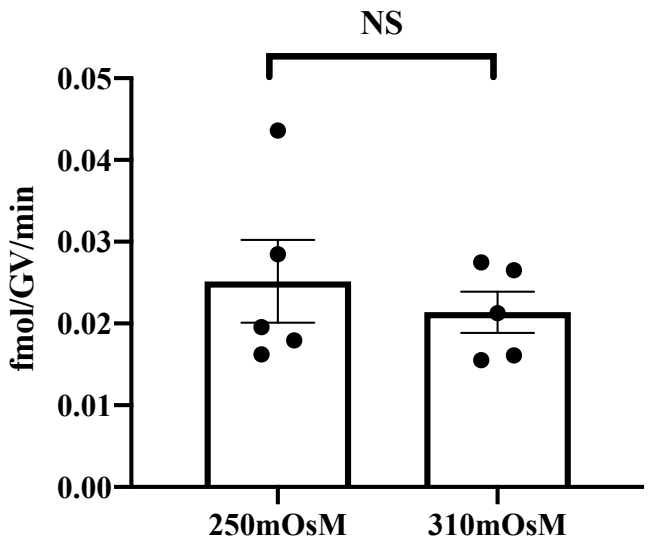

Figure 23: GLYT1 activity in ZP-free oocytes

The rate of [^{3}H]-glycine transport by GLYT1 was measured in ZP-free oocytes at 250 mOsM and 310 mOsM mKSOM. Media osmolarity was increased with the addition of Raffinose. The ZP was removed by short exposure to Acid Tyrode's. At 50 min post isolation from the follicle, all the oocytes were placed in 1 μM [^{3}H]-glycine mKSOM at an osmolarity of 310 mOsM for 10 min. An average was taken from an N = 5. The difference between means for GLYT1 activity in 250 mOsM and 350 mOsM mKSOM were analyzed by a two-tailed t-test and were not found to be significantly different (P = 0.5233).

5.3d. Inhibition of GLYT1 activity in ZP-intact and ZP-free oocytes

Since transmembrane proteins remain in the oocyte following ZP removal with Acid Tyrode's, it was of interest to examine whether the MP inhibitors act on transmembrane ZP and to thus in turn, suppress the activity of GLYT1. Oocytes were separated into four different treatments: no ZP with inhibitor, no ZP with no inhibitor, ZP with inhibitor and ZP with no inhibitor (Figure 24). The media for all groups was mKSOM that contained 10 μM of Milrinone, while the groups with inhibitors had the addition of either GI254023x, batimastat or marimastat that were used at a higher concentration of 40 μM. The GLYT1 activity assay protocol for groups used here was the same as described above. These results show that

MP inhibitors have an effect on ZP-intact oocytes in the presence of inhibitors as demonstrated previously. However, the MP inhibitors only have a slight effect in the absence of a ZP and that the effect is smaller than with a ZP and in two of three cases was not significant.

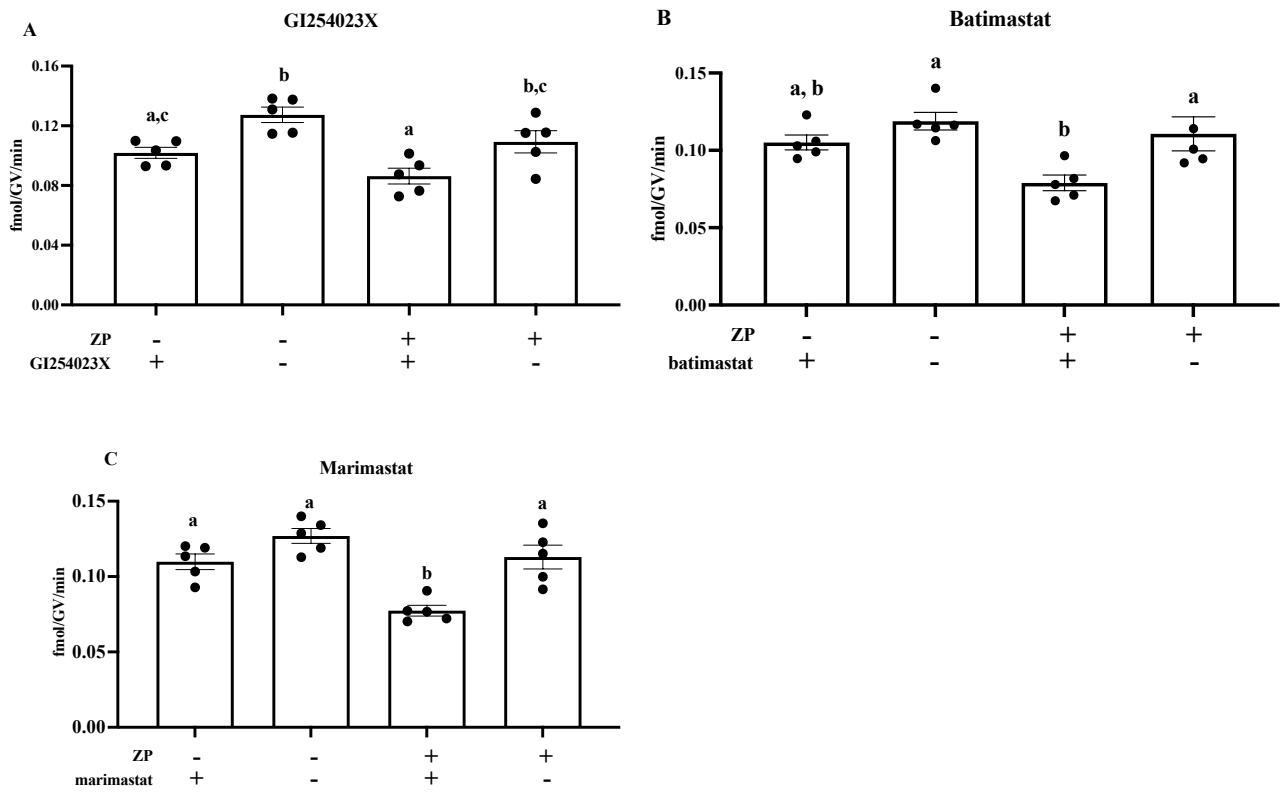

Figure 24: GLYT1 activity in ZP-intact and ZP-free oocytes in the presence or absence of MMP inhibitors

The rate of [^{3}H]-glycine transport by GLYT1 was measured in ZP-intact and ZP-free oocytes in the presence or absence of metalloprotease inhibitors, **(A)** GI254023x, **(B)** batimastat and **(C)** marimastat. The ZP was removed with short exposure to Acid Tyrode's. The various groups of oocytes were incubated for 4 hr post isolation from the follicle, with 10 µM of milrinone and some groups had the presence of 40 µM of inhibitor where listed. Oocytes were incubated in 1 µM [^{3}H]-glycine for 10 min. An average was taken from an N = 5. Bars that do not share the same letters are significantly different means ($P < 0.05$ by ANOVA with Tukey test). For GI254023X only, it is marginally significant with no ZP ($P = 0.03$).

5.4 TIMPs did not inhibit the release of the ZP from the oocyte

Since the chemical inhibitors showed successful inhibition of the MMPs responsible for ZP detachment from the oocyte, it was also of interest to examine whether physiological inhibitors of MMPs, TIMPs, were also able to prevent ZP detachment from oocytes (Figure 25). Thus, the oocyte ZP adhesion assay was performed on oocytes cultured with TIMPs-1,2,3 and 4. Groups of ~10 denuded oocytes were cultured for a total of 4 hr post isolation from the follicle. For the first 1.5 hr, oocytes were incubated with the chemical MMP inhibitor, GI254023x (control group) plus the addition of 1 μM TIMP (treatment group) to allow the TIMP, as it is a larger protein, to work its way through the ZP. Oocytes were washed and moved to either a control media (250mOsM mKSOM) or medium with 1 μM TIMPs only, for 2.5 hr. Once oocytes were incubated for a total of 4 hr, oocytes were hypertonically shocked with 1000 mOsM Hepes-mKSOM to determine their detachment score. Surprisingly, none of the four different TIMPs were able to prevent ZP detachment from the oocyte.

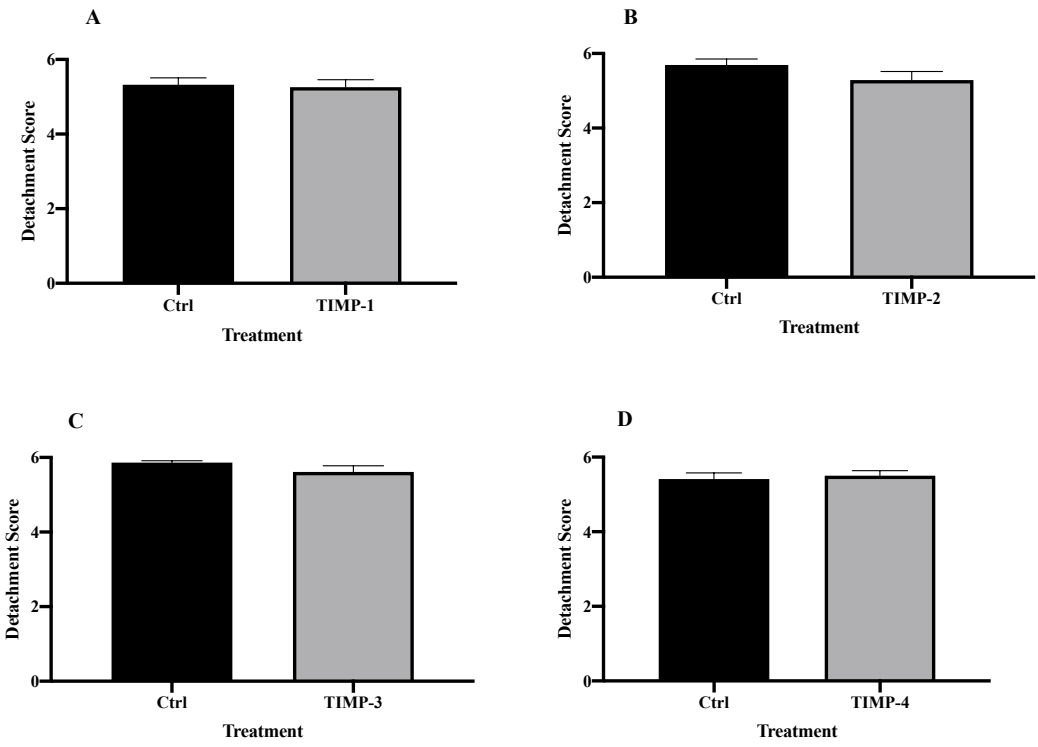

Figure 25: TIMPs and oocyte detachment

The oocyte-ZP adhesion assay was performed on oocytes exposed to the natural metalloproteinase inhibitors, TIMPs 1 to 4. Groups of oocytes were cultured for a total of 4 hr post isolation from the follicle. For the first 1.5 hr, oocytes were incubated with the chemical MP inhibitor, GI254023x (control group) plus the addition of 1 μM TIMP (treatment group). Oocytes were washed and switched for 2.5 hr to either mKSOM (control group) or with the addition 1 μM TIMPs (treatment group) only. At 4 hr, oocytes were shocked with 1000 mOsM Hepes-mKSOM to determine detachment score. An average was taken from an N = 5. There was no significant difference between means when two-tailed t-test was used to analyze the ZP detachment score in the presence and absence of TIMPs (figure (A) TIMP-1, P = 0.8100, figure (B) TIMP-2 = 0.1541, figure (C) TIMP-3, P = 0.1928, figure (D) TIMP-4, P = 0.6845).

6. Discussion

6.1 The oocyte-ZP release precedes the activation of GLYT1

Prior to ovulation or removal from the follicle, the oocyte is unable to regulate its own cell volume and is dependent on the tight adhesion through microvilli to the zona pellucida, which is responsible for maintaining oocyte cell volume (Richard et al., 2017). At this point, the ability of the ZP to detach from the oocyte and GLYT1 activity are suppressed by an unknown inhibitory mechanism. It has been suggested that the putative inhibitory signal arises from MGCs, as it has been demonstrated that a MGC monolayer was able to suppress the activation of GLYT1 in COCs *in vitro*, however the identity of this inhibitor and the signaling pathway involved remains to be elucidated (Richard et al., 2017). However, as ovulation is triggered, this inhibition is released shortly thereafter and followed by a decrease in oocyte cell volume. Within several hours, the initiation of independent cell volume commences with the detachment of the ZP from the oocyte and the activation of GLYT1, occurring well prior to ovulation where the oocyte leaves the follicle and enters the oviduct (occuring 12 – 16 hr post LH surge). In fully grown oocytes, these processes progress around the same time while following a similar time course. Previous research conducted in our laboratory focused on observing these two mechanisms in separate experiments carried out at different times and was not designed with the intention of comparing time courses (Richard et al., 2017; Tartia et al., 2009). Therefore, although it was found that these two processes occurred at a very similar time course, with the postulation that detachment of ZP from the oocyte slightly precede GLYT1 activation, it was not possible to determine this definitively. Thus, I sought to examine the precise temporal relationship between the two distinct cell

volume regulation processes of ZP-oocyte detachment and GLYT1 activation by performing time courses of each in a quantitative manner.

Here, I showed that upon isolation from the ovaries, the activity of GLYT1 is quiescent but quickly increases, reaching a half-maximal activity by 1.5 hr and maximal capacity by 4 hr, which was consistent with previous data (Tartia et al., 2009). Additionally, to determine the exact detachment score and the corresponding glycine uptake in an individual oocyte, the GLYT1 activity assay was performed on individual oocytes along with the standard protocol of performing on groups, and results demonstrated that the activation of GLYT1 showed the same time-dependence for both.

The results from the oocyte-ZP detachment assay I performed on fully grown oocytes demonstrated a clear similarity to the activation of GLYT1, supporting previous speculations from our laboratory. The results demonstrated that upon immediate removal from the follicle, oocytes remained completely attached to the ZP, while ~50% of fully grown GV oocytes were partially detached by ~1 hr following isolation from the follicle. By 2.5 hr, essentially all oocytes had become completely detached, demonstrating consistency with previous work (Richard et al., 2017).

Upon examination through separate experiments, I have found that oocyte-ZP detachment precedes GLYT1 activation, with a shift in the activation of GLYT1 by 20 min. However, as the time between oocyte-ZP detachment and GLYT1 activation is quite short, whether GLYT1 activation precedes oocyte-ZP detachment remained unclear. Therefore, I performed both assays on the same individual oocytes to demonstrate that detachment status of each oocyte predicts its GLYT1 activity. Moreover, this followed the same trend that, as the ZP-detachment increases, so does the rate of glycine uptake by the GLYT1 transporter. Although the mechanisms for how GLYT1 activates and oocyte-ZP detaches remains

unknown, this data demonstrated consistency with the possibility that detachment could be upstream of GLYT1 activation.

6.2 Oocyte-ZP detachment is required for GLYT1 activation

Although the time courses for oocyte-ZP detachment and GLYT1 activation were consistent with the hypothesis that detachment possibly triggers GLYT1 activation, demonstrating that detachment of the ZP from the oocyte was found to precede GLYT1 activation and that a greater detachment score is associated with a greater glycine uptake by the oocyte, it did not however establish causality. Therefore, I sought to prevent oocyte-ZP detachment to see if this would also prevent GLYT1 activation. Fortunately, it had been recently found in our laboratory that oocyte-ZP detachment required metallopeptidase activity that occurs during the early stages of meiotic maturation and that metallopeptidase activity could be prevented by several metallopeptidase inhibitors (Macaulay et al., 2023). Consequently, I was able to use the metallopeptidase inhibitors that had been shown to be effective, which were two broad-spectrum inhibitors for M10 and M12 families known as marimastat, batimastat along with one selective small molecule inhibitor for ADAM10 known as GI254023x to be able further study the relationship between oocyte-ZP detachment and GLYT1 activation.

To address the possibility of GLYT1 activation being associated with detachment, the GLYT1 activity assay was performed on oocytes in the presence of the protease inhibitors that demonstrated to be the most effective at preventing ZP-detachment, those being batimastat and GI254023x. Milirone was also added to maintain oocytes in meiotic arrest so that GLYT1 activation was unfolding (Tartia et al., 2009) without any other changes, such as

meiotic progression, to limit complication in interpretation of the data. Additionally, it has previously been shown in our laboratory that GLYT1 activation is the same with and without Milirone (Richard et al., 2017). The inhibitors responsible for preventing ZP detachment from the oocyte also inhibited the activity of GLYT1, suggesting the coupling of these two mechanisms and thus supporting the hypothesis that oocyte-ZP detachment is required for the activation of GLYT1. Alternatively, there is however a possibility that GLYT1 activity and oocyte-ZP detachment are independent of one another, with the activation of GLYT1 being directly controlled by a metallopeptidase rather than the metallopeptidase causing oocyte-ZP detachment which then induces GLYT1 activity. There is also the possibility for the metallopeptidase to be a different one than the one responsible for the oocyte-ZP detachment. In this case, if a metalloprotease is directly responsible, it could be acting through an inhibitory domain that is cleaved off SLC6A9, leading to the activation of GLYT1. This possibility does however seem less likely due to the data presented in Figure 24, since GLYT1 activates almost normally in the presence of metalloprotease inhibitors (GI254023x and batimastat) when the ZP has been removed from the oocyte. However, this remains to be elucidated, with further research required to uncover the mechanism responsible. Inhibitor reversibility was tested to confirm that results were not due to detrimental effects on the oocyte. Oocytes were incubated with inhibitors for 4 hr, at a time in which typically oocytes would be completely detached from their ZP and GLYT1 would be fully activated. Both inhibitors substantially blocked oocyte-ZP detachment and GLYT1 activation. After removing oocytes from the inhibitor, batimastat demonstrated poor reversibility, with oocytes remaining attached to the ZP. However, when GI254023x was washed out, oocytes were able to recover and completely regain the ability to detach from the ZP over time. In regard to the reversibility effects on GLYT1 activation, when comparing

the activation of GLYT1 in the presence of GI254023x and after washing it out, there was no significant difference. Although GI254023x had completely reversible effects on oocyte-ZP detachment, there seems to be a trend that GI254023x is not completely reversible on GLYT1 activity. However, data remains inconclusive as less repetitions were performed for this experiment, for a total of N=3. Thus it is possible that an increase in the number of repetitions would be able to demonstrate a difference in these results. Additionally, future studies could also explore this experiment using a longer oocyte incubation period after washing out the inhibitor, with a total of 4 hr (as opposed to 2.5 hr) at a time at which GLYT1 is completely active. It remains unknown whether the metalloprotease inhibitors effect on GLYT1 is toxic. This could however explain the lack of reversibility demonstrated in the results. However, further experimentation is required to confirm this.

Overall, these results suggest that oocyte-ZP detachment must occur in order for GLYT1 to activate, but the way in which these two mechanisms are coordinated remains unknown. As mentioned above, it is considered likely that upstream mechanisms involve an inhibitory factor in the follicle, however further investigation is required.

6.3 Removal of the ZP did not accelerate GLYT1 activation in oocytes

I was able to uncover the presence of an apparent relationship between oocyte-ZP detachment and GLYT1 activation, with detachment being required prior to GLYT1 activation. Accordingly, we further predicted that removal of the ZP would accelerate GLYT1 activity in oocytes. I first started by determining whether a volume decrease was accelerated upon ZP removal. However, at 250 mOsM, when oocytes had their ZP removed,

they showed no increase in their GLYT1 activity and decreased at the same rate over time as oocytes with intact ZPs.

I then followed by testing whether the removal of the ZP would accelerate the activation of GLYT1 when compared to ZP-intact oocytes in isotonic media, at 250 mOsM. To our surprise, the removal of the ZP from the oocyte showed no acceleration in GLYT1 activity compared to ZP-intact oocytes. Acid Tyrode's solution removes the extracellular ZP matrix, though the transmembrane proteins are unaffected and remain attached to the oocyte. This single layer of intact ZP surrounding the oocyte could possibly be responsible for preventing the acceleration of GLYT1 activity in oocytes. Thus, as the protease responsible cleaves these remaining transmembrane proteins, the detachment would be released and GLYT1 activity will accordingly increase, undergoing the same process at the same rate as ZP-intact oocytes.

As removal of the ZP from oocytes cultured in isotonic media did not accelerate GLYT1 activity, I sought to determine whether removing the ZP alongside inducing a cell volume change by increasing the osmolarity of the media would accelerate the activation of GLYT1. The theory behind this experiment was based on previous work conducted in our laboratory which showed that the total amount of glycine accumulated in one-cell embryos increased with external osmolarity, with accumulation approximately doubling when osmolarity was raised from 250 to 350 mOsM (Steeves & Baltz, 2005), although that occurred over a much longer time. Upon exposing ZP-free oocytes to hypertonic media, results revealed no difference in GLYT1 activity when compared with ZP-free oocytes in isotonic media. Thus, the activity of GLYT1 did not show any correlation to oocyte volume change, which suggests a volume decrease on its own does not initially activate GLYT1.

Lastly, as transmembrane proteins remain on the oocyte surface following ZP removal with Acid Tyrode's, I sought to determine whether metallopeptidase inhibitors act on these transmembrane ZP proteins, preventing their detachment from the oocyte and thus in turn, suppressing the activity of GLYT1. The results indicated that metallopeptidase inhibitors only have a slight effect on the inhibition of GLYT1 activity in ZP-free oocytes, while showing to be the most effective on ZP-intact oocytes. It remains unknown as to whether metallopeptidase inhibitors were actually able to prevent the detachment of the transmembrane proteins from the oocyte, leading to the initiation of GLYT1 activity. As an intact ZP is required for suppression of GLYT1, this could suggest the possibility for GLYT1 activation being due to a mechanotransduction, with the oocyte letting go of the rigid ZP and the release of tension as the oocyte shrinks could signal downstream effects. To test this hypothesis and for a better understanding of this mechanism, additional research is required.

6.4 TIMPs did not inhibit the release of the ZP from the oocyte

TIMPs play an important role in the extracellular matrix of cells, regulating the activity of MMPs through inhibition via tight, non-covalent binding (Brew & Nagase, 2010). As chemical inhibitors have been found to effectively inhibit the MMPs responsible for ZP-oocyte adhesion release, I hypothesized that physiological inhibitors, TIMPs, would similarly inhibit ZP release. TIMPs are large proteins that vary in size from 21 - 34 kDa, depending on the degree of glycosylation (Lambert et al., 2004). To allow time for the large TIMP proteins to work their way through the porous ZP to inhibit the MMP prior to triggering detachment, oocytes were incubated in media with TIMPs along with chemical inhibitors for 1.5 hr. This was followed by washing oocytes to remove the presence of any chemical inhibitor and

moving oocytes to a media with only TIMPs for another 2.5 hr. Unexpectedly, none of the four TIMPs were able to prevent the ZP detachment from the oocyte and in order to confirm these results to prove that TIMPs are indeed active, a control experiment for TIMPs activity is required. Due to lack of ability for TIMPs to inhibit detachment, we did not pursue this experiment further, however future studies through different ways of investigating inhibition via TIMPs, such as testing all TIMPs in combination or microinjecting TIMPs between the ZP and oocyte plasma membrane could be tested to confirm this. The inability of TIMPs to prevent oocyte-ZP detachment could suggest that it is not the TIMPs within the follicle that are responsible for inhibiting the activity of the metallopeptidase present between the ZP and the oocyte surface. There could be other factors responsible for inhibiting detachment in the follicle at play here, however future investigation is required to further understand this and to uncover the mechanism at play.

7. Conclusion

The results presented in my thesis have revealed certain aspects of the relationship between oocyte-ZP detachment and GLYT1 activation, providing further understanding into how oocytes independently regulation their own cell volume. My experimental data has shown that detachment of the ZP from the oocyte precedes GLYT1 activation. The ability for specific metalloprotease inhibitors (responsible for preventing oocyte-ZP detachment) to prevent the activation of GLYT1 suggests the coupling of these mechanisms. Based on my results, I hypothesized that removal of the ZP would accelerate the activation of GLYT1, however, the results showed no acceleration upon removal. This could potentially be due to the transmembrane proteins of the ZP that remain with the oocyte after removal, preventing the activation of GLYT1 until they detach. Additionally, as the ZP was removed from the oocyte and placed in isotonic or hypertonic media, the results showed a similar trend between groups, suggesting that a volume decrease on its own does not activate GLYT1, and that something else is at play here that remains to be elucidated. Lastly, as TIMPs, an important player of endogenous MMP inhibition, were unable to prevent oocyte-ZP detachment, this could suggest that it is not the TIMPs within the follicle inhibiting the metallopeptidase present at the oocyte surface responsible for the ZP detachment, but some other factor present in the follicle. However, further experimentation is required to elucidate the mechanisms of independent cell volume regulation in oocytes.

8. Significance

Here, I have shown that the detachment status of the ZP for each oocyte predicts its GLYT1 activity. Furthermore, I was able to show how these two important independent cell volume regulation mechanisms are coupled, as inhibiting the metalloprotease responsible for ZP detachment was able to inhibit the activity of GLYT1. Since the data suggests that TIMPs are not the factor inhibiting the metalloprotease responsible for ZP detachment from the oocyte, and since much about these two mechanisms and how they are suppressed within the follicle remains unknown, further investigations are required. A better understanding of these independent cell volume regulations will provide more insight into oocyte physiology before and after ovulation, contributing to the improvement of oocyte culture technologies and their outcomes. An important ART is cryopreservation of human gametes to allow for use at a later time, while keeping them in good health. However, this procedure is found to be a major source of osmotic stress on oocytes, as the cryoprotectants required for post-thaw survival greatly increases the osmolarity. The osmotic stress to the oocyte upon freezing and thawing may be damaging to the oocyte, however, it is suggested it may be rescued by the addition of glycine to culture media (Tscherner et al., 2021). Since glycine can play an important role in oocyte cell volume regulation, especially when involved in many different clinical techniques as oocytes spend extended periods outside their normal in vivo environment, it is crucial to uncover these indispensable mechanisms of cell volume regulation.

9. Literature cited

Adams, C.E. (1956). Egg transfer and fertility in the rabbit. Third Int. Congr. Anim. Reprod., Cambridge, Section 3, pp. 5-8.

Alam, M. H., & Miyano, T. (2019). Interaction between growing oocytes and granulosa cells in vitro. *Reproductive Medicine and Biology*, *19*(1), 13–23.

Alexandre, H. (2001). A history of mammalian embryological research. *The International Journal of Developmental Biology*, *45*(3), 457–467.

Andreini, C., Banci, L., Bertini, I., Elmi, S., & Rosato, A. (2005). Comparative analysis of the ADAM and ADAMTS families. *Journal of Proteome Research*, *4*(3), 881–888.

Aragón, C., & López-Corcuera, B. (2003). Structure, function and regulation of glycine neurotransporters. *European Journal of Pharmacology*, *479*(1–3), 249–262.

Araújo, V. R., Gastal, M. O., Figueiredo, J. R., & Gastal, E. L. (2014). In vitro culture of bovine preantral follicles: A review. *Reproductive Biology and Endocrinology : RB&E*, *12*, 78.

Aroeira, R. I., Sebastião, A. M., & Valente, C. A. (2014). GlyT1 and GlyT2 in brain astrocytes: Expression, distribution and function. *Brain Structure and Function*, *219*(3), 817–830.

Baena, V., & Terasaki, M. (2019). Three-dimensional organization of transzonal projections and other cytoplasmic extensions in the mouse ovarian follicle. *Scientific Reports*, *9*(1), 1262.

Baltz, J. M. (2001). Osmoregulation and cell volume regulation in the preimplantation embryo. *Current Topics in Developmental Biology*, *52*, 55–106.

Baltz, J. M. (2013). Connections between preimplantation embryo physiology and culture. *Journal of Assisted Reproduction and Genetics*, *30*(8), 1001–1007.

Baltz, J. M., & Zhou, C. (2012). Cell volume regulation in mammalian oocytes and preimplantation embryos. *Molecular Reproduction and Development*, *79*(12), 821–

Biggers, J. D. (1998). Reflections on the culture of the preimplantation embryo. *The International Journal of Developmental Biology*, *42*(7), 879–884.

Biggers, J. D., Lawitts, J. A., & Lechene, C. P. (1993). The protective action of betaine on the deleterious effects of NaCl on preimplantation mouse embryos in vitro. *Molecular Reproduction and Development*, *34*(4), 380–390.

Biggers, J. D., Whittingham, D. G., & Donahue, R. P. (1967). The pattern of energy metabolism in the mouse oöcyte and zygote. *Proceedings of the National Academy of Sciences of the United States of America*, *58*(2), 560–567.

Bleil, J. D., & Wassarman, P. M. (1980). Mammalian sperm-egg interaction: Identification of a glycoprotein in mouse egg zonae pellucidae possessing receptor activity for sperm. *Cell*, *20*(3), 873–882.

Blobel, C. P., & Apte, S. S. (2006). ADAMs AND ADAMTSs. In G. J. Laurent & S. D. Shapiro (Eds.), *Encyclopedia of Respiratory Medicine* (pp. 19–23). Academic Press.

Borowsky, B., Mezey, E., & Hoffman, B. J. (1993). Two glycine transporter variants with distinct localization in the CNS and peripheral tissues are encoded by a common gene. *Neuron*, *10*(5), 851–863.

Brew, K., & Nagase, H. (2010). The tissue inhibitors of metalloproteinases (TIMPs): An ancient family with structural and functional diversity. *Biochimica et Biophysica Acta*, *1803*(1), 55–71.

Brinster, R. L. (1963). A Method for in vitro cultivation of mouse ova from two-cell to blastocyst. *Experimental Cell Research*, *32*(1), 205–208.

Bruzzone, R., White, T. W., & Paul, D. L. (1996). Connections with Connexins: The Molecular Basis of Direct Intercellular Signaling. *European Journal of Biochemistry*, *238*(1), 1–27.

Chatot, C. L., Ziomek, C. A., Bavister, B. D., Lewis, J. L., & Torres, I. (1989). An improved culture medium supports development of random-bred 1-cell mouse embryos in vitro. *Journal of Reproduction and Fertility*, *86*(2), 679–688.

Chen, L., Russell, P. T., & Larsen, W. J. (1993). Functional significance of cumulus expansion in the mouse: Roles for the preovulatory synthesis of hyaluronic acid within the cumulus mass. *Molecular Reproduction and Development*, *34*(1), 87–93.

Collins, J. L., & Baltz, J. M. (1999). Estimates of mouse oviductal fluid tonicity based on osmotic responses of embryos. *Biology of Reproduction*, *60*(5), 1188–1193.

Coonrod, S. A., Calvert, M. E., Reddi, P. P., Kasper, E. N., Digilio, L. C., & Herr, J. C. (2004). Oocyte proteomics: Localisation of mouse zona pellucida protein 3 to the plasma membrane of ovulated mouse eggs. *Reproduction, Fertility, and Development*, *16*(1–2), 69–78.

Cooper, G. M., & Cooper, G. M. (2000). *The Cell* (2nd ed.). Sinauer Associates.

Cui, N., Hu, M., & Khalil, R. A. (2017). Biochemical and Biological Attributes of Matrix Metalloproteinases. *Progress in Molecular Biology and Translational Science*, *147*, 1–73.

Coticchio, Giovanni., et al. Oogenesis. Springer, 2013. pp.19-31

Da Silva-Buttkus, P., Jayasooriya, G. S., Mora, J. M., Mobberley, M., Ryder, T. A., Baithun, M., Stark, J., Franks, S., & Hardy, K. (2008). Effect of cell shape and packing density on granulosa cell proliferation and formation of multiple layers during early follicle development in the ovary. *Journal of Cell Science*, *121*(23), 3890–3900.

Dandekar, P., & Talbot, P. (1992). Perivitelline space of mammalian oocytes: Extracellular matrix of unfertilized oocytes and formation of a cortical granule envelope following fertilization. *Molecular Reproduction and Development*, *31*(2), 135–143.

Dawson, K. M., & Baltz, J. M. (1997). Organic Osmolytes and Embryos: Substrates of the Gly and β Transport Systems Protect Mouse Zygotes against the Effects of Raised Osmolarity1. *Biology of Reproduction*, *56*(6), 1550–1558.

Dawson, K. M., Collins, J. L., & Baltz, J. M. (1998). Osmolarity-dependent glycine accumulation indicates a role for glycine as an organic osmolyte in early preimplantation mouse embryos. *Biology of Reproduction*, *59*(2), 225–232.

Deneka, D., Sawicka, M., Lam, A. K. M., Paulino, C., & Dutzler, R. (2018). Structure of a volume-regulated anion channel of the LRRC8 family. *Nature*, *558*(7709), 254–259.

Egbert, J. R., Shuhaibar, L. C., Edmund, A. B., Van Helden, D. A., Robinson, J. W., Uliasz, T. F., Baena, V., Geerts, A., Wunder, F., Potter, L. R., & Jaffe, L. A. (2014). Dephosphorylation and inactivation of NPR2 guanylyl cyclase in granulosa cells contributes to the LH-induced decrease in cGMP that causes resumption of meiosis in rat oocytes. *Development (Cambridge, England)*, *141*(18), 3594–3604.

Egbert, J. R., Uliasz, T. F., Shuhaibar, L. C., Geerts, A., Wunder, F., Kleiman, R. J., Humphrey, J. M., Lampe, P. D., Artemyev, N. O., Rybalkin, S. D., Beavo, J. A., Movsesian, M. A., & Jaffe, L. A. (2016). Luteinizing Hormone Causes Phosphorylation and Activation of the cGMP Phosphodiesterase PDE5 in Rat Ovarian Follicles, Contributing, Together with PDE1 Activity, to the Resumption of Meiosis. *Biology of Reproduction*, *94*(5), 110.

Emori, C., & Sugiura, K. (2014). Role of oocyte-derived paracrine factors in follicular development. *Animal Science Journal*, *85*(6), 627–633.

Eppig, J. J. (2001). Oocyte control of ovarian follicular development and function in mammals. *Reproduction*, *122*(6), 829–838.

Eppig, J.J., Viveiros, M.M., Bivens, C.M. and De la Feunte, R. (2004). Regulation of Eppig mammalian oocyte maturation. In the ovary (Eds, Leung, P.C.K. and Adashi, E.Y.), pp. 113-129.

Eppig, J.J (1996) Coordination of nuclear and cytoplasmic oocyte matueation in eutherian mammals. Reprod. Fertil. Dev., 8:485-489.

Eulenburg, V., Armsen, W., Betz, H., & Gomeza, J. (2005). Glycine transporters: Essential regulators of neurotransmission. *Trends in Biochemical Sciences*, *30*(6), 325–333.

Fadini, R., Dal Canto, M. B., Mignini Renzini, M., Brambillasca, F., Comi, R., Fumagalli, D., Lain, M., Merola, M., Milani, R., & De Ponti, E. (2009). Effect of different gonadotrophin priming on IVM of oocytes from women with normal ovaries: A prospective randomized study. *Reproductive Biomedicine Online*, *19*(3), 343–351.

Fong, B., Watson, P. H., & Watson, A. J. (2007). Mouse preimplantation embryo responses to culture medium osmolarity include increased expression of CCM2 and p38 MAPK activation. *BMC Developmental Biology*, *7*, 2.

Franciosi, F., Coticchio, G., Lodde, V., Tessaro, I., Modina, S. C., Fadini, R., Dal Canto, M., Renzini, M. M., Albertini, D. F., & Luciano, A. M. (2014). Natriuretic Peptide Precursor C Delays Meiotic Resumption and Sustains Gap Junction-Mediated Communication in Bovine Cumulus-Enclosed Oocytes1. *Biology of Reproduction*, *91*(3), 61, 1–9.

Galliera, E., Tacchini, L., & Corsi Romanelli, M. M. (2015). Matrix metalloproteinases as biomarkers of disease: Updates and new insights. *Clinical Chemistry and Laboratory Medicine*, *53*(3), 349–355.

Garcia-Perez, A., & Burg, M. B. (1991). Role of organic osmolytes in adaptation of renal cells to high osmolality. *The Journal of Membrane Biology*, *119*(1), 1–13.

Gilula, N. B., Epstein, M. L., & Beers, W. H. (1978). Cell-to-cell communication and ovulation. A study of the cumulus-oocyte complex. *The Journal of Cell Biology*, *78*(1), 58–75.

Goddard, M. J., & Pratt, H. P. (1983). Control of events during early cleavage of the mouse embryo: An analysis of the "2-cell block." *Journal of Embryology and Experimental Morphology*, *73*, 111–133.

Goodenough, D. A., Goliger, J. A., & Paul, D. L. (1996). Connexins, connexons, and intercellular communication. *Annual Review of Biochemistry*, *65*, 475–502.

Gordon, J. W., & Talansky, B. E. (1986). Assisted fertilization by zona drilling: A mouse model for correction of oligospermia. *The Journal of Experimental Zoology*, *239*(3), 347–354.

Gross, J., & Lapiere, C. M. (1962). Collagenolytic activity in amphibian tissues: A tissue culture assay*. *Proceedings of the National Academy of Sciences*, *48*(6), 1014–1022.

Guastella, J., Brecha, N., Weigmann, C., Lester, H. A., & Davidson, N. (1992). Cloning, expression, and localization of a rat brain high-affinity glycine transporter.

Proceedings of the National Academy of Sciences of the United States of America, *89*(15), 7189–7193.

Hadi, T., Hammer, M.-A., Algire, C., Richards, T., & Baltz, J. M. (2005). Similar effects of osmolarity, glucose, and phosphate on cleavage past the 2-cell stage in mouse embryos from outbred and F1 hybrid females. *Biology of Reproduction*, *72*(1), 179–187.

Hammer, M. A., Kolajova, M., Léveillé, M.-C., Claman, P., & Baltz, J. M. (2000). Glycine transport by single human and mouse embryos. *Human Reproduction*, *15*(2), 419–426.

Hammer, M.-A., & Baltz, J. M. (2002). Betaine is a highly effective organic osmolyte but does not appear to be transported by established organic osmolyte transporters in mouse embryos. *Molecular Reproduction and Development*, *62*(2), 195–202.

Harris, S. E., Gopichandran, N., Picton, H. M., Leese, H. J., & Orsi, N. M. (2005). Nutrient concentrations in murine follicular fluid and the female reproductive tract. *Theriogenology*, *64*(4), 992–1006.

Hirshfield, A. N. (1991). Development of Follicles in the Mammalian Ovary. In K. W. Jeon & M. Friedlander (Eds.), *International Review of Cytology* (Vol. 124, pp. 43–101). Academic Press. https://doi.org/10.1016/S0074-7696(08)61524-7

Hoffmann, E. K., Lambert, I. H., & Pedersen, S. F. (2009). Physiology of Cell Volume Regulation in Vertebrates. *Physiological Reviews*, *89*(1), 193–277.

Hogan, B., Beddington, R., Constantini, F., & Lacy, E. (1994). Manipulating the mouse embryoL a laboratory manual. *Plainview: Cold Spring Harbor Press*.

Hw, J., V, D., P, W., & R, K. (2017). TIMPs: Versatile extracellular regulators in cancer. *Nature Reviews. Cancer*, *17*(1).

Inoue, A., Akiyama, T., Nagata, M., & Aoki, F. (2007). The perivitelline space-forming capacity of mouse oocytes is associated with meiotic competence. *The Journal of Reproduction and Development*, *53*(5), 1043–1052. https://doi.org/10.1262/jrd.19064

Jackson, B. C., Nebert, D. W., & Vasiliou, V. (2010). Update of human and mouse matrix metalloproteinase families. *Human Genomics*, *4*(3), 194–201.

Jain, M., & Singh, M. (2022). Assisted Reproductive Technology (ART) Techniques. In *StatPearls*. StatPearls Publishing. http://www.ncbi.nlm.nih.gov/books/NBK576409/

Jamnongjit, M., Gill, A., & Hammes, S. R. (2005). Epidermal growth factor receptor signaling is required for normal ovarian steroidogenesis and oocyte maturation. *Proceedings of the National Academy of Sciences of the United States of America*, *102*(45), 16257–16262.

Kanatsu-Shinohara, M., Schultz, R. M., & Kopf, G. S. (2000). Acquisition of Meiotic Competence in Mouse Oocytes: Absolute Amounts of p34cdc2, Cyclin B1, cdc25C,

and wee1 in Meiotically Incompetent and Competent Oocytes1. *Biology of Reproduction*, *63*(6), 1610–1616. https://doi.org/10.1095/biolreprod63.6.1610

Kelwick, R., Desanlis, I., Wheeler, G. N., & Edwards, D. R. (2015). The ADAMTS (A Disintegrin and Metalloproteinase with Thrombospondin motifs) family. *Genome Biology*, *16*, 113.

Kidder, G. M., & Vanderhyden, B. C. (2010). Bidirectional communication between oocytes and follicle cells: Ensuring oocyte developmental competence. *Canadian Journal of Physiology and Pharmacology*, *88*(4), 399–413.

Klein, T., & Bischoff, R. (2011). Physiology and pathophysiology of matrix metalloproteases. *Amino Acids*, *41*(2), 271–290.

König, B., & Stauber, T. (2019). Biophysics and Structure-Function Relationships of LRRC8-Formed Volume-Regulated Anion Channels. *Biophysical Journal*, *116*(7), 1185–1193.

Kristensen, A. S., Andersen, J., Jørgensen, T. N., Sørensen, L., Eriksen, J., Loland, C. J., Strømgaard, K., & Gether, U. (2011). SLC6 neurotransmitter transporters: Structure, function, and regulation. *Pharmacological Reviews*, *63*(3), 585–640.

Kwon, H. M., & Handler, J. S. (1995). Cell volume regulated transporters of compatible osmolytes. *Current Opinion in Cell Biology*, *7*(4), 465–471.

Lang, F., Busch, G. L., Ritter, M., Völkl, H., Waldegger, S., Gulbins, E., & Häussinger, D. (1998). Functional significance of cell volume regulatory mechanisms. *Physiological Reviews*, *78*(1), 247–306.

Lawitts, J. A., & Biggers, J. D. (1991). Overcoming the 2-cell block by modifying standard components in a mouse embryo culture medium. *Biology of Reproduction*, *45*(2), 245–251.

Lawitts, J. A., & Biggers, J. D. (1992). Joint effects of sodium chloride, glutamine, and glucose in mouse preimplantation embryo culture media. *Molecular Reproduction and Development*, *31*(3), 189–194.

Lawitts, J. A., & Biggers, J. D. (1993). [9] Culture of preimplantation embryos. In *Methods in Enzymology* (Vol. 225, pp. 153–164). Academic Press.

Litscher, E. S., Qi, H., & Wassarman, P. M. (1999). Mouse zona pellucida glycoproteins mZP2 and mZP3 undergo carboxy-terminal proteolytic processing in growing oocytes. *Biochemistry*, *38*(38), 12280–12287.

Liu, C., Litscher, E. S., Mortillo, S., Sakai, Y., Kinloch, R. A., Stewart, C. L., & Wassarman, P. M. (1996). Targeted disruption of the mZP3 gene results in production of eggs lacking a zona pellucida and infertility in female mice. *Proceedings of the National Academy of Sciences of the United States of America*, *93*(11), 5431–5436.

Liu, L., Kong, N., Xia, G., & Zhang, M. (2013). Molecular control of oocyte meiotic arrest and resumption. *Reproduction, Fertility, and Development*, *25*(3), 463–471.

López-Corcuera, B., Vázquez, J., & Aragón, C. (1991). Purification of the sodium- and chloride-coupled glycine transporter from central nervous system. *The Journal of Biological Chemistry*, *266*(36), 24809–24814.

Macaulay, A. D., Ortman, C. S., Moore, K. R. J., & Baltz, J. M. (2023). Initial detachment of the mouse oocyte from the zona pellucida is mediated by metallopeptidase activity. *Biology of Reproduction*, ioac185.

Makowski, L., Caspar, D. L., Phillips, W. C., & Goodenough, D. A. (1977). Gap junction structures. II. Analysis of the x-ray diffraction data. *The Journal of Cell Biology*, *74*(2), 629–645.

McLaren, A., & Biggers, J. D. (1958). Successful development and birth of mice cultivated in vitro as early as early embryos. *Nature*, *182*(4639), 877–878.

Mikkelsen, A. L., & Lindenberg, S. (2001). Benefit of FSH priming of women with PCOS to the in vitro maturation procedure and the outcome: A randomized prospective study. *Reproduction (Cambridge, England)*, *122*(4), 587–592.

Mongin, A. A., & Orlov, S. N. (2001). Mechanisms of cell volume regulation and possible nature of the cell volume sensor. *Pathophysiology: The Official Journal of the International Society for Pathophysiology*, *8*(2), 77–88.

Nagyová, E., Vanderhyden, B. C., & Procházka, R. (2000). Secretion of Paracrine Factors Enabling Expansion of Cumulus Cells Is Developmentally Regulated in Pig Oocytes1. *Biology of Reproduction*, *63*(4), 1149–1156.

Natale, D. R., Paliga, A. J. M., Beier, F., D'Souza, S. J. A., & Watson, A. J. (2004). P38 MAPK signaling during murine preimplantation development. *Developmental Biology*, *268*(1), 76–88.

Nicolson, G. L., Yanagimachi, R., & Yanagimachi, H. (1975). Ultrastructural localization of lectin-binding sites on the zonae pellucidae and plasma membranes of mammalian eggs. *The Journal of Cell Biology*, *66*(2), 263–274.

Norris, R. P., Freudzon, M., Mehlmann, L. M., Cowan, A. E., Simon, A. M., Paul, D. L., Lampe, P. D., & Jaffe, L. A. (2008). Luteinizing hormone causes MAP kinase-dependent phosphorylation and closure of connexin 43 gap junctions in mouse ovarian follicles: One of two paths to meiotic resumption. *Development (Cambridge, England)*, *135*(19), 3229–3238.

Norris, R. P., Freudzon, M., Nikolaev, V. O., & Jaffe, L. A. (2010). Epidermal growth factor receptor kinase activity is required for gap junction closure and for part of the decrease in ovarian follicle cGMP in response to LH. *Reproduction*, *140*(5), 655–662.

Norris, R. P., Ratzan, W. J., Freudzon, M., Mehlmann, L. M., Krall, J., Movsesian, M. A., Wang, H., Ke, H., Nikolaev, V. O., & Jaffe, L. A. (2009). Cyclic GMP from the surrounding somatic cells regulates cyclic AMP and meiosis in the mouse oocyte. *Development (Cambridge, England)*, *136*(11), 1869–1878.

Orlowski, J., & Grinstein, S. (1997). Na+/H+ Exchangers of Mammalian Cells. *Journal of Biological Chemistry*, *272*(36), 22373–22376.

Orlowski, J., & Grinstein, S. (2004). Diversity of the mammalian sodium/proton exchanger SLC9 gene family. *Pflugers Archiv: European Journal of Physiology*, *447*(5), 549–565.

Pan, B., & Li, J. (2019). The art of oocyte meiotic arrest regulation. *Reproductive Biology and Endocrinology*, *17*(1), 8. https://doi.org/10.1186/s12958-018-0445-8

Park, J.-Y., Su, Y.-Q., Ariga, M., Law, E., Jin, S.-L. C., & Conti, M. (2004). EGF-like growth factors as mediators of LH action in the ovulatory follicle. *Science (New York, N.Y.)*, *303*(5658), 682–684.

Pastor-Anglada, M., Felipe, A., Casado, F. J., Ferrer-Martínez, A., & Gómez-Angelats, M. (1996). Long-term osmotic regulation of amino acid transport systems in mammalian cells. *Amino Acids*, *11*(2), 135–151.

Porter, S., Clark, I. M., Kevorkian, L., & Edwards, D. R. (2005). The ADAMTS metalloproteinases. *Biochemical Journal*, *386*(1), 15–27.

Prochazka, R., & Nemcova, L. (2019). Mechanisms of FSH- and Amphiregulin-Induced MAP Kinase 3/1 Activation in Pig Cumulus-Oocyte Complexes During Maturation In Vitro. *International Journal of Molecular Sciences*, *20*(5), 1179.

Przemyslaw, L., Boguslaw, H. A., Elzbieta, S., & Malgorzata, S. M. (2013). ADAM and ADAMTS family proteins and their role in the colorectal cancer etiopathogenesis. *BMB Reports*, *46*(3), 139–150.

Raeeszadeh-Sarmazdeh, M., Do, L. D., & Hritz, B. G. (2020). Metalloproteinases and Their Inhibitors: Potential for the Development of New Therapeutics. *Cells*, *9*(5), E1313.

Rankin, T., Familari, M., Lee, E., Ginsberg, A., Dwyer, N., Blanchette-Mackie, J., Drago, J., Westphal, H., & Dean, J. (1996). Mice homozygous for an insertional mutation in the Zp3 gene lack a zona pellucida and are infertile. *Development (Cambridge, England)*, *122*(9), 2903–2910.

Rankin, T. L., O'Brien, M., Lee, E., Wigglesworth, K., Eppig, J., & Dean, J. (2001). Defective zonae pellucidae in Zp2-null mice disrupt folliculogenesis, fertility and development. *Development (Cambridge, England)*, *128*(7), 1119–1126.

Rankin, T., Talbot, P., Lee, E., & Dean, J. (1999). Abnormal zonae pellucidae in mice lacking ZP1 result in early embryonic loss. *Development (Cambridge, England)*, *126*(17), 3847–3855.

Razak, M. A., Begum, P. S., Viswanath, B., & Rajagopal, S. (2017). Multifarious Beneficial Effect of Nonessential Amino Acid, Glycine: A Review. *Oxidative Medicine and Cellular Longevity*, *2017*, 1716701.

Richard, S., & Baltz, J. M. (2014). Prophase I arrest of mouse oocytes mediated by natriuretic peptide precursor C requires GJA1 (connexin-43) and GJA4 (connexin-37) gap junctions in the antral follicle and cumulus-oocyte complex. *Biology of Reproduction*, *90*(6), 137.

Richard, S., Tartia, A. P., Boison, D., & Baltz, J. M. (2017). Mouse Oocytes Acquire Mechanisms That Permit Independent Cell Volume Regulation at the End of Oogenesis. *Journal of Cellular Physiology*, *232*(9), 2436–2446.

Richards, J. S. (2005). Ovulation: New factors that prepare the oocyte for fertilization. *Molecular and Cellular Endocrinology*, *234*(1–2), 75–79.

Robinson, J. W., Zhang, M., Shuhaibar, L. C., Norris, R. P., Geerts, A., Wunder, F., Eppig, J. J., Potter, L. R., & Jaffe, L. A. (2012). Luteinizing Hormone Reduces the Activity of the NPR2 Guanylyl Cyclase in Mouse Ovarian Follicles, Contributing to the Cyclic GMP Decrease that Promotes Resumption of Meiosis in Oocytes. *Developmental Biology*, *366*(2), 308–316.

Russell, D. L., Brown, H. M., & Dunning, K. R. (2015). ADAMTS proteases in fertility. *Matrix Biology: Journal of the International Society for Matrix Biology*, *44–46*, 54–63.

Salustri, A., Yanagishita, M., Underhill, C. B., Laurent, T. C., & Hascall, V. C. (1992). Localization and synthesis of hyaluronic acid in the cumulus cells and mural granulosa cells of the preovulatory follicle. *Developmental Biology*, *151*(2), 541–551.

Salustri, A. and Siracusa, G. (1983). Metabolic coupling, cumulus expansion and meiotic resumption in mouse cumuli oophori cultured in vitro in the presence of FSH or dcAMP , or stimulated in vivo by hCG. *J Reprod Fertil*. 68: 33-341

Schultz, G. A., Kaye, P. L., McKay, D. J., & Johnson, M. H. (1981). Endogenous amino acid pool sizes in mouse eggs and preimplantation embryos. *Journal of Reproduction and Fertility*, *61*(2), 387–393.

Sheikh-Hamad, D., & Gustin, M. C. (2004). MAP kinases and the adaptive response to hypertonicity: Functional preservation from yeast to mammals. *American Journal of Physiology. Renal Physiology*, *287*(6), F1102-1110.

Shuhaibar, L. C., Egbert, J. R., Edmund, A. B., Uliasz, T. F., Dickey, D. M., Yee, S.-P., Potter, L. R., & Jaffe, L. A. (2016). Dephosphorylation of juxtamembrane serines and threonines of the NPR2 guanylyl cyclase is required for rapid resumption of oocyte meiosis in response to luteinizing hormone. *Developmental Biology*, *409*(1), 194–201.

Shuhaibar, L. C., Egbert, J. R., Norris, R. P., Lampe, P. D., Nikolaev, V. O., Thunemann, M., Wen, L., Feil, R., & Jaffe, L. A. (2015). Intercellular signaling via cyclic GMP diffusion through gap junctions restarts meiosis in mouse ovarian follicles. *Proceedings of the National Academy of Sciences of the United States of America*, *112*(17), 5527–5532.

Silver, L.M. (1995). Mouse Genetics. Concepts and Applications. Oxford University Press. Available from: http://www.informatics.jax.org/silver/

Simon, A. M., Goodenough, D. A., Li, E., & Paul, D. L. (1997). Female infertility in mice lacking connexin 37. *Nature*, *385*(6616), 525–529.

Solc, P., Schultz, R. M., & Motlik, J. (2010). Prophase I arrest and progression to metaphase I in mouse oocytes: Comparison of resumption of meiosis and recovery from G2-arrest in somatic cells. *Molecular Human Reproduction*, *16*(9), 654–664.

Sorensen, R. A., & Wassarman, P. M. (1976). Relationship between growth and meiotic maturation of the mouse oocyte. *Developmental Biology*, *50*(2), 531–536.

Steeves, C. L., & Baltz, J. M. (2005). Regulation of intracellular glycine as an organic osmolyte in early preimplantation mouse embryos. *Journal of Cellular Physiology*, *204*(1), 273–279.

Steeves, C. L., Hammer, M.-A., Walker, G. B., Rae, D., Stewart, N. A., & Baltz, J. M. (2003). The glycine neurotransmitter transporter GLYT1 is an organic osmolyte transporter regulating cell volume in cleavage-stage embryos. *Proceedings of the National Academy of Sciences*, *100*(24), 13982–13987.

Steptoe, P. C., & Edwards, R. G. (1978). Birth after the reimplantation of a human embryo. *Lancet (London, England)*, *2*(8085), 366.

Strange, K. (2004). Cellular volume homeostasis. *Advances in Physiology Education*, *28*(1–4), 155–159.

Supplisson, S., & Bergman, C. (1997). Control of NMDA receptor activation by a glycine transporter co-expressed in Xenopus oocytes. *The Journal of Neuroscience: The Official Journal of the Society for Neuroscience*, *17*(12), 4580–4590.

Tartia, A. P., Rudraraju, N., Richards, T., Hammer, M.-A., Talbot, P., & Baltz, J. M. (2009). Cell volume regulation is initiated in mouse oocytes after ovulation. *Development*, *136*(13), 2247–2254.

Tscherner, A. K., Macaulay, A. D., Ortman, C. S., & Baltz, J. M. (2021). Initiation of cell volume regulation and unique cell volume regulatory mechanisms in mammalian oocytes and embryos. *Journal of Cellular Physiology*, *236*(10), 7117–7133.

van den Hurk, R., & Zhao, J. (2005). Formation of mammalian oocytes and their growth, differentiation and maturation within ovarian follicles. *Theriogenology*, *63*(6), 1717–1751. https://doi.org/10.1016/j.theriogenology.2004.08.005

Van Winkle, L. J., & Dickinson, H. R. (1995). Differences in amino acid content of preimplantation mouse embryos that develop in vitro versus in vivo: In vitro effects of five amino acids that are abundant in oviductal secretions. *Biology of Reproduction*, *52*(1), 96–104.

Van Winkle, L. J., Haghighat, N., & Campione, A. L. (1990a). Glycine protects preimplantation mouse conceptuses from a detrimental effect on development of the inorganic ions in oviductal fluid. *The Journal of Experimental Zoology*, *253*(2), 215–219.

Van Winkle, L. J., Haghighat, N., & Campione, A. L. (1990b). Glycine protects preimplantation mouse conceptuses from a detrimental effect on development of the inorganic ions in oviductal fluid. *The Journal of Experimental Zoology*, *253*(2), 215–219.

Van Winkle, L. J., Haghighat, N., Campione, A. L., & Gorman, J. M. (1988). Glycine transport in mouse eggs ad preimplantation conceptuses. *Biochimica et Biophysica Acta (BBA) - Biomembranes*, *941*(2), 241–256.

Vanderhyden, B. C., Caron, P. J., Buccione, R., & Eppig, J. J. (1990). Developmental pattern of the secretion of cumulus expansion-enabling factor by mouse oocytes and the role of oocytes in promoting granulosa cell differentiation. *Developmental Biology*, *140*(2), 307–317.

Wassarman, P., Chen, J., Cohen, N., Litscher, E., Liu, C., Qi, H., & Williams, Z. (1999). Structure and function of the mammalian egg zona pellucida. *The Journal of Experimental Zoology*, *285*(3), 251–258.

Wassarman, P. M. (1988). Zona pellucida glycoproteins. *Annual Review of Biochemistry*, *57*, 415–442.

Wassarman, P. M. (2005). Contribution of mouse egg zona pellucida glycoproteins to gamete recognition during fertilization. *Journal of Cellular Physiology*, *204*(2), 388–391.

Wassarman, P. M. (2008). Zona pellucida glycoproteins. *The Journal of Biological Chemistry*, *283*(36), 24285–24289.

Wassarman, P. M., & Litscher, E. S. (2013). Chapter Nine—Biogenesis of the Mouse Egg's Extracellular Coat, the Zona Pellucida. In P. M. Wassarman (Ed.), *Current Topics in Developmental Biology* (Vol. 102, pp. 243–266). Academic Press.

Wassarman, P. M., & Litscher, E. S. (2021). Zona Pellucida Genes and Proteins: Essential Players in Mammalian Oogenesis and Fertility. *Genes*, *12*(8), 1266.

Wassarman, P. M., Schultz, R. M., Letourneau, G. E., LaMarca, M. J., Josefowicz, W. J., & Bleil, J. D. (1979). Meiotic maturation of mouse oocytes in vitro. *Advances in Experimental Medicine and Biology*, *112*, 251–268.

Whitten, W. K. (1956). Culture of Tubal Mouse Ova. *Nature*, *177*(4498), Article 4498.

Whitten, W. K. (1957). Culture of tubal ova. *Nature*, *179*(4569), 1081–1082.

Whittingham, D. G. (1971). Culture of mouse ova. *Journal of Reproduction and Fertility. Supplement*, *14*, 7–21.

Wigglesworth, K., Lee, K.-B., O'Brien, M. J., Peng, J., Matzuk, M. M., & Eppig, J. J. (2013). Bidirectional communication between oocytes and ovarian follicular somatic cells is required for meiotic arrest of mammalian oocytes. *Proceedings of the National Academy of Sciences of the United States of America*, *110*(39), E3723-3729.

Williams, Z., & Wassarman, P. M. (2001). Secretion of mouse ZP3, the sperm receptor, requires cleavage of its polypeptide at a consensus furin cleavage-site. *Biochemistry*, *40*(4), 929–937.

Yancey, P. H., Clark, M. E., Hand, S. C., Bowlus, R. D., & Somero, G. N. (1982). Living with water stress: Evolution of osmolyte systems. *Science (New York, N.Y.)*, *217*(4566), 1214–1222.

Yong, V. W., Power, C., Forsyth, P., & Edwards, D. R. (2001). Metalloproteinases in biology and pathology of the nervous system. *Nature Reviews Neuroscience*, *2*(7), Article 7.

Zafra, F., & Giménez, C. (2008). Glycine transporters and synaptic function. *IUBMB Life*, *60*(12), 810–817.

Zhang, M., Su, Y.-Q., Sugiura, K., Xia, G., & Eppig, J. J. (2010). Granulosa cell ligand NPPC and its receptor NPR2 maintain meiotic arrest in mouse oocytes. *Science (New York, N.Y.)*, *330*(6002), 366–369.

Zhao, M., Gold, L., Dorward, H., Liang, L., Hoodbhoy, T., Boja, E., Fales, H. M., & Dean, J. (2003). Mutation of a conserved hydrophobic patch prevents incorporation of ZP3

into the zona pellucida surrounding mouse eggs. *Molecular and Cellular Biology*, *23*(24), 8982–8991.

Zhao, M., Gold, L., Ginsberg, A. M., Liang, L.-F., & Dean, J. (2002). Conserved Furin Cleavage Site Not Essential for Secretion and Integration of ZP3 into the Extracellular Egg Coat of Transgenic Mice. *Molecular and Cellular Biology*, *22*(9), 3111–3120.